# Report on alternative waste scenarios

OPERA-PU-NRG112

Radioactive substances and ionizing radiation are used in medicine, industry, agriculture, research, education and electricity production. This generates radioactive waste. In the Netherlands, this waste is collected, treated and stored by COVRA (Centrale Organisatie Voor Radioactief Afval). After interim storage for a period of at least 100 years radioactive waste is intended for disposal. There is a world-wide scientific and technical consensus that geological disposal represents the safest long-term option for radioactive waste.

Geological disposal is emplacement of radioactive waste in deep underground formations. The goal of geological disposal is long-term isolation of radioactive waste from our living environment in order to avoid exposure of future generations to ionising radiation from the waste. OPERA (OnderzoeksProgramma Eindberging Radioactief Afval) is the Dutch research programme on geological disposal of radioactive waste.

Within OPERA, researchers of different organisations in different areas of expertise will cooperate on the initial, conditional Safety Cases for the host rocks Boom Clay and Zechstein rock salt. As the radioactive waste disposal process in the Netherlands is at an early, conceptual phase and the previous research programme has ended more than a decade ago, in OPERA a first preliminary or initial safety case will be developed to structure the research necessary for the eventual development of a repository in the Netherlands. The safety case is conditional since only the long-term safety of a generic repository will be assessed. OPERA is financed by the Dutch Ministry of Economic Affairs and the public limited liability company Electriciteits-Produktiemaatschappij Zuid-Nederland (EPZ) and coordinated by COVRA. Further details on OPERA and its outcomes can be accessed at www.covra.nl.



OPERA-PU-NRG112
Title: Report on alternative waste scenarios
Authors: J. Hart (NRG), T.J. Schröder (NRG)
Date of publication: 7 July 2016
Keywords: fuel cycle, scenario, nuclear waste, nuclide inventory

Summary .... 5
Samenvatting .... 5
1. Introduction .... 7
1.1. Background .... 7
1.2. Objectives .... 7
1.3. Realization .... 7
1.4. Explanation contents .... 8
2. Alternative fuel cycles .... 9
2.1. Scenario 1 - No new nuclear power plants .... 10
2.2. Scenario 2 - Application of MOX fuel in Borssele NPP .... 10
2.3. Scenario 3 – No reprocessing of spent fuel .... 10
2.4. Scenario 4 - Deployment of MOX-fueled Gen III LWRs .... 11
2.5. Scenario 5 - Large-scale deployment of HTRs .... 11
2.6. Scenario 6 - Deployment of fast reactors .... 12
2.7. Scenario 7 - Deployment of thorium-based reactors. .... 12
3. Mapping of inventory to safety and performance indicator .... 15
3.1. Considered safety and performance indicators .... 16
3.2. Analysis of basic assumptions .... 18
3.3. Transformation and mapping of safety indicators .... 19
3.4. Construction of the PAMINA indicator and potential refinements .... 19
3.5. Conclusions .... 24
4. Computer tool - DANESS .... 25
5. Scenario Assumptions and Technology Characteristics .... 27
5.1. General assumptions .... 27
5.2. Nuclear energy demand .... 27
5.3. Reactor types .... 28
5.3.1. Gen II LWR – Borssele reactor .... 29
5.3.2. Gen III LWR .... 29
5.3.3. Sodium Fast Reactor (SFR) .... 29
5.3.4. HTR .... 31
5.3.5. Thorium reactor – PWR .... 32
5.4. Fuel cycle facilities .... 33
5.5. Fissile material .... 33
6. Back-end of the Fuel Cycle .... 34
6.1. Reprocessing plants .... 34
6.2. Storage and disposal .... 35
6.3. Waste Forms .... 35
7. DANESS Input Tables .... 38
7.1. Nuclear power plants .... 38
7.2. Fuel characteristics .... 38
7.3. Spent fuel and HLW isotopics .... 39
7.4. Fuel cycle facilities .... 39
8. Results of the DANESS Simulations .... 41
8.1. Scenario 1 – No new nuclear power plants .... 41
8.2. Scenario 2 – Application of MOX fuel .... 44
8.3. Scenario 3 – No reprocessing of spent fuel .... 48
8.4. Scenario 4 – Deployment of MOX-fueled Gen III LWRs .... 51
8.5. Scenario 5 – Large-scale deployment of HTRs .... 55
8.6. Scenario 6 - Deployment of fast reactors .... 59
8.7. Scenario 7 – Deployment of thorium-based reactors. .... 63
8.8. Summary and evaluation of the results .... 67
9. Concluding remarks .... 74
Index of Figures .... 75

Index of Tables ........................................................................................ 76
10. References ........................................................................................ 78

# Summary

The present report (*Alternative waste scenarios*, OPERA Report M1.1.2.1) is one of the outcomes of the OPERA Project *OPCHAR* (OPERA Waste Characteristics), as part of Task 1.1.2, *Alternative waste scenarios*. It describes a set of alternative future fuel cycle scenarios in the Netherlands, that are in compliance with scenarios formulated in the 'Energierapport 2008 (MinEZ, 2008; p.88), and that have been analysed with the computer code DANESS, "*Dynamic Analysis of Nuclear Energy System Strategies*". In addition, a new indicator based on the travel time of radionuclides in Boom Clay is introduced and tested with the outcomes of the DANESS analyses concerning the nuclide inventories of the different scenarios.

For the production of nuclear energy, several technological and logistic options are possible, i.e. reprocessing of waste, the utilisation of MOX-fuels in current reactors, the deployment of gas-cooled high temperature reactors (HTRs) or other 3$^{rd}$ or 4$^{th}$ generation technologies, including fast breeder reactors. Changes in the presently adopted nuclear fuel cycle strategy in the Netherlands impact both the quantities of generated radioactive waste as its composition. These have been quantified in the present analyses.

The present version of the DANESS code is essentially built as a uranium fuel cycle analysis tool. In order to apply DANESS to a thorium fuel cycle the code requires important modifications that are beyond the scope of the OPCHAR project. For those reasons, the results of the presently assessed thorium fuel cycle can only be regarded as indicative.

The elaboration of a dedicated performance indicator enables the (conservative) estimation of the impact of altered waste amounts on the long-term safety as will be calculated in OPERA WP7.3 (*Safety Assessment*).

# Samenvatting

Het onderhavige rapport (*Alternative waste scenarios*, OPERA Report M1.1.2.1) is een van de resultaten van het OPERA Project *OPCHAR* (OPERA Waste Characteristics), als onderdeel van Task 1.1.2, *Alternative waste scenarios*. Dit rapport beschrijft een set alternatieve toekomstige splijtstofcycli in Nederland, die in overeenstemming zijn met de scenario's die zijn geformuleerd in het 'Energierapport 2008 (MinEZ, 2008; p.88), en die zijn geanalyseerd met het computerprogramma DANESS, "*Dynamic Analysis of Nuclear Energy System Strategies*". Daarnaast wordt een nieuwe indicator beschreven die is gebaseerd op de verblijftijd van radionucliden in Boomse Klei, en die is getest aan de hand van de door DANESS berekende inventarissen van radionucliden.

Voor de productie van nucleaire energy zijn verschillende technologische en logistieke opties mogelijk, zoals het opwerken van gebruikte splijstof, het gebruik van MOX splijtstof in huidige reactoren, de inzet van hoge-temperatuur gasgekoelde ractoren of andere 3$^{e}$ of 4$^{e}$ generatie technologieën, inclusief snelle kweekreactoren. Veranderingen in de bestaande nucleaire splijtstofcyclus in Nederland beïnvloeden zowel de hoeveelheden van het geproduceerde radioactieve afval als de samenstelling ervan. Deze zijn gekwantificeerd in de onderhavige analyses.

De huidige versie van DANESS is in essentie opgezet als een analyse-tool voor de uranium splijtstofcyclus. Om de code geschikt te maken voor de analyse van thoriumcycli zijn significante aanpassingen vereist die buiten de scope van het OPCHAR project vallen. De resultaten van de analyse van de thoriumcyclus zijn derhalve als indicatief te beschouwen.

De ontwikkeling van een toepassingspecifieke indicator maakt het mogelijk een (conservatieve) afschatting te geven van de effecten van alternatieve hoeveelheden

radioactief afval op de lange-termijn veiligheid, zoals die zullen worden berekend in OPERA WP7.3 (*Safety Assessment*).

# 1. Introduction

## 1.1. Background

Reliable esimates of the radionuclide inventory and matrix composition are an important input for the long-term safety assessment of a deep geological facility for the disposal of radioactive waste. For OPERA's Task 1.1.1 (*Definition of radionuclide inventory and matrix composition*) the NRG project *OPCHAR* has compiled a detailed inventory of the total expected radioactive waste composition in the Netherlands foreseen to be disposed of in 2130. Based on the Dutch nuclear base scenario, a database has been compiled that integrated existing information, both in terms of the radionuclide inventory as well as of the matrix composition of all waste forms and fractions (Hart, 2014; Meeussen, 2014).

Changes in the presently adopted nuclear fuel cycle strategy in the Netherlands may impact both the quantities of generated radioactive waste as its composition: for the production of nuclear energy, several technological and logistic options are possible, i.e. reprocessing of spent fuel, the utilisation of MOX-fuels in current reactors, the deployment of gas-cooled high temperature reactors (HTRs) or other 3$^{rd}$ or 4$^{th}$ generation technologies, including fast breeder reactors.

The present report is one of the outcomes of the OPERA Project *OPCHAR* (OPERA Waste Characteristics), as part of Task 1.1.2, *Alternative waste scenarios*. It describes a set of alternative future fuel cycle scenarios in the Netherlands, that are in compliance with scenarios formulated in the 'Energierapport 2008 (MinEZ, 2008; p.88), and that have been analysed with the computer code DANESS, "*Dynamic Analysis of Nuclear Energy System Strategies*". In addition, a new indicator based on the travel time of radionuclides in Boom Clay is introduced and tested with the outcomes of the DANESS analyses concerning the nuclide inventories of the different scenarios.

OPERA's Task 1.1.2 (*Alternative waste scenario's*) sets out to quantify the consequences of several possible alternative nuclear fuel cycle scenarios in the Netherlands in terms of waste amounts and compositions. In addition, the elaboration of a dedicated performance indicator enables the (conservative) estimation of the impact of altered waste amounts on the long-term safety on basis of the calculated results of OPERA WP7.3 (*Safety Assessment*).

## 1.2. Objectives

The aim of the task is to provide an estimation of the radionuclide inventory of the radioactive waste that is expected to be stored in a radioactive waste repository in the year 2130, taking into account a set of alternative nuclear energy scenarios in the Netherlands. In addition, a new indicator based on the travel time of radionuclides in Boom Clay is introduced that will serve as basis for an elaborated indicator, to be developed later in the project.

## 1.3. Realization

To estimate the impact of altered radioactive waste scenarios on the long-term safety of a disposal concept, the *OPCHAR* contribution to Task 1.1.2 aims to a) quantify the radioactive waste in terms of amounts and compositions for several altered nuclear fuel cycle scenarios at the foreseen time of disposal (i.e. the year 2130) and b) to develop a plausible indicator that allows to compare these scenarios in terms of long-term behaviour of the relevant radionucides in a semi-quantitative manner.

In order to assess the functionality of the proposed indicator, radionuclide specific spectra for a number of nuclear fuel cycle scenarios, which may be relevant within the Dutch context, have been elaborated. To get a realistic representation of possible future nuclear scenarios in the Netherlands, the state-of-the-art code DANESS, "Dynamic Analysis of Nuclear Energy System Strategies" (ANL, 2005), has been applied. DANESS is an integrated dynamic nuclear process model for the analysis of today's and future nuclear energy systems which simulates the flows of fissile material, fresh fuel, spent fuel, high level waste, all intermediate stocks and fuel cycle facilities' throughput.

By the use of DANESS nuclide inventories that are generated within different nuclear energy scenarios have been estimated, which can be used as input for safety assessment calculations.

Moreover, a performance indicator developed by NRG as part of the EU-FP-7 project PAMINA (Schröder et al., 2009) is developed further for the particular purpose of the present study. Under certain conditions, the outcomes of the DANESS calculations can be linked in a rather straightforward way to the set of safety indicators proposed in (OPERA M7.3.1, OPERA M7.3.2).

## 1.4. Explanation contents

A description of alternative fuel cycles in the Netherlands is presented in Chapter 2. In Chapter 3, we analyse which indicators can be used to perform such an analysis, and describe how and under which conditions the inventory estimated by DANESS can be mapped on different indicators of the OPERA Safety Case. Chapter 4 provides a general overview of the computer program DANESS that has been applied to assess the alternative fuel cycles. In Chapter 5 technologies and assumptions are described that are relevant to the respective scenarios and fuel cycles. Details about the back-end of the fuel cycle are described in Chapter 6, and input data to the DANESS code are provided in Chapter 7. Results of the DANESS simulations are provided in Chapter 8. Finally, Chapter 9 provides the concluding remarks.

# 2. Alternative fuel cycles

The aim of the present project is to compose a database with detailed descriptions of the total expected radioactive waste inventory for each waste fraction on radionuclide level, taking into account a selected set of future nuclear fuel cycles in the Netherlands. In addition to the Dutch nuclear base scenario '1a' in the 'Energierapport 2008 (MinEZ, 2008; p.88) that assumes no new nuclear power plants and operation of the present Borssele reactor until 2033, several alternative future nuclear energy scenarios have been assessed in terms of waste impact. Two groups of future nuclear scenarios are assumed to be relevant and have been analysed with *DANESS* and compared to the 'base scenario' in terms of the resulting radionuclide inventory:

1. Changing fuel cycle/reprocessing options on basis of the existing nuclear power plant Borssele
2. Deployment of new future nuclear power plants

The alternative scenarios of the second group deviate also from the present Dutch strategy of reprocessing of spent fuel from nuclear power reactors and will result in other types of high-level wastes with deviating radionuclide spectra that need be disposed of.

The nuclear fuel cycle scenarios that have been selected for the present study are the following:

- Scenario 1 - No new nuclear power plants;
- Scenario 2 - Application of MOX fuel;
- Scenario 3 - No reprocessing of spent fuel;
- Scenario 4 - Deployment of MOX-fuelled Generation III Light Water Reactors;
- Scenario 5 - Large-scale deployment of HTRs;
- Scenario 6 - Deployment of fast reactors;
- Scenario 7 - Deployment of thorium-based reactors.

The present study is an update and extension of a paper by Hart and Van Heek (2008), describing options for renewing the current Dutch electricity generating park in the next decades. The analyses performed in that study were also performed with DANESS and examined the consequences of a transition from the present primarily fossil-fuel based electricity generating park towards a more sustainable situation with a larger share of nuclear energy and renewable energy. In a dynamic analysis with the DEEA and DANESS computer codes the future electricity supply distribution in the Netherlands by source, the required capacities of nuclear facilities, and the emissions of exhaust gases and high-level radioactive waste have been determined. The future deployment of nuclear reactors in the Netherlands was assumed to be shared by the evolutionary reactor design EPR and the smaller-scale alternative PBMR. Two different scenarios were assumed for the foreseen growth of the Dutch electricity demand. The analyses have been compared with the consequences of a nuclear phase-out. The 2008 study clearly revealed that, in addition to the foreseen substantial growth of renewable energy in the Netherlands, the possible deployment of nuclear energy may result in significantly reduced emissions of CO2 and other exhaust gases.

The present study elaborates the 2008 study significantly by analysing different scenarios and assuming the deployment of other types of nuclear reactors. In addition, the distribution of the radionuclides generated by the different nuclear fuel cycles by the year

2130 has been estimated, which may serve as input and source term for the long term safety assessment to be performed in OPERA WP7.3 *Safety Assessment*.

The following sections describe the alternative nuclear fuel cycle scenarios investigated in the present study in more detail.

## *2.1. Scenario 1 - No new nuclear power plants*

Scenario 1, the base scenario, assumes that no new nuclear power plants will be introduced in the Netherlands and that the present Borssele reactor, a “Gen II reactor”, continues to operate until its close-down in 2033. The spent fuel continues to be reprocessed, and the HLW will be stored at COVRA until it is finally disposed of in a deep geological disposal facility by 2130. The process scheme is depicted in Figure 2-1.

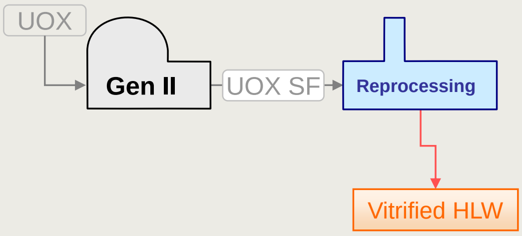


**Figure 2-1 Process scheme of Scenario 1 - No new nuclear power plants**

## *2.2. Scenario 2 - Application of MOX fuel in Borssele NPP*

Scenario 2 assumes changing the fuel cycle options for the existing nuclear power plant Borssele. This scenario assumes that 40% of the nuclear fuel of the Borssele NPP will consist of MOX (EPZ, 2010; p.24), and 60% “c-ERU[1]” UOX fuel (EPZ, 2010; p.24). It is assumed that both the spent UOX and MOX fuel are reprocessed.

The simplified process scheme is depicted in Figure 2-2.

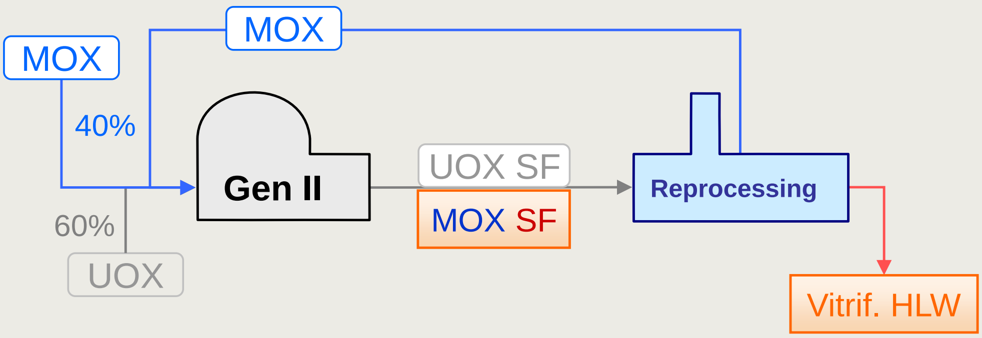


**Figure 2-2 Process scheme of Scenario 2 - Application of MOX fuel**

## *2.3. Scenario 3 – No reprocessing of spent fuel*

This scenario assumes that spent fuel of the Borssele NPP, the Gen II reactor, will no longer be reprocessed after the year 2013 but, after conditioning, will be directly disposed instead. This once-through cycle process scheme is depicted in Figure 2-3.

[1] C-ERU UOX: “compensated enriched recycled uranium”, 4,6% enriched in U-235

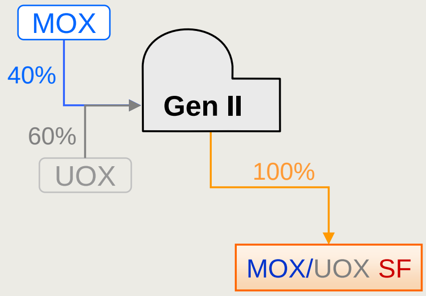


**Figure 2-3 Process scheme of Scenario 3 - No reprocessing of spent fuel**

## 2.4. Scenario 4 - Deployment of MOX-fueled Gen III LWRs

This scenario assumes that from 2020 on the Gen II Borssele NPP will be supplemented by Gen-III type LWRs, which will partially (i.e. by 40%) use MOX fuel (EPZ, 2008; p.2). In this scenario it will be assumed that spent both UOX and MOX fuel will be reprocessed. This scenario is in line with Scenario 2 of the Energy Council of the Dutch Ministry of Economic Affairs (MinEZ, 2008; p. 89).

The simplified process scheme is depicted in Figure 2-4.

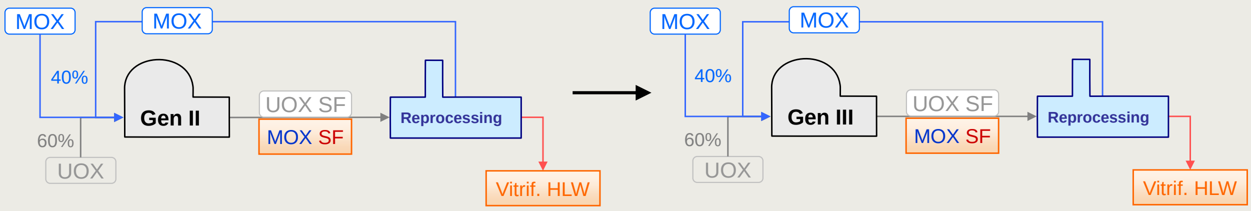


**Figure 2-4 Process scheme of Scenario 4 - Deployment of MOX-fueled Gen III LWRs**

## 2.5. Scenario 5 - Large-scale deployment of HTRs

This scenario is in line with Scenario 1b of the Energy Council of the Dutch Ministry of Economic Affairs (MinEZ, 2008p; p. 88). The deployment of HTRs is assumed to be feasible from approximately 2020 on. The HTR UOX spent fuel pebbles will not be reprocessed but instead stored on surface prior to their disposal starting in 2130. In a previous study is was established that the deployment of gas cooled high temperature reactors may result in large volumes of graphite pebbles, containing U/PuOx spent fuel, and activated carbon (Hart, 2008).

The simplified process scheme is depicted in Figure 2-5.

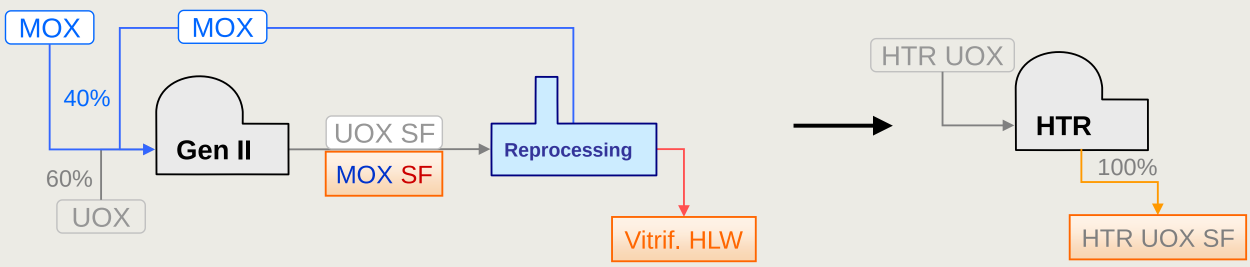


**Figure 2-5 Process scheme of Scenario 5 - Large-scale deployment of HTRs**

### 2.6. Scenario 6 - Deployment of fast reactors

In this scenario is has been assumed that the nuclear electricity demand is initially covered by LWR Gen III reactors, as Gen IV type reactors are not presently available on a commercial basis. The deployment of fast reactors, starting around 2040, and assuming full reprocessing of the spent fuel, will result in a different type of HLW since actinides will be removed from the waste in order to be applied in the manufacturing of FR-MOX fuel.

This scenario is in line with Scenario 3 of the Energy Council of the Dutch Ministry of Economic Affairs (MinEZ, 2008; p. 89).

The simplified process scheme is depicted in Figure 2-6.

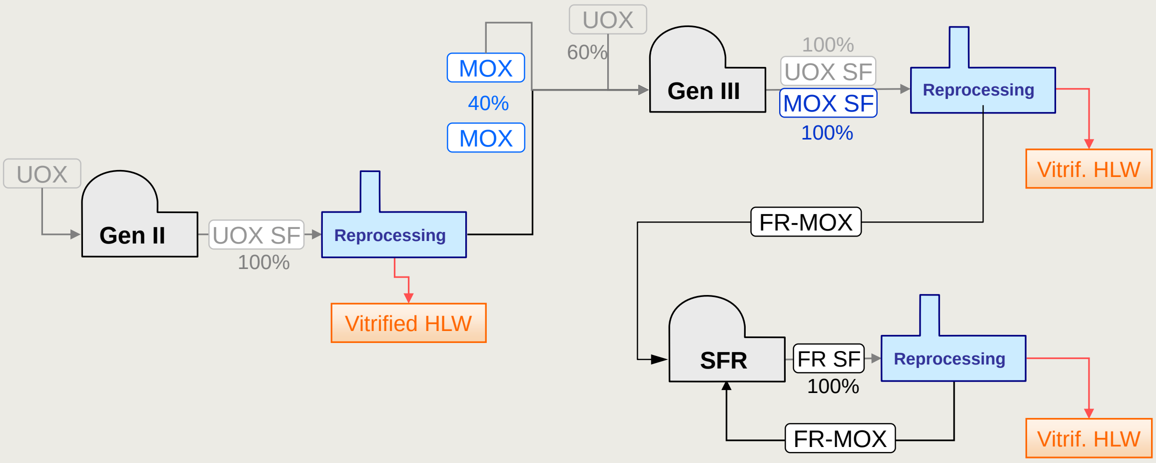


**Figure 2-6 Process scheme of Scenario 6 - Deployment of fast reactors**

### 2.7. Scenario 7 - Deployment of thorium-based reactors.

An alternative future nuclear cycle may partially utilize thorium-based fuels. Thorium has been considered as an alternative to the uranium-based fuel since the beginning of nuclear industry. This was initially based on considerations of resource utilization (thorium is approximately three times more abundant than uranium), and more recently as a result of concerns about proliferation and waste management, since the thorium fuel cycle promises reduced production of plutonium and higher actinides, improved physical and nuclear properties for reactor and potential waste management applications (IAEA, 2005; p.1). Thorium can be used both in once-through and recycle options, and in thermal and fast spectrum systems. Since there are no naturally-occurring thorium isotopes that can fission under reactor conditions, thorium is only useful as a resource for breeding new fissile materials.

Thorium (Th-232) is the fertile material that can be used to produce the fissile isotope uranium-233 (U-233) in a reactor, which in turn could be used as fissile material in fuel for nuclear reactors. Uranium-233 is an isotope of uranium with very favorable neutronic properties, as an alternative option for fuel for a thermal reactor. Reasons for considering the introduction of a thorium-based fuel cycle include (Todosow, 2010; p.1892):

a) Increasing fissile resources by breeding U-233 from thorium,
b) Improving fissile fuel utilization in thermal reactors,
c) Significantly reducing U-235 enrichment requirements,
d) Decreasing production of Pu and other transuranic (TRU) elements compared to uranium fuel cycle,
e) Taking advantage of the improved neutronic and physical properties of thorium-based fuel (e.g., higher thermal conductivity, melting point).

The thorium based fuel cycles are particularly attractive for countries which have significant thorium deposits and small, or no uranium reserves. However, there are significant proliferation risks associated with U-233 (which is a weapons usable isotope similar to Pu-239) which must be addressed in any implementation scenario.

The feasibility of the thorium based fuel cycle has already been demonstrated for high temperature gas cooled reactors (HTGR), light water reactors (LWR), pressurized heavy water reactors (PHWR), liquid metal cooled fast breeder reactors (LMFBR), and molten salt breeder reactors (MSBR) as documented in several extensive publications published by the International Atomic Energy Agency (e.g. IAEA, 2005).

The difference of fissile material compared to the uranium fuel cycle results in different types of waste, including a different spectrum of HLW-fission products, which may impact the long-term safety (Bultman, 1996; p. 11). Since the thorium-based fuel cycle is still under development and its implementation may start only several decades from now, it is assumed that the transition from the present situation to a thorium-based fuel cycle will be managed by the deployment of LWR Gen III reactors.

The fuel cycle is depicted schematically in Figure 2-7. In accordance with the present status in the Netherlands, 100% of the current LWR Gen II Borssele reactor is fuelled with UOX fuel. After having been irradiated, the LWR Gen II UOX spent fuel is reprocessed and the remaining HLW is disposed into a geological disposal facility taking into account a sufficient cooling time. The reprocessed material is partially converted to MOX fuel for the LWR Gen-III reactors.

The LWR Gen III reactors utilize UOX/MOX fuel. Spent UOX fuel is reprocessed and the resulting material is converted to MOX, which is fed back into the LWR Gen III reactors. The vitrified HLW will be stored until 2130. Spent MOX fuel from the LWR Gen III reactors is also reprocessed, leaving the HLW as waste to be stored on surface until 2130.

The assumed thorium cycle is taken from the ideas put forward in a paper by Todosow (2010; Section IIIC)) in which PWR are initially loaded with the TRU-Th fuel. For subsequent cycles, the discharged spent fuel is cooled for several years, the uranium, neptunium and plutonium are separated, and then cooled for an additional 2 years. The charge fuel for the next cycle consists of this fuel with any needed makeup required to achieve an 18-month cycle from PWR discharged fuel. The remaining vitrified HLW is stored on surface until 2130.

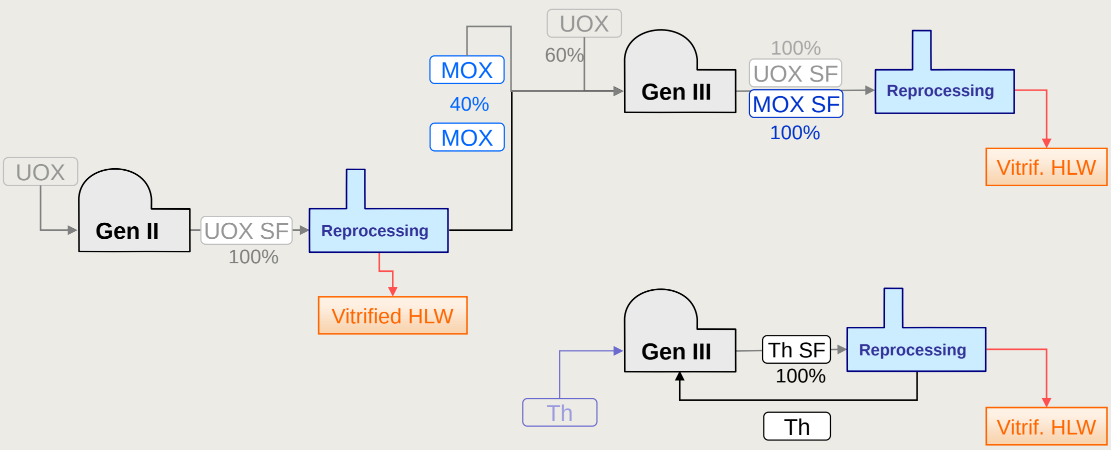


**Figure 2-7 Process scheme of Scenario 7 - Deployment of thorium-based reactors**

It has to be noted that the DANESS has been set up as a uranium fuel cycle analysis tool. In order to apply DANESS to a thorium fuel cycle the code would need significant modifications, e.g. including the thorium mining, conversion, enrichment steps in the fuel cycle, provisions to properly model thorium reprocessing steps, and adding other thorium-specific features (resources, price, etc.). For those reasons, the results of the presently assessed thorium fuel cycle can only be regarded as indicative.

# 3. Mapping of inventory to safety and performance indicator

The outcome of a Safety Case for deep geological disposal is in first instance valid only for the considered inventory/waste forms. Whenever the inventory or its chemical composition change, for example by adopting other nuclear strategies, one need to reassess the effects on the back-end of the fuel cycle, including the relevant safety functions applicable for deep geological disposal. Aspects that need to be considered are e.g.:

- thermal load of the waste
- chemical composition of the waste
- packaging of the waste/necessary adaptation of the disposal concept
- volume of the waste/necessary surface area of the disposal facility

An altered radionuclide inventory influences the outcome of the safety assessment calculations quantitatively. The outcomes of the OPERA safety assessment are expressed in a set of so-called '*safety and performance indicators*' as proposed in (Rosca-Bocancea, 2013; Schröder, 2013). The safety and performance indicators are computed for each (future evolution) scenario considered (Grupa, 2013) and therefore the entities of interest. A selection of indicators to be considered will be discussed in the next section.

An important prerequisite for mapping of the outcome is that the applied PA-model is based on a collection of equations that are linearly related to the source term. This is the case when diffusion and advective transport is described by linear sorption ('$K_d$ approach'), and the biospheric exposure is described by a (constant) dose conversion factor. This approach is followed in e.g. (Schröder, 2009; Schröder, 2009a). An increase of the inventory of a certain radionuclide will then result in a proportional increase of the indicators' values for that particular radionuclide.

Currently it is unknown[2] how the final PA model, being developed in OPERA task 7.2.4, will look like. Section 3.2 gives a short discussion of relevant determinants and features that need to be considered from the current point of view is given. Section 3.3 outlines a general approach on how and under which conditions the DANESS outcome can be mapped to the Safety Indicators provided in (Rosca-Bocancea, 2013; Schröder, 2013).

Furthermore, Section 3.4 reassesses a performance indicator developed by NRG as part of the EU-FP-7 project PAMINA (Schröder, 2009). That indicator was judged to provide meaningful additional information concerning the travel time of radionuclides through the Boom Clay, and is in principal capable to be mapped against different inventories. It will be discussed whether the proposed indicator has an added value, and if so, whether this indicator can be refined for the particular purpose of this study.

[2] An update will be provided at a later stage (M1.1.2.1), when the outline of the PA-model is set.

## 3.1. Considered safety and performance indicators

The set of safety and performance indicators proposed in (Rosca-Bocancea, 2013; Table 5-1, p.26) is summarized in Table 3-1:

**Table 3-1 Safety and performance indicators recommended for OPERA**

| | |
|---|---|
| **Safety Indicators** | |
| Effective dose rate | + |
| Radiotoxicity concentration in biosphere water | + |
| Radiotoxicity flux from geosphere | + |
| Power density in the groundwater | o |
| **Performance Indicators** | |
| Radiotoxicity in compartments | + |
| Radiotoxicity flux from compartments | + |
| Time-integrated radiotoxicity flux from compartments | + |
| Radiotoxicity concentration in compartment water | + |
| Transport time through compartments | + |
| Host rock retention factor | + |
| Contribution of each safety function | + |
| **Performance indicators based on safety functions[3]** | |
| Containment (*C-RT*): | + |
| Limitation of release (*R1-RT*): | + |
| Retardation due to migration through buffer and host formation (*R3-RT*) | + |
| Retardation due to migration through geosphere (*R4-RT*) | + |
| Performance of the integrated repository system (*PI-RT*) | + |
| Activity based indicators (*C*, *R1*, *R3*, *R4*, *PI*) | 0 |

o = potential additional candidate parameter

Three groups of indicators are distinguished:

***Safety Indicators***
All four safety indicators in Table 3-1 are relevant quantities that can and should be calculated for altered waste inventories, because they provide essential information over the long-term safety.

***Performance Indicators***
These indicators provide additional information on compartment level. For the reasons discussed in the next section, it is not recommended to map this group of indicators against altered waste inventories without detailed analyses of the

[3] See also (Rosca-Bocancea, 2013; p.25):
- Containment (C-RT): radiotoxocity in waste package at time of overpack failure (T1)/ initial radiotoxocity in waste package (T0= time of disposal);
- Limitation of release (R1-RT): time-integrated (up to time t) radiotoxocity flux released from waste package/radiotoxocity in waste package at time of overpack failure (T1);
- Retardation due to migration through buffer and host formation (R3 - RT): time integrated radiotoxocity flux released from host formation/time-integrated (up to time t) radiotoxocity flux released from waste package;
- Retardation due to migration through geosphere (R4 - RT): time integrated radiotoxicity flux released to biosphere / time integrated radiotoxicity flux released from host formation
- Performance of the integrated repository system (PI-RT): time integrated radiotoxocity flux released from host formation / initial radiotoxocity in waste package (T0= time of disposal).

impact of the specific combination of radionuclide, compartment and indicator. Because the objective of the present project was to provide a simple, straightforward method, this group of indicators is not evaluated further, except for the indicator *Transport time through compartments*. That indicator has been developed in the PAMINA project and is judged to provide added value to the present set of safety indicators (Schröder, 2009).

***Performance indicators based on safety functions***
This group of indicators is already expressed relative to the inventory. Therefore no added value is expected of mapping these indicators against altered waste inventories. However, these indicators are expected to be of particular use in providing evidence that assumptions behind the mapping are reasonably covered (see Section 3.2).

The four safety indicators selected can be computed according to (Becker, 2013) for each individual radionuclides *n* by

*Effective dose rate [Sv/a]* = $c_n DCF_n$ *Equation 1*

*Radiotoxicity concentration in biosphere water [Sv/m³]* = $c_n e(50)_n$ *Equation 2*

*Radiotoxicity flux from geosphere [Sv/a]* = $s_n e(50)_n$ *Equation 3*

*Power density in ground water [MeV/s·m³]* = $c_n E_n$ *Equation 4*

With:

- $c_n$ the *activity concentration* [Bq/m³] of radionuclide *n* in the biosphere water or ground water
- $DCF_n$ the *biosphere dose conversion factor* in [(Sv/a)/(Bq/m³)]
- $e(50)_n$ the *ingestion dose coefficient* in [Sv per Bq intake]
- $s_n$ the *activity flux*[4] [Bq/a] of radionuclide *n* from the geosphere to the biosphere
- $E_n$ the decay energy [MeV/s] of a radionuclide *n*

The generic dose conversion factors $DCF_n$ will be deduced for OPERA within OPERA Task 6.3.1 '*Modelling approach for transport & uptake processes*'. The values for $e(50)_n$ can be found in (VROM, 2001; Appendix 4, Table 4.1)[5], and the $E_n$ value in (Kellett, 2009). All indicator values are provided for the individual radionuclides by OPERA performance assessment calculations (OPERA Task 7.2.4). The total value of the indicators can be derived by adding up the contributions of all individual radionuclides.

[4] Although strictly speaking *flux* is defined as the rate of *flow* of a property per unit area, we follow here the definitions as used in the literature on safety and performance indicators.
[5] Note there is currently no *e(50)*-value defined for Po-209 in (VROM, 2001) or the underlying ICRP reports.

## 3.2. Analysis of basic assumptions

***Dissolution behaviour of the waste***

In PAMINA, several exercises have been performed with generic, simplified representation of disposal concepts in Boom Clay, limited to vitrified high-level-waste. However, in the OPERA disposal concept (Verhoef, 2011a), also other waste sections than for HLW have to be assessed, each its own composition (Hart, 2014; Meeussen, 2014) and dissolution characteristics. The concerned indicators can be transformed section-wise as will be discussed in the next chapter. The contributions of all sections can then be summed up again in order to derive an indicator for the whole disposal concept.

However, uncertainty analysis on a generic disposal concept in clay (Schröder, 2009a) shows that the influence of the dissolution rate, varied between 100 and 10,000 years, was not significant for the resulting dose rate to the biosphere. In case that the dissolution behaviour of the different waste sections in the OPERA concept have minor impact on the overall outcome, the approach described in the next section can be applied directly. This statement can however only be properly judged when details on the final OPERA performance assessment (PA) model representations are known (OPERA Task 7.2.4).

Analysis of the indicator '*Contribution of each safety function*' (see Table 3-1) might be of help when deciding which approach should be used: if it appears that the safety functions '*Containment (C-RT)*' and '*Limitation of release (R1-RT)*' have ample influence on the overall safety of the disposal concept, one may consider to envisage the different waste sections as one. The indicator *Contribution of each safety function* than provides an estimation on how large the error of the chosen approach will be for each scenario, for each radionuclide and for each timestep. More support for such a simplification may be provided from uncertainty analyses (see Becker, 2013).

***Radionuclide transport behaviour***

In a radiological performance assessment (PA) the migration of radionuclides in the Boom Clay is often addressed by a '*$K_d$ approach*', resulting in a linear relation between risk and inventory. However, when looking more into detail, the underlying processes are more complex. The probably most relevant process to consider here is the precipitation of radionuclides, leading in the most ideal case to a constant concentration of radionuclides in solution, independent of the total inventory. Precipitation is usually expected to take place at rather high concentrations (>$10^{-9}$ mol/l; (SCK•CEN, 2002). The condition under which precipitation occurs, however, are complex, see e.g. (Berner, 1998; Grauer, 1997; Ganor, 1998; Temmam, 2000; Astilleros, 2002; Heberling, 2008; Lützenkirchen, 2009; Vercouter, 2009, De Cannière, 2010). Moreover, for a disposal concept in clay, where diffusion is the most relevant migration mechanism, the relevance of precipitation as protective mechanism might be rather limited for most radionuclides. As consequence, in simplified PA models, precipitation is not always accounted for.

***Representation of uncertainty***

It is the intention of OPERA to explicitly address uncertainties (Verhoef, 2011b), e.g. numerical uncertainty of applied parameters. Although in (Becker, 2013) different aspects of uncertainties are addressed in detail, it is currently still unclear how this aspect will be integrated in the final OPERA PA model (M7.2.4). In any case, one needs to weigh up the added value of depicting several uncertainty measures (e.g. 95-percentile & mean) against the increasing complexity of the graphical representation.

Next to the presentation of measures of uncertainty in the indicators outcomes, uncertainty calculation can be of use in evaluating the assumptions discussed in the previous paragraphs.

## 3.3. Transformation and mapping of safety indicators

If the outcome of a safety indicator $I_n$ can be assumed linearly related to the inventory $N_n$, for most of the radionuclides *n,* the indicator value $I_n(t)$ can be directly transformed by multiplying with the ratio of the new and original inventory for each radionuclide:

$$I_{n,\,new}(t) = I_{n,original}(t)\frac{N_{n,new}}{N_{n,original}} \qquad \text{Equation 5}$$

The above equation can be applied for the fission products without relevant daughter nuclides, but for actinides or other members of nuclide chains, such a simple approach cannot be used. In PAMINA, a simple algorithm is proposed to address this group of radionuclides (see Section 3.4 and (Schröder, 2009). However, the approach is judged too conservative for OPERA, in particular because of the large amounts of depleted uranium foreseen for geological disposal (Hart, 2014; Section 5.1.2; Verhoef, 2011a). Instead, indicator values should be transformed as function of time *t* by

$$I_{n,\,new}(t) = I_{n,original}(t)\frac{N_{n,new}(t)}{N_{n,original}(t)} \qquad \text{Equation 6}$$

and the inventory *N* of each radionuclide has to be calculated by adding up the contribution of all *m* mother nuclides:

$$N_n(t)\,[-] = \sum_{k=1}^{m} N_k(t) \qquad \text{Equation 7}$$

with

$$N_k(t)[-] = N_1(t_0)\left(\prod_{i=1}^{k-1} y_i\lambda_i\right)\sum_{j=1}^{k}\frac{e^{-\lambda_j t}}{\prod_{i=1,i\neq j}^{k}(\lambda_i-\lambda_j)} \qquad \text{Equation 8}$$

and

$\lambda_i$ the *decay constant* [1/s] of radionuclide *i*

$N_1(t_0)$ the number of atoms of the mother nuclide on $t_0$

$y_i$ the yield of radionuclide *i*

For $\lambda_i$ *and* $y_i$, values are provided in (Kellett, 2009). The initial inventory $N_1(t_0)$ can be found in (Hart, 2014), or is computed by DANESS for a number of nuclear energy scenarios considered (see Chapter 8).

## 3.4. Construction of the PAMINA indicator and potential refinements

***Indicator description***

One of the restrictions of the safety indicators discussed in the previous section is that it is not straightforward from which feature or characteristic of a radionuclide the indicators evolution and accompanying risk is affected. In the PAMINA study (Schröder, 2009), a new type of travel-time based indicator was proposed (Figure 3-1) that allows to visualize for each radionuclide three basic characteristics that are important to understand the overall migration behaviour in case a disposal concept in clay. These characteristics are:

- inventory in terms of radiotoxicity,
- half-life,
- retardation factor $R_f$ in the host rock.

Figure 3-1 shows an example radionuclide inventory [Sv] as function of the nuclide half-life (diamonds), with the presence of nuclide chains covered in a conservative manner. Here, the inventory of mother nuclides was added to their daughter nuclide, applying the following rules:

- if the mother nuclide has a longer half-life, equilibrium with the daughter nuclide is assumed and the activity of the mother is added to that of the daughter;
- in case the mother nuclide has a shorter halve-life, the mother activity is added to that of the daughter in molar amounts.

These additions are performed cumulative for all consecutive nuclides of the four nuclide chains; an example of the resulting effective inventory is given in Table 3-2. Note that due to the chosen scale, the long-living $^{238}U$ is not visible in Figure 3-1 ($4.5 \cdot 10^9$ a).

A second adjustment needs to be made to correct for short living daughter nuclides: when they are in equilibrium with the mother nuclides, they may appear at later times than would be expected due to their half-life. In case a mother nuclide contributes more than 10% to the radiotoxicity inventory of a shorter living daughter nuclide, the half-life of all were replaced by the half-life of their mother. Examples of original and adjusted inventories are summarized in Table 3-2.

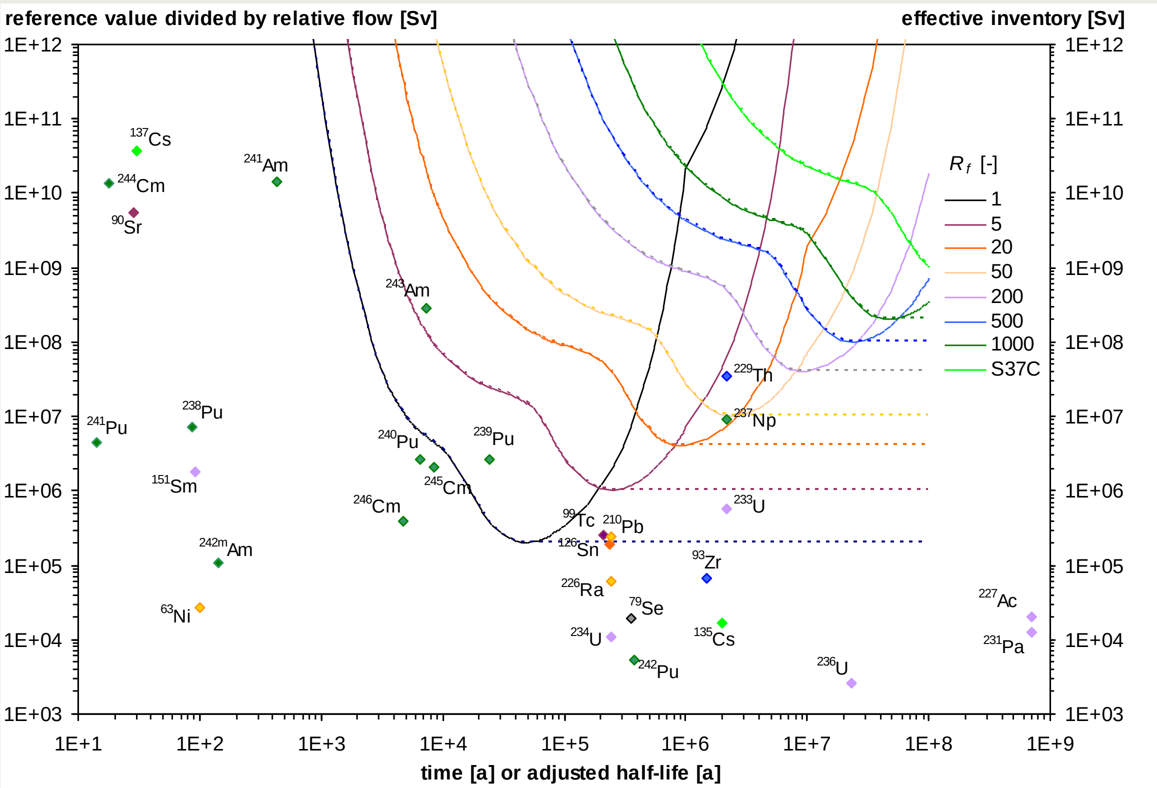


**Figure 3-1 Reference value divided by relative flow rate and radiotoxicity inventory as function of adjusted radionuclide half-life, example adapted from (Schröder, 2011)**

In Figure 3-1, also a group of lines is depicted, derived from calculated 'relative flow rates' of stable isotopes with different retardation factors $R_f$. The lines can be calculated for each scenario and are expressed in terms of a 'dilution' factor by dividing a reference value (here: the radiotoxicity flow into the geosphere) by the computed relative flow rates.

$I_n(t)\ [Sv] = \quad rv\ [Sv/a] \dfrac{X_{in}\ [mol]}{S(t)\ [mol/a]}$ *Equation 9*

with

*rv* the reference value;

$X_{in}$ the initial amount of a stable isotope; and

*S(t)* the flow rate of a stable isotope over the boundary of interest.

Likewise, one may use radiotoxicity concentrations or dose rates and divide these by the reference values for radiotoxicity or dose rate, respectively. In any case, the lines are expressed in Sv, and can be compared with the inventory, expressed in Sv, too[6].

Each curve can be envisaged as the initial inventory of a radionuclide equivalent to the chosen reference value, i.e. inventory values below the line will result in values below the reference value and vice versa. The dashed lines extend the minimum values of each of the curves horizontally in time to the right, to reflect the assumption that radionuclides with a half-life longer than the maximum travel time will leave the repository with the maximum relative flow rate.

**Table 3-2 Example of original and adjusted radionuclide half-lives and effective radionuclide inventory, adapted from (Schröder et al., 2009)**

| nuclide | half life [a] | adjusted half life [a] | Inventory [Sv] | effective inventory [Sv] |
|---|---|---|---|---|
| **Cm-248** | 3.4E+05 | 3.4E+05 | 9.2E-03 | 9.2E-03 |
| **Pu-244** | 8.0E+07 | 8.0E+07 | 1.5E-04 | 1.6E-04 |
| **Cm-244** | 1.8E+01 | 1.8E+01 | 4.6E+07 | 4.6E+07 |
| **Pu-240** | 6.6E+03 | 6.6E+03 | 3.9E+03 | 9.0E+03 |
| **U-236** | 2.3E+07 | 2.3E+07 | 1.5E+00 | 8.7E+00 |
| **Th-232** | 1.4E+10 | 1.4E+10 | 1.1E-05 | 7.0E-01 |
| **U-232** | 6.9E+01 | 1.4E+10 | 2.0E-01 | 2.7E-01 |

When both radionuclide inventories and the normalized breakthrough curves are depicted in one graph as in Figure 3-1, the inventory of individual radionuclides can be easily compared with the breakthrough curves belonging to a scenario. All nuclides below the black line ($R_f$=1, no retardation) will leave in any case the repository in flow rates below the chosen reference value. A number of radionuclides appear above the $R_f$=1-curve, but due to their strong sorption behaviour, large retardation factors are assumed for them[7]. However, as can be seen in Figure 3-1, in all but one case, already a moderate retardation ($R_f$ < 50) is sufficient to limit the emission out of the repository to values below the assumed reference value.

The described travel-time based indicator was judged by the authors to be useful in understanding the impact of radionuclide migration behaviour in the PAMINA project. Despite some shortcoming, it gives a simple visual overview on the overall inventory, and allows making rough visual estimations of the migration behaviour. In the next subsection it will be evaluated how the indicator can be applied for the purpose of this study, and what options exists to improve the indicator.

[6] the power density indicator can be depicted likewise, by presenting the inventory in this case in $MeV/s{\cdot}m^3$

[7] all inventory markers are color-coded according to their assumed retardation behaviour

***Indicator construction and potential refinements***

All four safety indicators considered in (Rosca-Bocancea, 2013) can be represented in the PAMINA indicator by proper transformation and application of the accompanying reference value. The following definitions can be made:

Effective dose rate (Edr):

$$I_{Edr}(t)[Sv] = \quad rv_{Edr}\,[Sv/a]\frac{X_{in}\,[mol]}{S(t)\,[mol/a]} \qquad \textit{Equation 10}$$

Radiotoxicity concentration in biosphere water (RtoxBw):

$$I_{RtoxBw}\,[Sv] = \quad rv_{RtoxBw}\,[Sv/m^3]\frac{X_{in}\,[mol]}{C(t)\,[mol/m^3]} \qquad \textit{Equation 11}$$

Radiotoxicity flux from geosphere (RtoxFG):

$$I_{RtoxFG}\,[Sv] = \quad rv_{RtoxFG}\,[Sv/a]\frac{X_{in}\,[mol]}{S(t)\,[mol/a]} \qquad \textit{Equation 12}$$

Power density in ground water (PdGw):

$$I_{PdGw}\,[MeV/s] = \quad rv_{PdGw}\,[MeV/s\cdot m^3]\frac{X_{in}\,[mol]}{C(t)\,[mol/m^3]} \qquad \textit{Equation 13}$$

with *C(t)* the concentration [mol/m$^3$] of a stable isotope in the biosphere water or ground water. With exception of the last indicator, all indicators are expressed in [Sv][8]. The time dependent concentrations and fluxes can be computed as part of the OPERA PA calculations, using the same model representations and parameterizations as for the safety assessments. The four reference values will be provided in OPERA Task 1.2.2 (project *ENGAGED*).

All discussions in the Section 2.1 on the linearity of safety indicators apply here, too. The graphical approach chosen in Figure 3-1 in principle allows it for this indicator to represent the influence of precipitation on the migration behaviour directly by plotting additional curves for different assumed equilibrium concentration, and from current point of view this should not add too much detail since it is expected that solubility limitation will be of relevance for only a small number of elements. This option will be addressed in a later stage of this project, when the final conceptual design of the OPERA PA model is available.

With respect to the handling of nuclide chains, it is recommend for the purpose of this study not to use the simplified approach followed in PAMINA, but instead to use the approach as discussed in the previous section and summarized in Equation 6 to Equation 8, which can be applied to the present indicator, too.

One particular point of discussion for the PAMINA contribution was whether to represent the inventory as a single point, or as function of time. Figure 3-2 gives an example in which for one nuclide, $^{90}$Sr, the exact evolution of the inventory is given as function of time (red line) and as single point (red diamond). Although the line gives precise

[8] although also for the last indicator a transformation into [Sv] is possible in principle, this is not recommended

information on the decay of the radionuclides in time, it is quite obvious that depicting lines for all individual radionuclides (68 radionuclides are considered in (Hart, 2014)) will make the graph rather complicated. The general decay behaviour on log-log scale is visually the same for all nuclides not part of a nuclide chain, which favours the use of single points as in PAMINA.

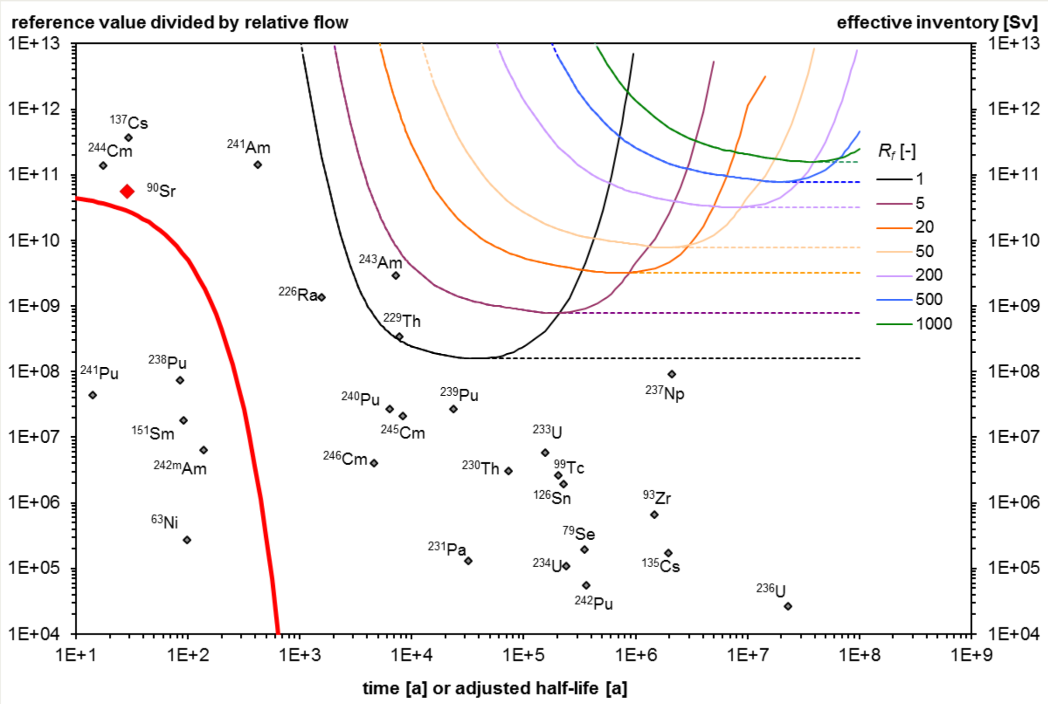


**Figure 3-2 Reference value divided by relative flow rate and radiotoxicity inventory as function of adjusted radionuclide half-life, example adapted from (Schröder, 2011)**

Equation 6 to Equation 8 can be applied to evaluate the simplified approach for addressing decay chains as described in the previous section, making use of the actual OPERA reference inventory (Hart, 2014) or the scenarios analysed with DANESS (Chapter 8). Figure 3-3 shows selected radionuclide evolutions based on Equation 6 to Equation 8 as example. From the selected radionuclides depicted, it is evident that this kind of representation gives a much more detailed representation than the simplified approach followed in PAMINA. It has to be evaluated in a next step, whether a combination of both approaches can be followed, e.g. by depicting radionuclides of clearly no relevance as single points, and the more relevant radionuclides and member of decay chains as lines.

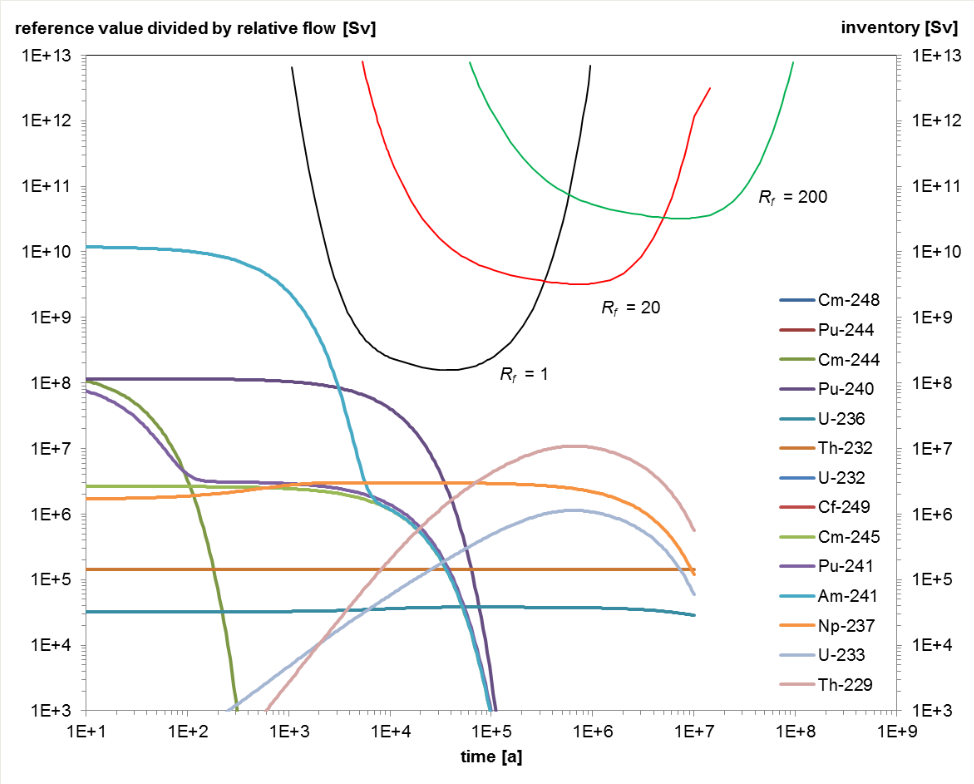


**Figure 3-3 Reference value divided by relative flow rate and radiotoxicity inventory of selected radionuclides as function time**

### *3.5. Conclusions*

The investigation of the possibility to construct an indicator that easily allows comparing different nuclear energy usage scenarios resulted in two sets of indicators:

- safety indicators,
- modified, travel-time-based indicators based on safety indicators.

Both sets of indicators have been discussed, and calculation methods for their construction have been described. For the modified, travel-time-based indicator introduced in PAMINA, refinements have been discussed that allow complex nuclide chains to be presented in a more sensible way.

Basic consideration for the applicability of the indicators is whether the indicators are sufficiently linear related to the inventories. A number of potential processes have briefly been discussed, and methods to verify this have been suggested. Furthermore, a method to integrate radionuclide chains has been described.

# 4. Computer tool - DANESS

For the assessment of the nuclear fuel cycle strategies, the DANESS code ("Dynamic Analysis of Nuclear Energy System Strategies") version 4.0 (Van den Durpel et al., 2008) has been applied to simulate the flows of fissile material, fresh fuel, spent fuel, high level waste as well as all intermediate stocks and fuel cycle facility throughput.

DANESS is based on a system dynamics model, using the iThink-software (Isee Systems, 2009), allowing to simulate the dynamic behaviour of systems including multiple components and to simulate and investigate the dynamic interdependence of these components interacting between each other via feedback loops. System dynamics software also provides a transparent way of communicating the set-up of models and the outcome of the simulations.

DANESS allows to simulate time-varying nuclear energy systems from cradle-to-grave and to support nuclear energy assessment processes from a technological, economic and environmental perspective. DANESS evaluates quantities like mass flows and costs as a function of time, typically spanning time-periods of coming decades or century. Both resources and waste quantities development are being determined, for any modelled combination of reactor systems and fuel cycles.

New reactors are introduced based on the requirement to cover the nuclear energy demand and on the economic and technological ability to build new reactors. The timeline of technological development of reactors and fuel cycle facilities is modelled to simulate delays in the availability of new technologies by means of technological readiness levels (TRL) determined for the different reactor and facility types. Levelized fuel cycle costs are calculated for each nuclear fuel batch for each type of reactor over time and are combined with capital cost models to arrive at energy generation costs per reactor and, by aggregation, into a cost of energy for the whole nuclear energy system. It is clear that such modelling does demand significant amounts of reactor and fuel cycle facility specifications (i.e. technical, economic and environmental attributes). These specifications are discussed in more detail in Section 5.

The architecture of the DANESS v4.0 code is depicted schematically in Figure 4-1, whereas Figure 4-2 shows the fuel cycle model as implemented in the code. A more detailed description of DANESS v4.0 can be found is provided by Van den Durpel et al. (2008). A variety of benchmark and verification activities have been undertaken with DANESS within various international projects, e.g. the IAEA-INPRO project (IAEA, 2008) and PUMA (Kuijper, 2010). Additional benchmarking activities are reported in Van Den Durpel (2008).

The most recent version of *DANESS* allows tracking of waste flows on radionuclide level, by means of a 'Fuel Isotopic Evolution Module'. That module enables the user to estimate nuclide specific stocks at different steps in the fuel cycle and for different types of nuclear power reactors.

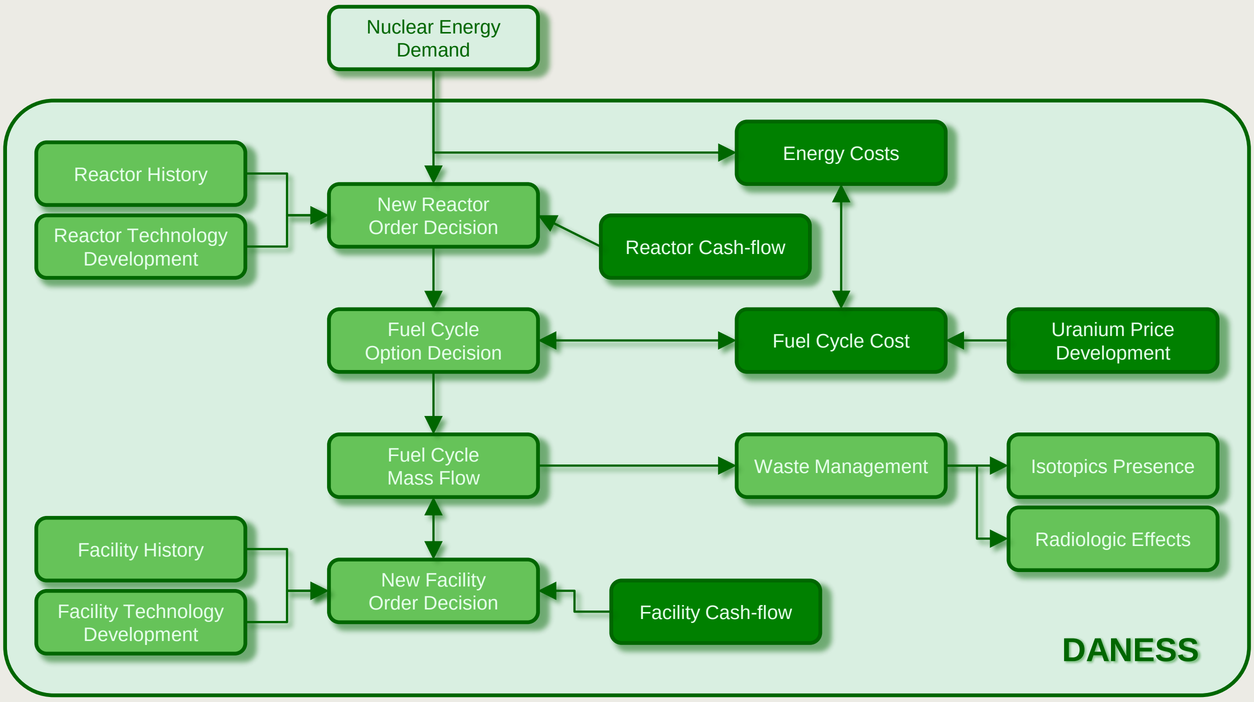


**Figure 4-1 Architecture of the DANESS model**

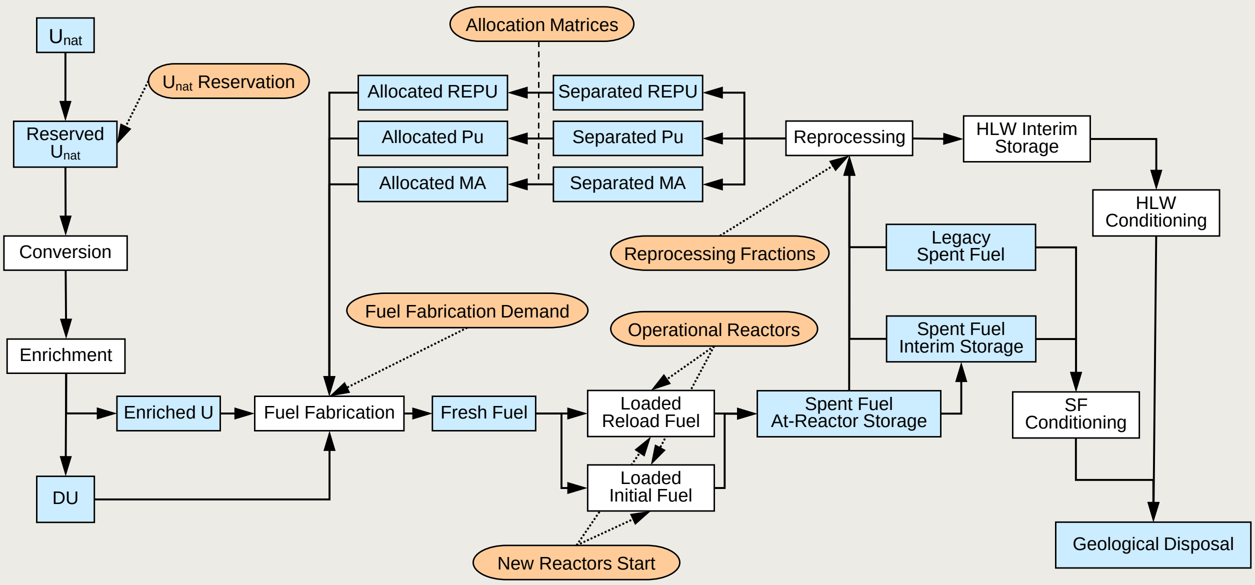


**Figure 4-2 Fuel cycle model of the DANESS program**

# 5. Scenario Assumptions and Technology Characteristics

For the quantitative analysis of future nuclear deployment strategies utilizing the DANESS program, a variety of assumptions apply to future trends and technology characteristics of the nuclear fuel cycle and fuel cycle facilities. A summary of the technology characteristics and related assumptions is provided in the sections below. An overview of the considered fuel cycle scenarios is provided in Chapter 2.

## *5.1.General assumptions*

The fuel cycle assessments are performed in an intra-nuclear mode without considering full energy market competition (e.g. fossil fuels, renewables, import, etc.). The different scenarios are based on a given nuclear energy demand, the existing nuclear reactor (Borssele) and its foreseen phase-out, the introduction of Gen-III and Gen-IV reactors, various fuel cycles, and unlimited fuel cycle facility capacity. This last assumption is justified considering the relatively small nuclear program in the Netherlands compared to other European countries.

The following assumptions have been made for the analyses of the considered scenarios.

- The time horizon of the analyses is 2130, which at present is the foreseen start of the final disposal of the radioactive waste in the Netherlands;
- The current Gen II reactor, i.e. the Borssele NPP, may be replaced by Gen III Light Water Reactor(s) (LWRs), wich are immediately available. The High Temperature gas-cooled Reactors (HTRs) are assumed to be available around 2020, whereas the Fast Reactors (FRs) will be commercially available after 2040. The FRs operate as breeder to ensure minimal uranium use, and minimise waste;
- For a future thorium fuel cycle, available around 2040, it is assumed that thorium is utilized in a pressurized water reactor (PWR);
- Uranium or thorium resources pose no limit to the deployment of new nuclear reactors in the Netherlands.

The next paragraphs provide additional details of the different data types and assumptions that have been implemented in the DANESS model.

## *5.2.Nuclear energy demand*

An important boundary condition of the integrated dynamic modelling of nuclear fuel cycles is the future nuclear energy demand. Nuclear energy demand scenarios are given as input to the DANESS-model. Starting from the existing reactor park the DANESS-model aims to match this demand by generating energy with a mix of nuclear reactors. The reactor types and their nuclear fuels are selected by the code user.

In the present analyses the future nuclear energy demand in the Netherlands is based on the ideas laid down in recently published reports from the Netherlands Energy Research Foundation ECN (Seebregts, 2010, 2011), which have been prepared for the Dutch Ministries of Economic Affairs (EZ) and of the Environment (VROM). They present facts and figures on new nuclear energy in the Netherlands in the period after 2020. Their content was intended to support a stakeholder discussion process on the role of new nuclear power in the transition to a sustainable energy supply for the Netherlands.

The set of senarios considered in the ECN reports are a practical interpretation of the scenarios put forward in the ‘Energierapport 2008’ (MinEZ, 2008; p.88). The timelines of these scenarios is up to 2040, the so-called “Target year” (“Zichtjaar”) (Seebregts, 2010; p.42). Of the scenario’s considered in the ECN reports, Scenario 3: *New nuclear power* *plants shortly after 2020* (2000 to 5000 MWe, Generation 3) leads to the highgest deployment of new nuclear reactors (Seebregts, 2010; p.19).

Based on the above-mentioned considerations, for the growth scenarios, viz. in the cases of newly deployed reactors the nuclear energy demand in the present analyses has been implemented as follows:

- From 2015 on, the nuclear energy demand increases linearly from the present value to a value of 5000 MWe, corresponding to approximately five to six 900 MWe reactors, or about 28 180 MWe reactors (i.e. HTRs);
- From 2040 on, the nuclear energy demand remains constant throughout the simulated time frame, i.e. up to 2130.

The nuclear energy demand curve in terms of TWhe/yr is depicted in Figure 5-1.

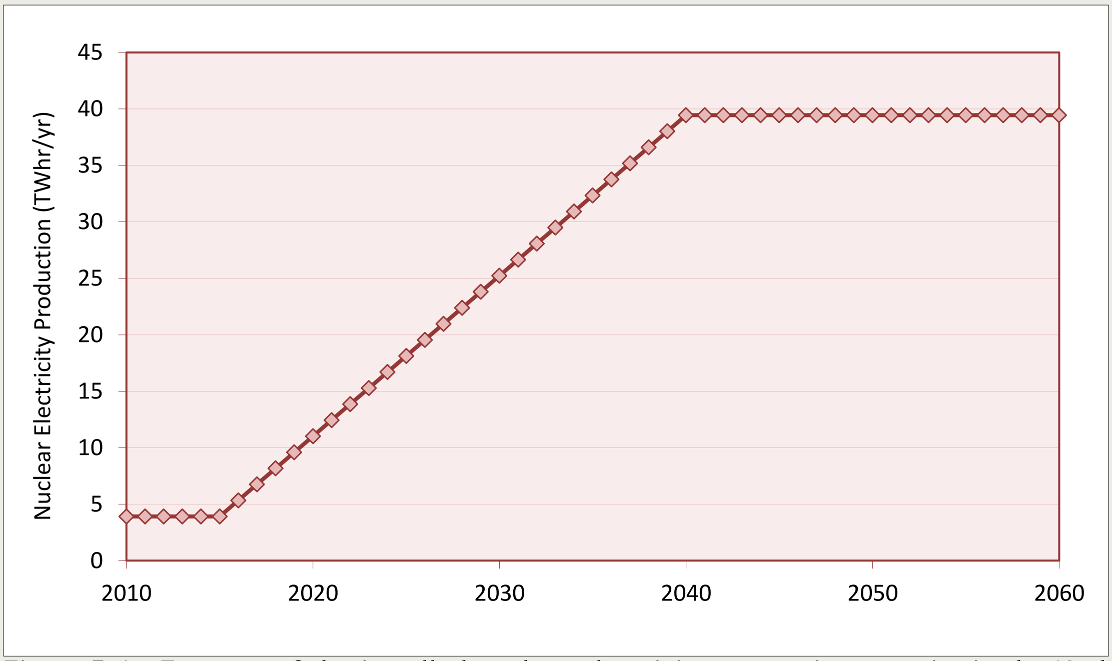


**Figure 5-1 Forecast of the installed nuclear electricity generating capacity in the Netherlands for the adopted growth scenario**

## *5.3. Reactor types*

In the present analyses, it is assumed that several types of new reactors may be utilized for electricity production, viz. Gen-III LWRs, and Gen-IV reactors taking into account the introduction dates, viz. the Sodium Fast Reactor (SFR), and the high temperature reactor (HTR) respectively. Specific reactor characteristics and features of these two reactor types are discussed in the following paragraphs.

### 5.3.1. Gen II LWR – Borssele reactor

The main features of the Borssele reactor have been taken from the PRIS database (IAEA, 2012), and are listed in Table 5-1.

**Table 5-1 Main features of the Borssele reactor**

| Feature | Value |
|---|---|
| **Thermal Power** | 1366 MW |
| **Electric Power** | 482 MW |
| **Net Efficiency** | 35,3% |
| **Primary Loops** | 4 |
| **Availability** | 92,6% |
| **Plant Design Lifetime** | Close-down in 2033 |

### 5.3.2. Gen III LWR

In the present study the characteristics of the adopted LWR are less relevant than the characteristics of the fuels, more specifically the spent fuels and vitrified waste residues. For that reason a generic type Gen III PWR has been modelled for which the characteristics have been obtained from the relevant documentation of the EU FP6 project RED-IMPACT (González Romero, 2005; Chapter 2, Annex 1). These reactor characteristics have been implemented and utilized in a previous study analyzing several of the RED-IMPACT scenarios with the DANESS code (Hart, 2009).

In the analyzed RED-IMPACT scenarios the generic Gen III LWR was supposed to be fuelled with both UOX and/or MOX type fuels (González Romero, 2005; Chapter 2, Annex 1). In the present analyses the generic Gen III LWR may also be fuelled with thorium-based fuel, in analogy with a study performed by Todosow (2010).

Main features of the Gen III LWR are listed in Table 5-2.

**Table 5-2 Main features of the Gen III LWR**

| Feature | Value |
|---|---|
| **Thermal Power** | 2700 MW |
| **Electric Power** | 900 MW |
| **Net Efficiency** | 33% |
| **Primary Loops** | 4 |
| **Availability** | 90% |
| **Plant Design Lifetime** | 60 years |

### 5.3.3. Sodium Fast Reactor (SFR)

The Sodium-cooled Fast Reactor (SFR) is one of the six selected nuclear systems within the Generation IV International Forum (GIF, 2011; p.23). This reactor uses liquid sodium instead of water as a coolant. An important characteristic of this reactor type is the possibility to breed plutonium and burn (minor) actinides and fission products which together determine the waste characteristics. Experimental and demonstration SFRs have been and are operating all around the world. However, within the context of Gen IV, the sodium cooled reactor should improve mainly in safety and economics. For the Generation IV SFR no licensing efforts have been made yet.

The SFR uses liquid sodium as reactor coolant, allowing high power density with low coolant volume fraction. Sodium reacts chemically with air and water and therefore requires a sealed coolant system. At the same time, an oxygen-free environment prevents corrosion.

The current study considers the pool type SFR design. In the fuel cycle assessment reported here, the fuel and burn-up characteristics of the SFR are assumed to be similar to the SFR assumed for the RED-IMPACT scenario B1 (González Romero, 2005; Chapter 2, Annex 1), except for the rated power. Axial and radial blankets and their fuels, which have different characteristics compared to the fissil part, have not been modelled in the present analyses, since they comprise only about 8% of the total fuel inventory.

Figure 5-2 shows an overview of the system whereas Table 5-3 summarizes the main characteristics of the SFR.

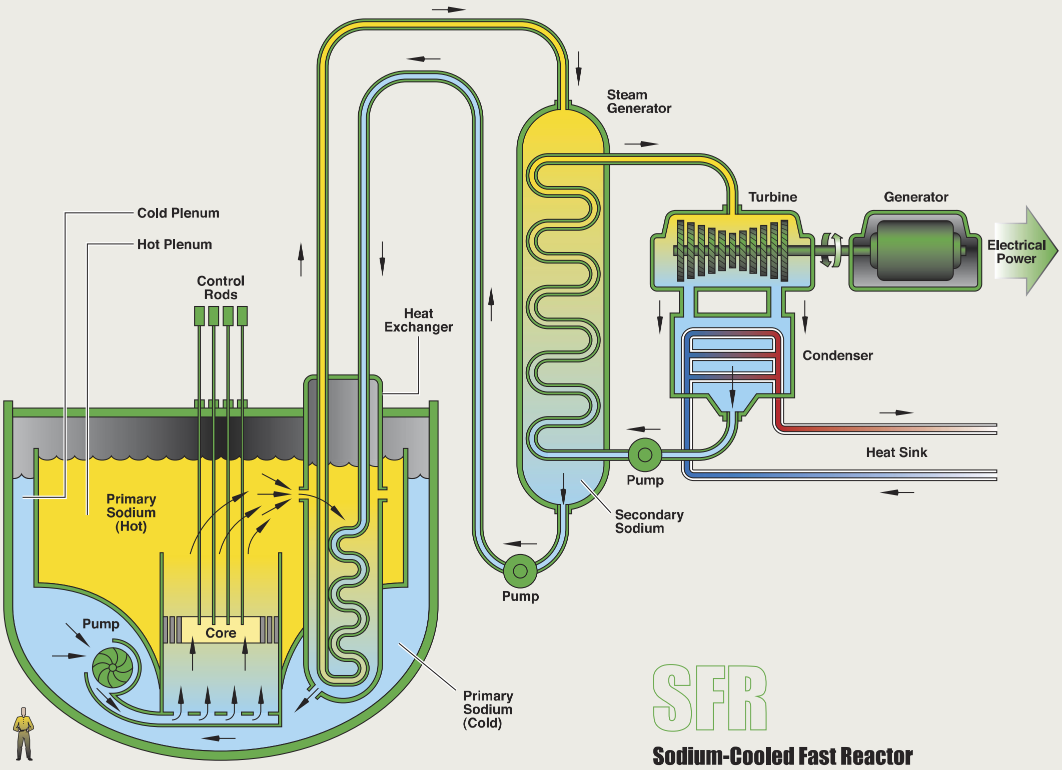


**Figure 5-2 Overview of the Sodium-cooled Fast Reactor**

**Table 5-3 Main characteristics of the SFR**

| Feature | Value |
|---|---|
| **Thermal Power** | 2250 MW |
| **Electric Power** | 900 MW |
| **Net Efficiency** | 40% |
| **Primary Loops** | 3 |
| **Availability** | 90% |
| **Plant Design Lifetime** | 60 years |

### 5.3.4. HTR

The High Temperature Reactor (HTR) is one of the six selected nuclear systems within the Generation IV International Forum (GIF, 2010; p.17). This reactor type, which is also indicated as Very High Temperature Reactor (VHTR) in the GIF documentation, uses helium gas instead of water as a coolant, and the moderator function is taken by carbon in the form of graphite. An important feature of this reactor type is the high coolant temperature and therefore high electric efficiency. This also brings a high suitability for coupled cogeneration. On the other hand, the existing operational experience is limited compared to water-cooled reactor designs.

Although many designs of high temperature reactors have been conceived, for the present assessment the HTR-PM was selected (Zhang, 2009). That reactor design is based on the modular pebble bed reactor of German origin, as this is the only design with both successful experience from the past, a currently operating test reactor (the Chinese HTR-10), and construction activity going-on.

The pebble fuel element was developed in Germany from the 1960s as an alternative to the traditional pellet-with-cladding fuel element, able to reach significantly higher temperatures by replacing the welded metallic cladding of LWR fuels by ceramic coatings. The fuel element is a tennisball-sized graphite sphere containing about 10’000 coated $UO_2$ fuel kernels, as shown in Figure 5-4 (IAEA, 2010; p.35). The fuel elements are randomly stacked together in a cylindrical cavity to form the reactor core. The core is surrounded by graphite a reflector of about 1 meter thickness, with openings for the control rods.

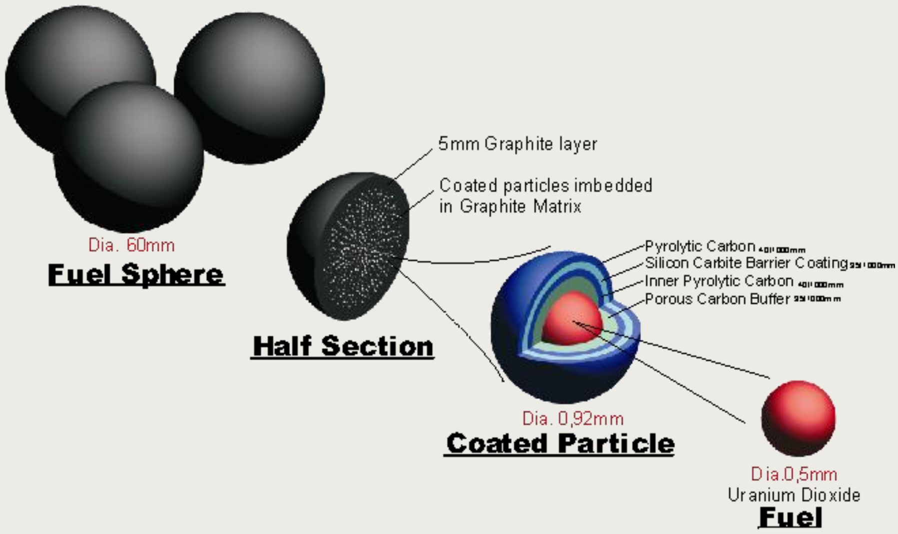


**Figure 5-3 Spherical fuel element**

During operation, the fuel pebbles are loaded and unloaded continuously. Pebbles removed from the bottom are led to a burnup measuring device by an automated pneumatic transfer system. Depending on the outcome of the burnup measurement the pebble is redirected towards the core for further use or designated as used and transported to a transport container for used fuel.

In the present analyses, the HTR-PM concept has been modelled in DANESS. The HTR-PM combines two reactor modules on one turbine-generator unit and utilizes an alternative steam generator design, see Figure 5-4 (Zhang, 2007; p.40).

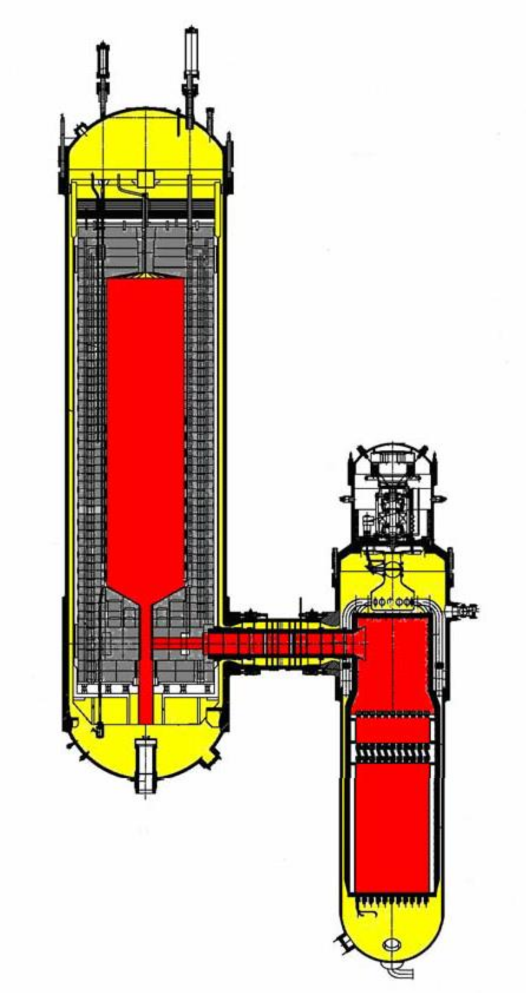

Figure 5-4 View of the HTR-PM

The main characteristics of the HTR-PM are tabulated below.

Table 5-4 Main charactistics of the HTR-PM

| Feature | Value |
|---|---|
| **Thermal Power** | 2x200MW |
| **Electric Power** | 180 MW |
| **Net Efficiency** | 45% |
| **Primary Loops** | 2x1 |
| **Availability** | 90% |
| **Plant Design Lifetime** | 40 years |

### 5.3.5. Thorium reactor – PWR

The assumptions for the present DANESS analyses are based on the ideas put forward by Todosow (2010) regarding the use of thorium based fuel in PWRs. In that study analyses were performed assuming that generic Gen III LWR reactors may be fuelled with thorium-based fuel.

The characteristics of the PWR are summarized in Table 5-5. For the present analysis, the actual design of the reactor is less relevant, therefore the characteristics are assumed the same as for Gen III LWRs (cf. Section 5.3.2). Only the applied thorium fuel composition and the spent fuel/HLW characteristics are important since they determine the isotopic composition of the material to be disposed in a deep geological repository. These characteristics are elaborated in Section 7.2.

**Table 5-5 Main features of the thorium PWR**

| Feature | Value |
|---|---|
| **Thermal Power** | 2700 MW |
| **Electric Power** | 900 MW |
| **Net Efficiency** | 33% |
| **Primary Loops** | 4 |
| **Availability** | 90% |
| **Plant Design Lifetime** | 60 years |

## *5.4. Fuel cycle facilities*

The fuel cycle facilities that have been implemented in DANESS comprise all relevant steps in the nuclear uranium fuel cycle, such as mining, enrichment, fuel fabrication, reprocessing, storage, conditioning and disposal (see also Figure 4-2). In the present DANESS code, no provisions have yet been implemented to properly model all these steps for the thorium fuel cycle. In the present assessment this aspect has been by-passed by assuming unlimited fuel cycle capacities and fuel resources. This assumption is justified considering the relatively limited nuclear infrastructure in the Netherlands.

## *5.5. Fissile material*

The front-end of the fuel cycle comprises the mining and milling of uranium, the conversion, enrichment and the fuel fabrication of UOX, MOX or Fast Reactor MOX fuel, as well as thorium fuel. The present study assumes an unlimited supply of the different nuclear fuel types considered, which is justified considering the relatively small nuclear infrastructure in the Netherlands.

# 6. Back-end of the Fuel Cycle

After the unloading of spent fuel from a reactor the spent fuel assemblies are stored in spent fuel storage pools for a certain time-period, usually several years. After a sufficient cool-down period, and depending on the available interim storage capacity and reprocessing capacity, the spent fuel will be transferred to the reprocessing plants or a so-called interim spent fuel storage facility.

In the reprocessing step, irradiated uranium, plutonium and, if applicable, minor actinides (MA), will be separated from the fission products based on the characteristics for different reprocessing technologies. The loss fractions for these actinides together with the fission products are vitrified and poured into steel canisters. This vitrified High Level Waste (HLW) is then sent to the 'HLW Interim Storage' stock before it is conditioned for geological disposal. The cooling time for HLW in the interim storage can take several decades.

In case the spent fuel is not reprocessed, the spent fuel elements are stored in the spent fuel pools for several decades. After that period the spent fuel is conditioned before it is transferred to a deep geological disposal facility.

The subsequent fuel cycle facilities are summarily discussed in the following sections, whereas the technology parameters that are representative for the fuel cycle facilities and storage and disposal facilities, and that have been input into the DANESS program are summarized in Chapter 7.

## *6.1.Reprocessing plants*

In several of the nuclear fuel cycles described in Chapter 2 spent fuel is assumed to be reprocessed. The conventional reprocessing of spent fuel allows for the separation of uranium and plutonium from the fission products in the case of LWR spent UOX fuel. The plutonium is separated by reprocessing irradiated $UO_2$ fuel using an aqueous partitioning system. Recovered plutonium is then mixed with depleted uranium to prepare conventional MOX fuel that can be applied in Gen II and Gen III LWRs. In the conventional reprocessing route the MA (Minor Actinides) and FP (Fission Products) are vitrified and, after a necessary period of several decades to cool down, disposed in a geological disposal facility.

In addition to the conventional reprocessing, where only plutonium is re-used for the manufacturing of MOX, in the scenarios utilizing Fast Reactors also an advanced reprocessing technology is considered. In addition to plutonium, also the MA are separated after which these components are mixed with depleted uranium to form the Fast Reactor MOX fuel, FR-MOX. In principle this process can be repeated many times, although in an "equilibrium" situation a steady inflow of DepU in fresh FR-MOX will be necessary since during the irradiation in the Fast Reactor part of the fissile material is lost since it is converted to fission products. The fission products are subsequently separated from the Fast Reactor spent fuel, vitrified, and finally disposed as HLW.

The present analyses also assume the reprocessing of the spent thorium fuel after eight cycles in the reactor, in analogy of the assumptions made by Todosow (2010; Section III).

## 6.2. Storage and disposal

Irradiated spent fuel and HLW have to cool down for several years up to several decades before it can either be reprocessed or finally disposed into a geological disposal facility. In the present analyses two stages have been distinguished for the spent fuel and HLW:

- At reactor storage – it has been assumed that the irradiated spent fuel is stored in the spent fuel pools for five years before it can be reprocessed or transferred to the interim storage facility;
- Interim storage – spent fuel that is not reprocessed and HLW resulting from the reprocessing step needs to cool down further before it can be sent to a geological disposal facility.

For the present scenarios, the geological disposal itself is not modelled as a waste management option reflecting the policy of long-term storage of the waste forms in the Netherlands, i.e. up to 2130.

## 6.3. Waste Forms

Different types of radioactive waste forms will be managed and disposed of in geological repositories in each of the scenarios: collos loaded with UOX/MOX spent fuel assemblies (SFA) and Universal Canisters loaded with vitrified HLW (CSD-V) and remains of the compacted hulls and ends (CSD-C) from the different reprocessing operations. The technology parameters have been taken from the RED-IMPACT project (Von Lensa, 2007).

LWR-UOX Spent Fuel Assemblies

In the RED-IMPACT project it has been assumed that four PWR UOX spent fuel assemblies (SFA), if not reprocessed, will be loaded in each waste package, or collo. Before its irradiation in the reactor, the mass of initial heavy metal is about 459 kg per fuel assembly.

An example of an LWR-UOX SFA is shown in Figure 6-1 (from Von Lensa, 2007).

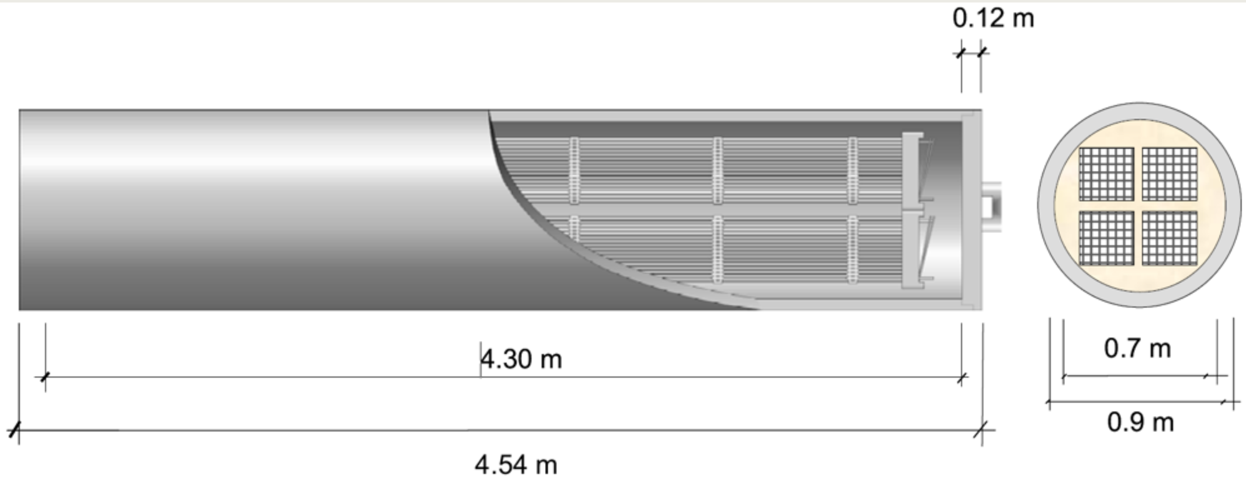


**Figure 6-1 Spent fuel assembly for spent UOX fuel**

LWR-MOX SFA

The main characteristics of the MOX spent fuel assemblies used in the cycle with mono-recycling of plutonium are similar to those of UOX spent fuel. The only difference with the UOX fuel, before its irradiation in the reactor, is the presence of an enhanced fraction of plutonium in the fresh fuel. The higher heat output from spent MOX fuel as compared to spent UOX fuel, caused primarily by the higher content of curium in spent MOX fuel, is the reason that only one MOX SFA is loaded per waste package, or collo. As a consequence, the amount of waste packages produced per TWh(e) is four times larger for MOX spent fuel than for UOX spent fuel.

An example of an LWR-MOX SFA is shown in Figure 6-2 (from Von Lensa, 2007).

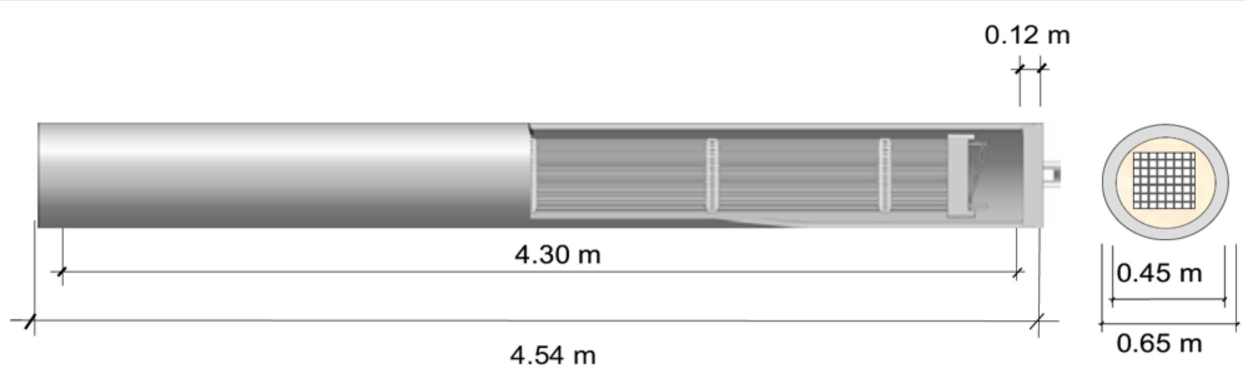


**Figure 6-2 Spent fuel assembly for spent MOX fuel**

HTR Spent Fuel Pebbles

For the final disposal in a geological repository, presently for the HTR spent fuel pebbles presently no dedicated container is foreseen. Two facilities to store spent HTR fuel in dry CASTOR (*cask for storage and transport of radioactive material*) type casks are being operated in Julich and Ahaus (IAEA, 1998; p.161). Figure 6-3 shows a dry storage facility partially filled with CASTOR casks[9]. A CASTOR cask, height 3.74 diameter 1,38 m (IAEA, 2010; p.174), can hold about 2030 HTR spent fuel pebbles (IAEA, 2010; p.210).

**Figure 6-3 Spent fuel storage in CASTOR casks**

LWR-HLW CSD-V

The main companies offering spent fuel reprocessing services in the world (BNFL and Areva) make use of a standard CSD-V vitrified wastes canister. A load of 40 kg of fission products plus actinides per CSD-V has been assumed in all cases where vitrified HLW is produced (Gonzalez, 2005; p.11). That amount of fission products results from the reprocessing of an equivalent amount of about 900 kg of initial heavy metal, depending on the burn-up (Von Lensa, 2007; Table 6.7).

[9] http://www.gns.de/language=en/4976/packaging-for-radioactive-materials (last accessed on 10 March 2014

**Figure 6-4 Universal canister for vitrified high level waste**

FR-HLW CSD-V

For the conditioning of high level waste generated by the reprocessing of spent FR-MOX fuel, also the standard CSD-V vitrified wastes canisters are applied. A load of 40 kg of fission products plus actinides per CSD-V has been assumed (Gonzalez, 2005; p.11).

Long lived ILW packages for final disposal – CSD-C

DANESS does not track the mass flows of low- and intermediate level waste. The new heat generating ILW consists of the compacted hulls and ends from the reprocessing process and are stored in CSD-C canisters, which have the same dimension as the CSD-V canisters. For the present analyses it has been assumed that the amount of CSD-C canisters equals twice the amount of the CSD-V canisters. The inventory of the radionuclides contained in a single CSD-C container has been obtained from COVRA, and is tabulated in the OPERA radionuclide inventory report (Hart, 2014; Table 4-11).

Depleted Uranium – DepU

Depleted uranium (DepU) originates from the uranium enrichment facility of URENCO (EL&I, 2011; p.22). The DepU is presently stored in DV-70 containers (volume 3,5 $m^3$). For the purpose of OPERA it is assumed that the DU of one DV-70 container will be immobilized in concrete (1:1) and finally disposed of in two KONRAD type II containers (volume 4,6 $m^3$ per KONRAD II container).

# 7. DANESS Input Tables

Based on the assumptions described in the previous chapters, the relevant technology data have been converted to parameter values needed as input for the DANESS code.

## *7.1.Nuclear power plants*

The characteristics of the nuclear power plants that are input in DANESS have been collected as part of several fuel cycle studies performed earlier:

- Characteristics of the Borssele NPP: Hart, 2008;
- Characteristics of the LWR Gen-III: González. 2005; Van Heek, 2012;
- Characteristics of the HTR: Van den Durpel, 2009;
- Characteristics of the SFR, sodium-cooled fast reactor: González. 2005; Van Heek, 2012;
- Characteristics of the thorium-fueled PWR: similar as LWR Gen III.

The data are summarized in Table 7-1. It should be noted that the cost factors are estimates and that they contribute in a relatively minor extent to the transition and NPP deployment schemes analysed in the present study.

**Table 7-1 NPP-type characteristics used in scenario analysis**

| | *Borssele NPP* | *LWR Gen III* | *HTR 180 UOX* | *FR Gen IV* | *Thorium PWR* |
|---|---|---|---|---|---|
| **Unit Power [MWe]** | 482 | 900 | 180 | 900 | 900 |
| **Thermal Efficiency [%]** | 35 | 33 | 45 | 40 | 33.3 |
| **Average Capacity Factor [%]** | 93 | 90 | 90 | 90 | 90 |
| **Licensing Time [yrs]** | 2 | 2 | 1 | 3 | 2 |
| **Construction Time [yrs]** | 4 | 4.75 | 3 | 6 | 4 |
| **Technical Lifetime [yrs]** | 20 | 60 | 40 | 60 | 60 |
| **Construction Cost [B€/unit]** | 1.00 | 4.2 | 0.25 | 5.25 | 2.4 |
| **OtherCapitalCost [B€/unit]** | 0.0 | 0.00 | 0.00 | 0.00 | 0.00 |
| **DecomCost [B€/unit]** | 0.50 | 1.4 | 0.12 | 1.74 | 0.8 |
| **Contingencies [B€/unit]** | 0.0 | 0.42 | 0.00 | 0.525 | 0.25 |
| **Variable O&M Cost [€/MWhe]** | 6.0 | 5.7 | 8.45 | 6.7 | 9.4 |

## *7.2.Fuel characteristics*

The characteristics of the nuclear fuels that are input in DANESS have been collected as part of several fuel cycle studies performed earlier:

- Characteristics of a generic Gen II LWR UOX fuel, representative for the presently applied Borssele NPP fuel (UOX, 39 GWd/tHM): Liljenzin, 2001, Table 21.2; NEI, 2009; p.146);
- Characteristics of the presently applied Borssele NPP fuel (UOX, MOX): EPZ, 2011, Section 6.4; Gonzalez, 2005: Tables 1,2,5,6 (spent fuel isotopic compositions);
- Characteristics of the LWR Gen-III fuel (UOX, MOX): Gonzalez, 2005: Tables 1,2,5,6 (spent fuel isotopic compositions);
- Characteristics of the standard HTR fuel pebbles: Van den Durpel, 2009;
- Characteristics of the SFR fuel, sodium-cooled fast reactor (FR-MOX): Gonzalez, 2005: Tables 9, 10 (spent fuel isotopic compositions).

Characteristics of the thorium-fuel have been obtained from (Todosow, 2010; Table VI). It should be noted that DANESS does not run properly if the input parameter "*Initial U [t/tIHM]*" is set at 0.0, as should be the case for Thorium fuel. Therefore the initial U-235 composition is set as 0.8586, which is equal to the initial Th-232 fuel fraction of the thorium fuel applied in the analysis of Scenario 7 (thorium cycle). Essentialy this means that in the present analysis of the thorium cycle, the fresh thorium fuel is simulated by fresh uranium fuel. From the amount of HLW produced, the thorium HLW nuclide composition is extracted by taking into account the thorium spent fuel composition as tabulated in (Todosow, 2010; Table VI) and (Carter, 2012; Table O-3).

The data are summarized in Table 7-2 below.

## 7.3. Spent fuel and HLW isotopics

For the standard set of radionuclides which are presently tracked in DANESS, the isotopic composition of the spent fuels and HLWs have been obtained from a variety of sources:

- For the CSD-V canisters, resulting from the reprocessing of the Gen II LWR (Borssele): Hart, 2014, Table 4-10;
- For all CSD-C canisters, resulting from the reprocessing of spent fuels: Hart, 2014, Table 4-11;
- For the reprocessed presently applied Borssele NPP UOX fuel, and the Gen-III LWR UOX fuel: Cuñado, 2006, Table 3.13;
- For the reprocessed presently foreseen Borssele NPP MOX fuel, and the Gen-III LWR MOX fuel: Cuñado, 2006, Table 11.10;
- For the standard HTR fuel pebbles: Van den Durpel, 2009;
- For the reprocessed SFR fuel, sodium-cooled fast reactor (FR-MOX): Cuñado, 2006, Table 5.1.
- For the thorium HLW: Todosow, 2010, Table VI; and Carter, 2012; Table O-3.

The total inventory at 2130 is calculated from the spent fuel isotopic inventory that is added yearly during and after the operations of the reactors to the DANESS stocks "*SF_Conditioning*" and "*HLW_Conditioning*" cf. Figure 4-2. Thereby, decay of the radionuclides is taken into account. Because of the relatively large quantities of depleted uranium, only for the DepU ingrowth of uranium daughter nuclides has been taken into account.

The present version of DANESS tracks a set of 68 radionuclides in total, which includes radionuclides with half-lives shorter than 10 years. For the present analysis, only radionuclides are reported with half lives longer than 10 years, and which are present in the considered spent fuels and/or HLWs. That list comprises a set of 49 radionuclides in total.

## 7.4. Fuel cycle facilities

The characteristics of the nuclear fuel cycle facilities that are input in DANESS have been collected as part of an earlier fuel cycle study (Van Heek, 2012). It is reminded that for the analyses unlimited fuel cycle facility capacities have been assumed, which is justified regarding the relatively small nuclear program in the Netherlands. Also to be noted is that, for the present application of DANESS, the system parameters of the fuel cycle facilities are less relevant.

Table 7-2 Fuel-type characteristics used in scenario analysis

| | *EPZ UOX 39 GWd/tHM* | *EPZ UOX c-ERU* | *EPZ MOX* | *LWR Gen III UOX* | *LWR Gen III MOX* | *HTR UOX* | *FR Gen IV* | *Thorium* |
|---|---|---|---|---|---|---|---|---|
| **BU [GWd/tIHM]** | 39 | 53 | 53.0 | 50.0 | 50.0 | 100.3 | 136 | 50.0 |
| **Cycle Length [months]** | 11 | 11 | 11.0 | 18.0 | 18.0 | 25.6 | 14.6 | 18.0 |
| **Number of Batches [#]** | 3 | 4 | 4 | 5 | 5 | 5 | 5 | 3 |
| **Initial U [t/tIHM]** | 1.0 | 1.0 | 0.915 | 1.0 | 0.915 | 1.0 | 0.0 | 0.859 |
| **Inital REPU [t/tIHM]** | 0.0 | 0.0 | 0.0 | 0.0 | 0.0 | 0.0 | 0.0 | 0.0 |
| **Initial DU [t/tIHM]** | 0.0 | 0.0 | 0.0 | 0.0 | 0.0 | 0.0 | 0.7155 | 0.0 |
| **Initial Enrichment 235U [%]** | 4.00 | 4.60 | 0.25 | 4.2 | 0.229 | 9.0 | 0.186 | 0.81 |
| **Initial Pu [t/tIHM]** | 0.0 | 0.0 | 0.0846 | 0.0 | 0.0849 | 0.0 | 0.232 | 0.132 |
| **Initial MA [t/tIHM]** | 0.0 | 0.0 | 0.0 | 0.0 | 0.0 | 0.0 | 0.026 | 0.0086 |
| **Initial Np [t/tIHM]** | 0.0 | 0.0 | 0.0 | 0.0 | 0.0 | 0.0 | 0.005 | 0.0 |
| **Initial Am [t/t/IHM]** | 0.0 | 0.0 | 0.0013 | 0.0 | 0.0 | 0.0 | 0.016 | 0.0015 |
| **Initial Cm [t/tIHM]** | 0.0 | 0.0 | 0.0 | 0.0 | 0.0 | 0.0 | 0.005 | 0.0 |
| **Spent U [t/tIHM]** | 0.948 | 0.982 | 0.969 | 0.9354 | 0.8796 | 0.8820 | 0.7509 | 0.0407 |
| **Spent Enrichment 235U [%]** | 0.80 | 1.574 | 0.9836 | 0.743 | 0.115 | 1.2660 | 0.0917 | 0.4053 |
| **Spent Pu [t/tIHM]** | 0.008 | 0.0098 | 0.0242 | 0.0116 | 0.0624 | 0.0145 | 0.1456 | 0.1628 |
| **Spent MA [t/tIHM]** | 0.0012 | 0.0016 | 0.0015 | 0.0015 | 0.0074 | 0.0013 | 0.0105 | 0.0281 |
| **Spent Np [t/tIHM]** | 0.0002 | 0.0014 | 0.0004 | 0.0007 | 0.0002 | 0.0008 | 0.0016 | 0.0055 |
| **Spent Am [t/tIHM]** | 0.0058 | 0.0000 | 0.0004 | 0.0000 | 0.0058 | 0.0003 | 0.0075 | 0.0173 |
| **Spent Cm [t/tIHM]** | 0.0013 | 0.0001 | 0.0003 | 0.0001 | 0.0013 | 0.0002 | 0.0030 | 0.0052 |
| **Spent FP [t/tIHM]** | 0.040 | 0.0512 | 0.0499 | 0.0512 | 0.0499 | 0.1030 | 0.0915 | 0.0147 |

c-ERU: Compensated Enriched Recycled Uranium

# 8. Results of the DANESS Simulations

## *8.1. Scenario 1 – No new nuclear power plants*

The following figures show the development of relevant deployment and waste parameters for this scenario. The characteristics of the waste packages are summarized in Table 8-1, whereas Table 8-2 contains the estimated radionuclide inventory in 2130.

The operating reactor capacity of the Borssele NPP is shown in Figure 8-1. The termination of the reactor operation is as planned in 2033.

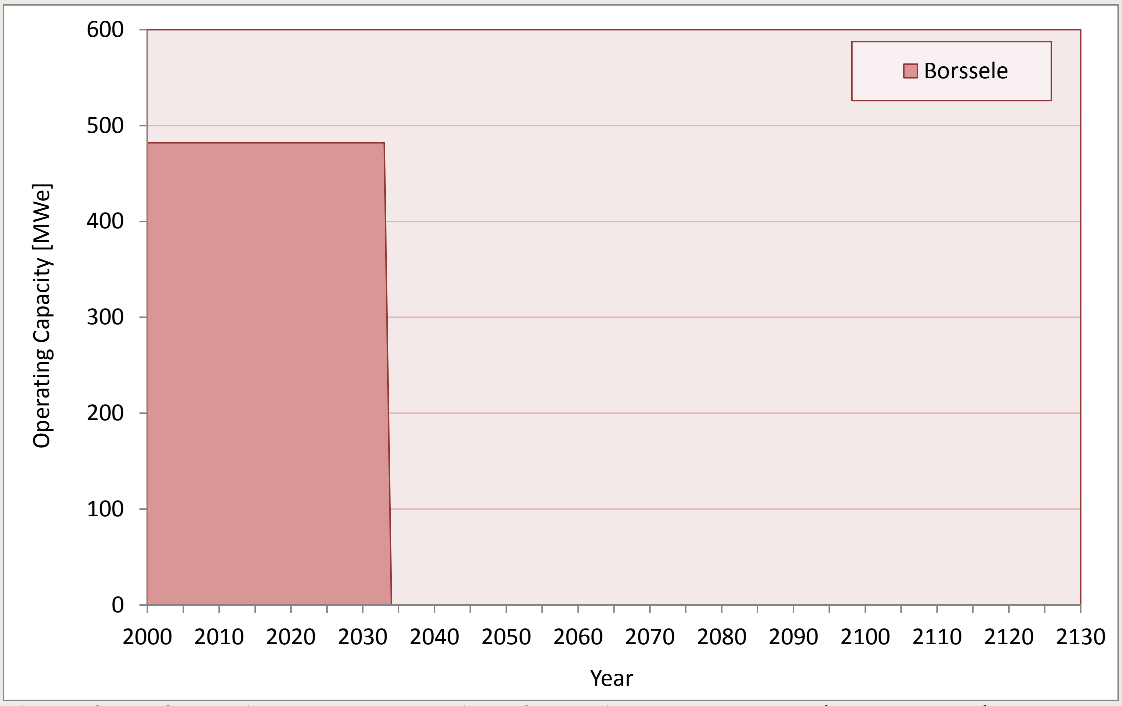


**Figure 8-1 Operating reactor capacity - Scenario 1 - No new nuclear power plants**

The amount of HLW CSD-V containers is shown in Figure 8-2 and Table 8-1. It is noted that the total amount of CSD-V containers is approximately aligned with the expected inventory of HLW intended for disposal, i.e. 625 colli (Verhoef, 2011a; Table A-2). The total estimated number of CSD-V containers, i.e. 624, is composed of the following stocks:

- 196 containers, presently stored at COVRA (COVRA, 2013; p.11);
- 339 containers, resulting from the continuing operation of the Borssele NPP up to 2033;
- 89 containers, resulting from the reprocessing of spent fuel presently stored in the spent fuel pool[10] or at other locations.

[10] In NEI, 2009 (p.146) it is mentioned that 50 $t_{HM}$ of spent fuel is stored in the fuel pool.

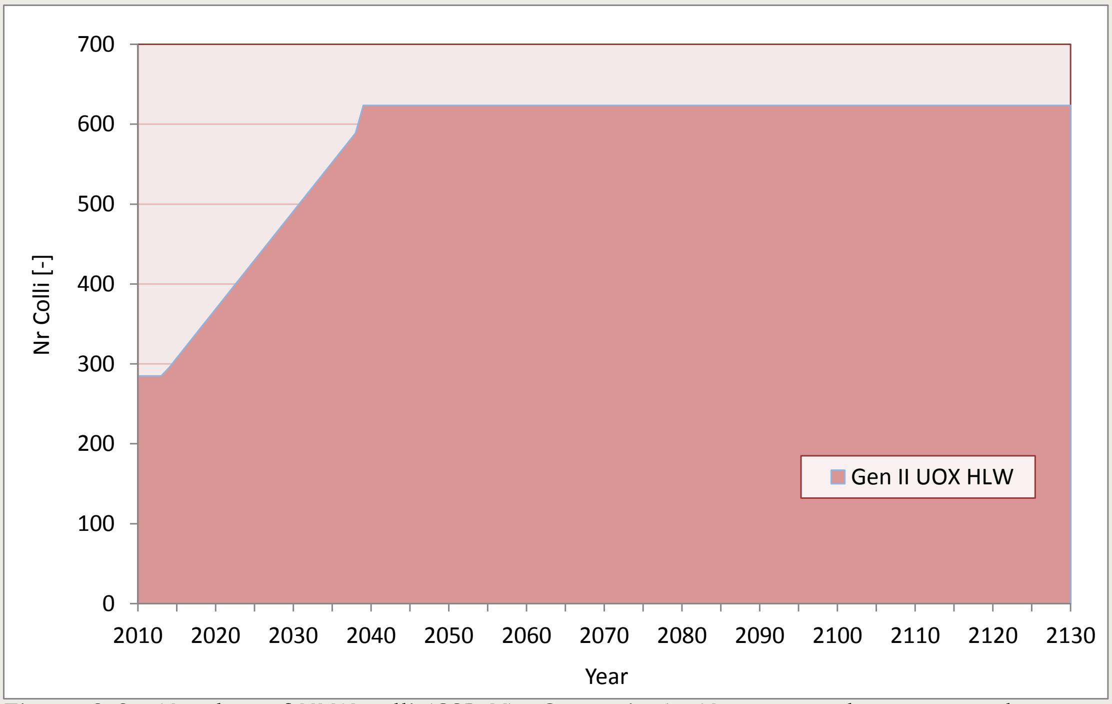


**Figure 8-2 Number of HLW colli (CSD-V) - Scenario 1 - No new nuclear power plants**

The amount of depleted uranium (DepU), generated during reactor operations from 2010, is depicted in Figure 8-3. Assuming that the DepU is conditioned in KONRAD II containers (9,40 tHM DepU per container), the total amount of approximately 4480 $t_{HM}$ of DepU requires 477 KONRAD II containers.

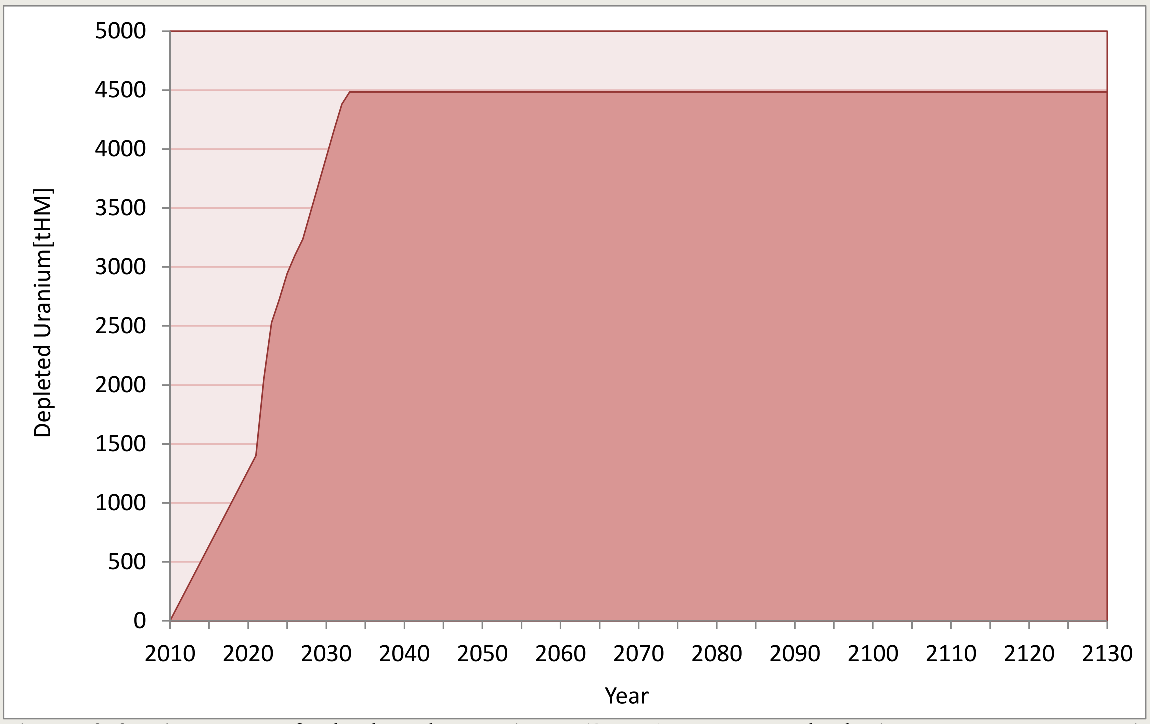


**Figure 8-3 Amount of depleted uranium (DepU) generated during reactor operations - Scenario 1 - No new nuclear power plants**

Table 8-1 Waste characteristics per 2130 – Scenario 1 – No new nuclear power plants

| | Gen II UOX |
|---|---|
| Number of CSD-V canisters | 624 |
| Number of CSD-C canisters | 1247 |
| Number of CSD-V canisters per TWh(e) | 3.08 |
| Number of CSD-C canisters per TWh(e) | 6.36 |
| Number of KONRAD II containers (DepU) | 477 |

The radionuclide inventory estimated in the year 2130 is tabulated in Table 8-2 for the vitrified HLW, and in Table 8-3 for the depleted uranium. Because of the significant quantities of DepU, the ingrowth of relevant uranium daughter nuclides has been taken into account.

Table 8-2 Estimated radionuclide inventory in 2130 - Scenario 1 – No new nuclear power plants

| | *Activity [Bq]* | | | |
|---|---|---|---|---|
| **Nuclide** | ***Half-life [years]*** | ***CSD-V*** | ***CSD-C*** | ***Total*** |
| C-14 | 5.70E+03 | 0.00E+00 | 1.72E+13 | 1.72E+13 |
| Cl-36 | 3.01E+05 | 0.00E+00 | 0.00E+00 | 0.00E+00 |
| Ca-41 | 1.40E+05 | 0.00E+00 | 0.00E+00 | 0.00E+00 |
| Ni-59 | 7.60E+04 | 0.00E+00 | 4.47E+14 | 4.47E+14 |
| Ni-63 | 1.01E+02 | 0.00E+00 | 1.57E+16 | 1.57E+16 |
| Se-79 | 3.77E+05 | 2.91E+12 | 6.86E+10 | 2.98E+12 |
| Kr-85 | 1.08E+01 | 0.00E+00 | 0.00E+00 | 0.00E+00 |
| Sr-90 | 2.88E+01 | 2.06E+17 | 2.50E+15 | 2.09E+17 |
| Zr-93 | 1.53E+06 | 6.57E+13 | 3.74E+11 | 6.61E+13 |
| Mo-93 | 4.00E+03 | 0.00E+00 | 7.24E+12 | 7.24E+12 |
| Nb-94 | 2.00E+04 | 0.00E+00 | 6.92E+13 | 6.92E+13 |
| Tc-99 | 2.14E+05 | 7.81E+14 | 2.87E+12 | 7.84E+14 |
| Pd-107 | 6.50E+06 | 4.23E+12 | 1.46E+10 | 4.24E+12 |
| Ag-108m | 4.18E+02 | 0.00E+00 | 0.00E+00 | 0.00E+00 |
| Sn-126 | 1.00E+05 | 2.37E+13 | 1.10E+11 | 2.38E+13 |
| I-129 | 1.61E+07 | 1.62E+11 | 6.61E+10 | 2.28E+11 |
| Cs-135 | 2.30E+06 | 1.88E+13 | 8.85E+10 | 1.88E+13 |
| Cs-137 | 3.00E+01 | 3.28E+17 | 1.49E+15 | 3.30E+17 |
| Sm-151 | 9.00E+01 | 0.00E+00 | 3.19E+13 | 3.19E+13 |
| U-232 | 6.88E+01 | 0.00E+00 | 4.47E+08 | 4.47E+08 |
| U-233 | 1.59E+05 | 0.00E+00 | 3.99E+05 | 3.99E+05 |
| U-234 | 2.46E+05 | 5.09E+10 | 4.65E+10 | 9.74E+10 |
| U-235 | 7.04E+08 | 4.06E+08 | 1.56E+09 | 1.96E+09 |
| U-236 | 2.37E+07 | 6.04E+09 | 1.51E+10 | 2.11E+10 |
| U-238 | 4.47E+09 | 7.16E+09 | 2.35E+10 | 3.06E+10 |
| Pu-238 | 8.77E+01 | 5.52E+13 | 8.57E+13 | 1.41E+14 |
| Pu-239 | 2.41E+04 | 1.24E+13 | 1.94E+13 | 3.19E+13 |
| Pu-240 | 6.56E+03 | 3.19E+14 | 2.45E+13 | 3.43E+14 |
| Pu-241 | 1.43E+01 | 1.85E+13 | 6.72E+13 | 8.57E+13 |
| Pu-242 | 3.74E+05 | 9.62E+10 | 1.23E+11 | 2.19E+11 |
| Pu-244 | 8.00E+07 | 0.00E+00 | 6.12E+04 | 6.12E+04 |
| Np-236 | 1.15E+05 | 0.00E+00 | 0.00E+00 | 0.00E+00 |
| Np-237 | 2.14E+06 | 1.48E+13 | 8.98E+09 | 1.48E+13 |

| | Activity [Bq] | | | |
|---|---|---|---|---|
| **Nuclide** | ***Half-life [years]*** | ***CSD-V*** | ***CSD-C*** | ***Total*** |
| Am-241 | 4.33E+02 | 5.90E+16 | 3.65E+13 | 5.90E+16 |
| Am-242m | 1.52E+02 | 0.00E+00 | 1.17E+11 | 1.17E+11 |
| Am-243 | 7.36E+03 | 1.07E+15 | 4.32E+13 | 1.12E+15 |
| Cm-243 | 2.85E+01 | 0.00E+00 | 2.43E+10 | 2.43E+10 |
| Cm-244 | 1.80E+01 | 1.69E+15 | 1.81E+12 | 1.69E+15 |
| Cm-245 | 8.50E+03 | 1.26E+13 | 1.36E+10 | 1.26E+13 |
| Cm-246 | 4.73E+03 | 0.00E+00 | 5.96E+09 | 5.96E+09 |
| Cm-247 | 1.56E+07 | 0.00E+00 | 3.28E+04 | 3.28E+04 |
| Cm-248 | 3.39E+05 | 0.00E+00 | 2.03E+05 | 2.03E+05 |
| Cm-250 | 6.90E+03 | 0.00E+00 | 0.00E+00 | 0.00E+00 |
| Th-229 | 7.34E+03 | 0.00E+00 | 1.47E+03 | 1.47E+03 |
| Th-230 | 7.54E+04 | 0.00E+00 | 2.09E+04 | 2.09E+04 |
| Th-232 | 1.41E+10 | 0.00E+00 | 2.52E+00 | 2.52E+00 |
| Ra-226 | 1.60E+03 | 0.00E+00 | 1.30E+01 | 1.30E+01 |
| Pa-231 | 3.28E+04 | 0.00E+00 | 3.02E+05 | 3.02E+05 |
| Ac-227 | 2.18E+01 | 0.00E+00 | 1.47E+02 | 1.47E+02 |

**Table 8-3 Estimated radionuclide inventory (DepU) in 2130 - Scenario 1 - No new nuclear power plants**

| **Nuclide** | ***Half-life [years]*** | ***Activity [Bq]*** |
|---|---|---|
| U-238 | 4.47E+09 | 5.56E+13 |
| U-235 | 7.04E+08 | 1.28E+12 |
| U-234 | 2.46E+05 | 1.28E+13 |
| Pa-231 | 3.28E+04 | 2.91E+09 |
| Th-230 | 7.54E+04 | 1.27E+10 |
| Ac-227 | 2.18E+01 | 2.10E+09 |
| Ra-226 | 1.60E+03 | 2.91E+08 |
| Rn-222 | 1.05E-02 | 2.91E+08 |

## *8.2. Scenario 2 – Application of MOX fuel*

The following figures show the development of relevant deployment and waste parameters for this scenario. The characteristics of the waste packages are summarized in Table 8-4, whereas Table 8-5 contains the estimated radionuclide inventory in 2130.

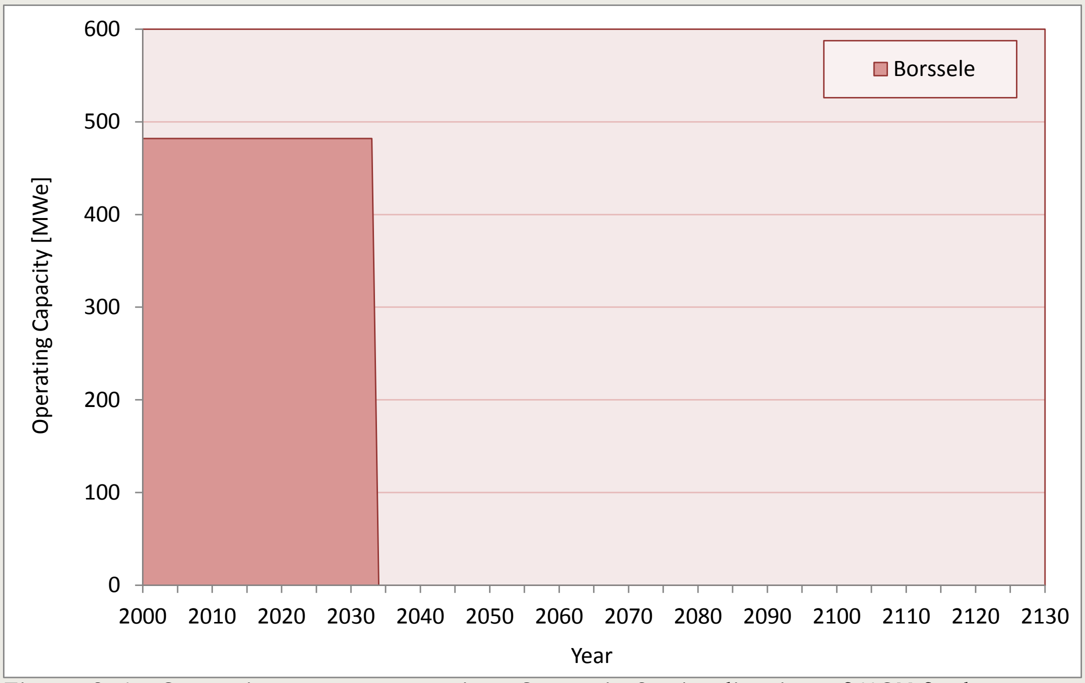

**Figure 8-4 Operating reactor capacity - Scenario 2 - Application of MOX fuel**

The total final number of HLW containers consist of the following contributions:

- 347 CSD-V containers, resulting from the reprocessing of the presently applied UOX fuel;
- 167 CSD-V containers, resulting from the future reprocessing of the c-ERU[11] fuel;
- 109 CSD-V containers, resulting from the future reprocessing of the MOX fuel.

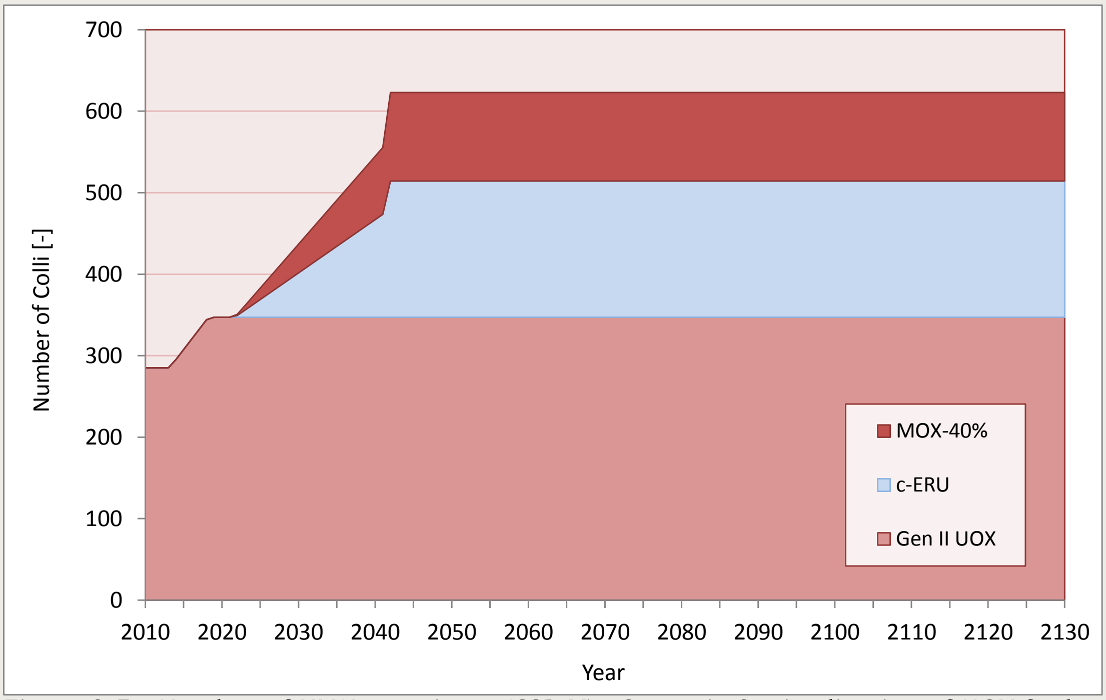

**Figure 8-5 Number of HLW containers (CSD-V) - Scenario 2 - Application of MOX fuel**

[11] c-ERU: compensated enriched recycled uranium

The amount of depleted uranium (DepU), generated during reactor operations from 2010, is depicted in Figure 8-6. Assuming that the DepU is conditioned in KONRAD II containers (9,40 tHM DepU per container), the total amount of approximately 2960 $t_{HM}$ of DepU requires 315 KONRAD II containers. The amount of generated DepU is less than for Scenario 1 due to the reprocessing of part of the core inventory.

**Table 8-4 Waste characteristics per 2130 - Scenario 2 - Application of MOX fuel**

| | Gen II UOX | c-ERU | MOX-40% |
|---|---|---|---|
| Number of CSD-V canisters | 347 | 167 | 109 |
| Number of CSD-C canisters | 694 | 334 | 218 |
| Number of CSD-V canisters per TWhr | | 2.76 | |
| Number of CSD-C canisters per TWhr | | 5.52 | |
| Number of KONRAD II containers (DepU) | 319 | | |

The radionuclide inventory estimated in the year 2130 is tabulated in Table 8-5 for the HLW, and in Table 8-6 for the depleted uranium. Because of the significant quantities of DepU, the ingrowth of relevant uranium daughter nuclides has been taken into account.

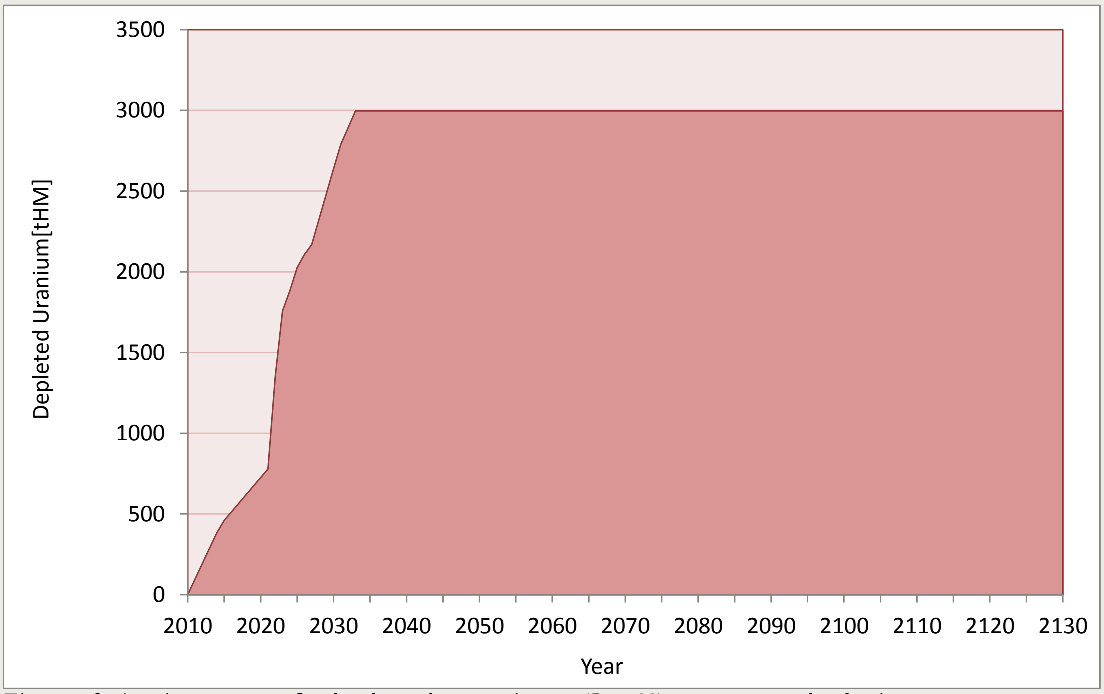


**Figure 8-6 Amount of depleted uranium (DepU) generated during reactor operations - Scenario 2 - Application of MOX fuel**

**Table 8-5 Estimated radionuclide inventory in 2130 - Scenario 2 - Application of MOX fuel**

| | | *Activity [Bq]* | | |
|---|---|---|---|---|
| **Nuclide** | ***Half-life [years]*** | ***CSD-V*** | ***CSD-C*** | ***Total*** |
| C-14 | 5.70E+03 | 5.20E+11 | 1.72E+13 | 1.77E+13 |
| Cl-36 | 3.01E+05 | 4.03E+11 | 0.00E+00 | 4.03E+11 |
| Ca-41 | 1.40E+05 | 1.67E+11 | 0.00E+00 | 1.67E+11 |
| Ni-59 | 7.60E+04 | 1.37E+12 | 4.47E+14 | 4.48E+14 |
| Ni-63 | 1.01E+02 | 1.77E+16 | 1.58E+16 | 3.35E+16 |
| Se-79 | 3.77E+05 | 2.35E+12 | 6.85E+10 | 2.42E+12 |

| Nuclide | Half-life [years] | Activity [Bq] CSD-V | CSD-C | Total |
|---|---|---|---|---|
| Kr-85 | 1.08E+01 | 0.00E+00 | 0.00E+00 | 0.00E+00 |
| Sr-90 | 2.88E+01 | 1.12E+17 | 2.54E+15 | 1.15E+17 |
| Zr-93 | 1.53E+06 | 5.79E+13 | 3.74E+11 | 5.83E+13 |
| Mo-93 | 4.00E+03 | 0.00E+00 | 7.23E+12 | 7.23E+12 |
| Nb-94 | 2.00E+04 | 6.04E+11 | 6.92E+13 | 6.98E+13 |
| Tc-99 | 2.14E+05 | 6.19E+14 | 2.86E+12 | 6.22E+14 |
| Pd-107 | 6.50E+06 | 4.77E+12 | 1.46E+10 | 4.78E+12 |
| Ag-108m | 4.18E+02 | 1.44E+08 | 0.00E+00 | 1.44E+08 |
| Sn-126 | 1.00E+05 | 2.37E+13 | 1.10E+11 | 2.38E+13 |
| I-129 | 1.61E+07 | 9.47E+10 | 6.60E+10 | 1.61E+11 |
| Cs-135 | 2.30E+06 | 1.97E+13 | 8.85E+10 | 1.98E+13 |
| Cs-137 | 3.00E+01 | 1.93E+17 | 1.52E+15 | 1.94E+17 |
| Sm-151 | 9.00E+01 | 2.35E+15 | 3.21E+13 | 2.39E+15 |
| U-232 | 6.88E+01 | 2.22E+10 | 4.49E+08 | 2.27E+10 |
| U-233 | 1.59E+05 | 5.75E+08 | 3.99E+05 | 5.75E+08 |
| U-234 | 2.46E+05 | 9.41E+10 | 4.63E+10 | 1.40E+11 |
| U-235 | 7.04E+08 | 3.24E+08 | 1.55E+09 | 1.88E+09 |
| U-236 | 2.37E+07 | 5.52E+09 | 1.51E+10 | 2.06E+10 |
| U-238 | 4.47E+09 | 6.81E+09 | 2.35E+10 | 3.03E+10 |
| Pu-238 | 8.77E+01 | 1.02E+14 | 8.61E+13 | 1.88E+14 |
| Pu-239 | 2.41E+04 | 1.55E+13 | 1.94E+13 | 3.50E+13 |
| Pu-240 | 6.56E+03 | 2.94E+14 | 2.45E+13 | 3.19E+14 |
| Pu-241 | 1.43E+01 | 1.01E+13 | 7.04E+13 | 8.05E+13 |
| Pu-242 | 3.74E+05 | 1.79E+11 | 1.23E+11 | 3.02E+11 |
| Pu-244 | 8.00E+07 | 7.13E+04 | 6.12E+04 | 1.32E+05 |
| Np-236 | 1.15E+05 | 0.00E+00 | 0.00E+00 | 0.00E+00 |
| Np-237 | 2.14E+06 | 1.12E+13 | 8.97E+09 | 1.12E+13 |
| Am-241 | 4.33E+02 | 3.92E+16 | 3.65E+13 | 3.92E+16 |
| Am-242m | 1.52E+02 | 3.29E+13 | 1.18E+11 | 3.30E+13 |
| Am-243 | 7.36E+03 | 8.38E+14 | 4.32E+13 | 8.81E+14 |
| Cm-243 | 2.85E+01 | 1.14E+13 | 2.48E+10 | 1.14E+13 |
| Cm-244 | 1.80E+01 | 7.65E+14 | 1.87E+12 | 7.67E+14 |
| Cm-245 | 8.50E+03 | 1.28E+13 | 1.35E+10 | 1.28E+13 |
| Cm-246 | 4.73E+03 | 1.26E+12 | 5.96E+09 | 1.27E+12 |
| Cm-247 | 1.56E+07 | 6.67E+06 | 3.28E+04 | 6.71E+06 |
| Cm-248 | 3.39E+05 | 4.49E+07 | 2.02E+05 | 4.51E+07 |
| Cm-250 | 6.90E+03 | 0.00E+00 | 0.00E+00 | 0.00E+00 |
| Th-229 | 7.34E+03 | 3.16E+06 | 1.47E+03 | 3.16E+06 |
| Th-230 | 7.54E+04 | 6.83E+08 | 2.09E+04 | 6.83E+08 |
| Th-232 | 1.41E+10 | 7.53E+02 | 2.52E+00 | 7.56E+02 |
| Ra-226 | 1.60E+03 | 0.00E+00 | 1.30E+01 | 1.30E+01 |
| Pa-231 | 3.28E+04 | 2.12E+08 | 3.02E+05 | 2.12E+08 |
| Ac-227 | 2.18E+01 | 7.12E+06 | 1.51E+02 | 7.12E+06 |

**Table 8-6 Estimated radionuclide inventory (DepU) in 2130 – Scenario 2 – Application of MOX fuel**

| Nuclide | Half-life [years] | Activity [Bq] |
|---|---|---|
| U-238 | 4.47E+09 | 3.43E+13 |

| Nuclide | *Half-life [years]* | *Activity [Bq]* |
|---|---|---|
| U-235 | 7.04E+08 | 7.91E+11 |
| U-234 | 2.46E+05 | 7.92E+12 |
| Pa-231 | 3.28E+04 | 1.78E+09 |
| Th-230 | 7.54E+04 | 7.76E+09 |
| Ac-227 | 2.18E+01 | 1.28E+09 |
| Ra-226 | 1.60E+03 | 1.74E+08 |
| Rn-222 | 1.05E-02 | 1.74E+08 |

## *8.3. Scenario 3 – No reprocessing of spent fuel*

The following figures show the development of relevant deployment and waste parameters for this scenario. The characteristics of the waste packages are summarized in Table 8-7, whereas Table 8-8 contains the estimated radionuclide inventory in 2130.

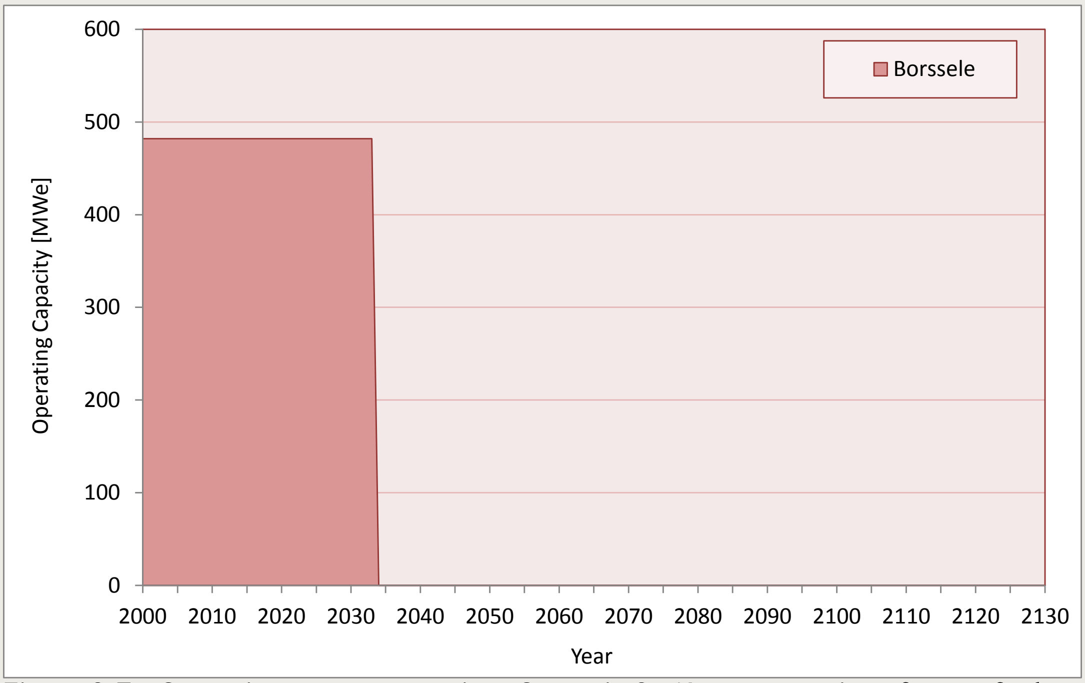


**Figure 8-7 Operating reactor capacity - Scenario 3 - No reprocessing of spent fuel**

Figure 8-8 and Table 8-7 show the total amount of spent fuel (UOX and MOX) and HLW CSD-V containers. The 285 HLW CSD-V containers result from the already reprocessed Gen II UOX spent fuel, and from the Gen II UOX spent fuel assumed to be present in the “reprocessing pipeline” (see also Section 8.1).

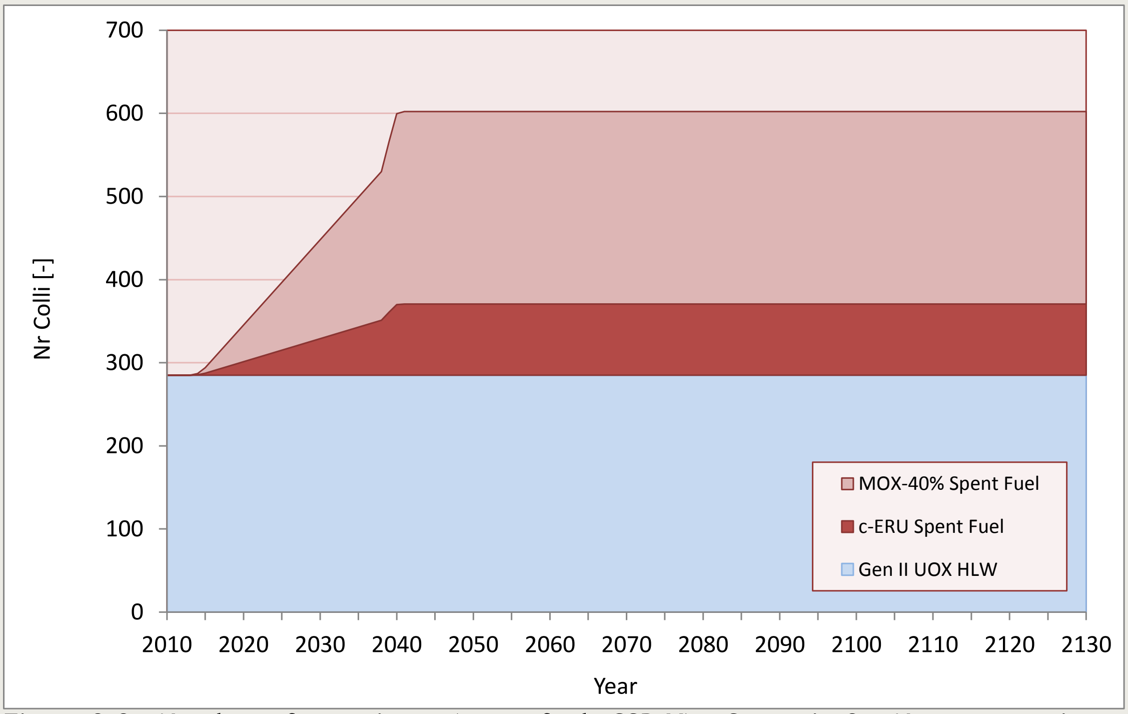


**Figure 8-8 Number of containers (spent fuel; CSD-V) - Scenario 3 - No reprocessing of spent fuel**

Note that the amount of c-ERU spent fuel UOX containers is significantly less than that of the MOX spent fuel. The reason is that a single spent fuel container can hold four spent fuel c-ERU UOX assemblies, and only one spent fuel MOX assembly (see also Section 6.3).

**Table 8-7 Waste characteristics per 2130 - Scenario 3 - No reprocessing of spent fuel**

| | Gen II UOX-33 HLW | c-ERU Spent Fuel | MOX-40% Spent Fuel |
|---|---|---|---|
| Number of CSD-V canisters | 285 | | |
| Number of CSD-C canisters | 570 | | |
| Number of SF canisters | | 86 | 232 |
| Number of SF canisters per TWhr | | 0.73 | 1.97 |
| Number of KONRAD II containers (DepU) | 295 | | |

The amount of depleted uranium (DepU), generated during reactor operations from 2010, is depicted in Figure 8-9. Assuming that the DepU is conditioned in KONRAD II containers (9,40 tHM DepU per container), the total amount of approximately 2770 tHM of DepU requires 590 KONRAD II containers. The amount of generated DepU is equal to that of Scenario 2 and likewise less than for Scenario 1 due to the reprocessing of part of the core inventory.

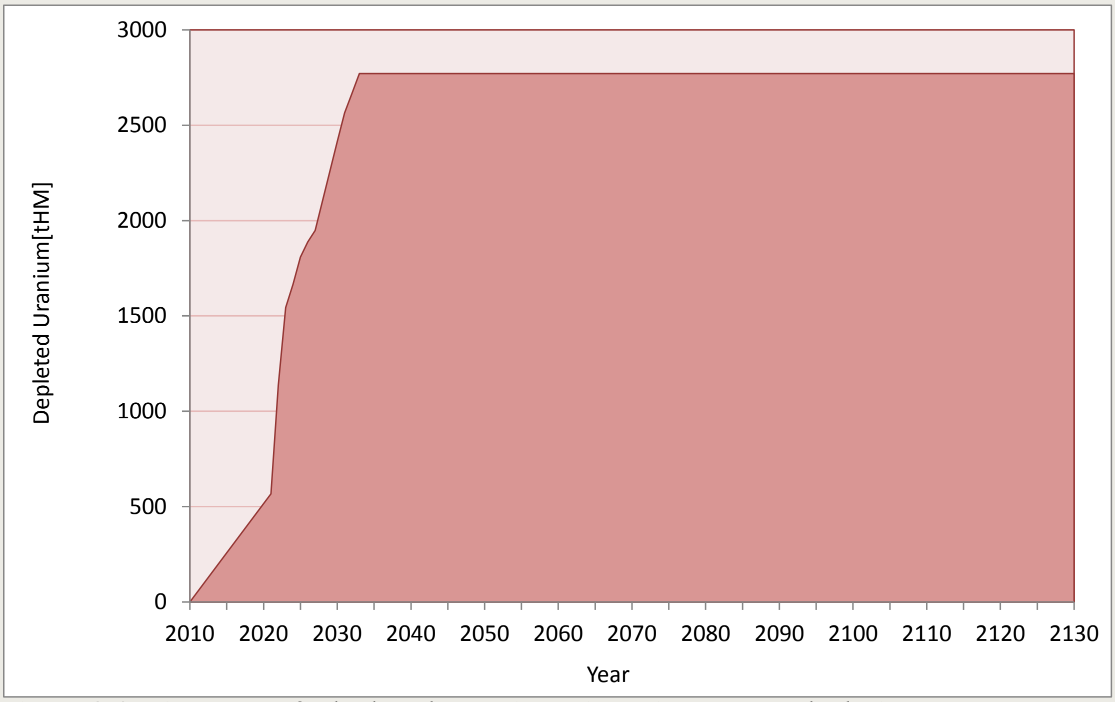


**Figure 8-9 Amount of depleted uranium (DepU) generated during reactor operations - Scenario 3 - No reprocessing of spent fuel**

The radionuclide inventory estimated in the year 2130 is tabulated in Table 8-8 for the spent fuel and HLW, and in Table 8-9 for the depleted uranium. Because of the significant quantities of DepU, the ingrowth of relevant uranium daughter nuclides has been taken into account.

**Table 8-8 Estimated radionuclide inventory in 2130 - Scenario 3 - No reprocessing of spent fuel**

| | *Activity [Bq]* | | | | | |
|---|---|---|---|---|---|---|
| | ***Half-life [years]*** | ***Vitrified HLW*** | | ***Spent Fuel*** | | |
| **Nuclide** | | ***CSD-V*** | ***CSD-C*** | ***c-ERU*** | ***MOX-40%*** | ***Total*** |
| C-14 | 5.70E+03 | 0.00E+00 | 7.86E+12 | 3.58E+12 | 1.89E+12 | 1.33E+13 |
| Cl-36 | 3.01E+05 | 0.00E+00 | 0.00E+00 | 4.24E+11 | 1.30E+11 | 5.54E+11 |
| Ca-41 | 1.40E+05 | 0.00E+00 | 0.00E+00 | 1.32E+11 | 4.37E+10 | 1.75E+11 |
| Ni-59 | 7.60E+04 | 0.00E+00 | 2.04E+14 | 1.07E+12 | 3.58E+11 | 2.06E+14 |
| Ni-63 | 1.01E+02 | 0.00E+00 | 6.69E+15 | 7.31E+13 | 2.44E+13 | 6.78E+15 |
| Se-79 | 3.77E+05 | 1.33E+12 | 3.13E+10 | 4.82E+11 | 2.85E+11 | 2.13E+12 |
| Kr-85 | 1.08E+01 | 0.00E+00 | 0.00E+00 | 8.06E+13 | 3.04E+13 | 1.11E+14 |
| Sr-90 | 2.88E+01 | 7.16E+16 | 8.67E+14 | 4.59E+16 | 1.53E+16 | 1.34E+17 |
| Zr-93 | 1.53E+06 | 3.00E+13 | 1.71E+11 | 1.52E+13 | 7.05E+12 | 5.25E+13 |
| Mo-93 | 4.00E+03 | 0.00E+00 | 3.30E+12 | 0.00E+00 | 0.00E+00 | 3.30E+12 |
| Nb-94 | 2.00E+04 | 0.00E+00 | 3.16E+13 | 0.00E+00 | 0.00E+00 | 3.16E+13 |
| Tc-99 | 2.14E+05 | 3.57E+14 | 1.31E+12 | 1.17E+14 | 7.65E+13 | 5.51E+14 |
| Pd-107 | 6.50E+06 | 1.93E+12 | 6.67E+09 | 1.02E+12 | 1.49E+12 | 4.45E+12 |
| Ag-108m | 4.18E+02 | 0.00E+00 | 0.00E+00 | 8.34E+07 | 1.07E+08 | 1.90E+08 |
| Sn-126 | 1.00E+05 | 1.08E+13 | 5.03E+10 | 5.37E+12 | 5.52E+12 | 2.18E+13 |
| I-129 | 1.61E+07 | 7.41E+10 | 3.02E+10 | 2.58E+11 | 2.08E+11 | 5.70E+11 |
| Cs-135 | 2.30E+06 | 8.57E+12 | 4.05E+10 | 4.43E+12 | 5.18E+12 | 1.82E+13 |
| Cs-137 | 3.00E+01 | 1.15E+17 | 5.24E+14 | 7.60E+16 | 5.10E+16 | 2.43E+17 |
| Sm-151 | 9.00E+01 | 0.00E+00 | 1.35E+13 | 1.27E+15 | 2.06E+15 | 3.35E+15 |

| Nuclide | Half-life [years] | Activity [Bq] | | | | |
|---|---|---|---|---|---|---|
| | | Vitrified HLW | | Spent Fuel | | |
| | | CSD-V | CSD-C | c-ERU | MOX-40% | Total |
| U-232 | 6.88E+01 | 0.00E+00 | 1.84E+08 | 8.52E+10 | 2.03E+10 | 1.06E+11 |
| U-233 | 1.59E+05 | 0.00E+00 | 1.82E+05 | 1.43E+08 | 3.85E+07 | 1.81E+08 |
| U-234 | 2.46E+05 | 2.40E+10 | 2.24E+10 | 1.36E+13 | 4.04E+13 | 5.40E+13 |
| U-235 | 7.04E+08 | 1.85E+08 | 7.11E+08 | 9.34E+10 | 9.64E+09 | 1.04E+11 |
| U-236 | 2.37E+07 | 2.76E+09 | 6.90E+09 | 2.10E+12 | 7.04E+10 | 2.18E+12 |
| U-238 | 4.47E+09 | 3.27E+09 | 1.07E+10 | 1.80E+12 | 1.14E+12 | 2.96E+12 |
| Pu-238 | 8.77E+01 | 2.32E+13 | 3.61E+13 | 1.56E+16 | 7.96E+16 | 9.52E+16 |
| Pu-239 | 2.41E+04 | 5.69E+12 | 8.88E+12 | 2.18E+15 | 6.11E+15 | 8.31E+15 |
| Pu-240 | 6.56E+03 | 1.47E+14 | 1.12E+13 | 3.85E+15 | 1.72E+16 | 2.12E+16 |
| Pu-241 | 1.43E+01 | 4.51E+12 | 1.64E+13 | 5.99E+15 | 2.46E+16 | 3.06E+16 |
| Pu-242 | 3.74E+05 | 4.40E+10 | 5.61E+10 | 2.14E+13 | 1.07E+14 | 1.29E+14 |
| Pu-244 | 8.00E+07 | 0.00E+00 | 2.80E+04 | 7.85E+06 | 6.56E+07 | 7.35E+07 |
| Np-236 | 1.15E+05 | 0.00E+00 | 0.00E+00 | 1.16E+08 | 4.53E+07 | 1.62E+08 |
| Np-237 | 2.14E+06 | 6.76E+12 | 4.10E+09 | 3.01E+12 | 5.66E+11 | 1.03E+13 |
| Am-241 | 4.33E+02 | 2.65E+16 | 1.64E+13 | 7.46E+15 | 4.04E+16 | 7.44E+16 |
| Am-242m | 1.52E+02 | 0.00E+00 | 5.12E+10 | 4.06E+13 | 8.47E+14 | 8.87E+14 |
| Am-243 | 7.36E+03 | 4.89E+14 | 1.97E+13 | 2.54E+14 | 1.67E+15 | 2.44E+15 |
| Cm-243 | 2.85E+01 | 0.00E+00 | 8.41E+09 | 3.19E+13 | 2.01E+14 | 2.33E+14 |
| Cm-244 | 1.80E+01 | 4.80E+14 | 5.13E+11 | 7.26E+14 | 6.89E+15 | 8.10E+15 |
| Cm-245 | 8.50E+03 | 5.74E+12 | 6.19E+09 | 6.02E+12 | 1.30E+14 | 1.42E+14 |
| Cm-246 | 4.73E+03 | 0.00E+00 | 2.72E+09 | 1.32E+12 | 1.62E+13 | 1.75E+13 |
| Cm-247 | 1.56E+07 | 0.00E+00 | 1.50E+04 | 6.91E+06 | 1.29E+08 | 1.36E+08 |
| Cm-248 | 3.39E+05 | 0.00E+00 | 9.26E+04 | 4.52E+07 | 1.30E+09 | 1.34E+09 |
| Cm-250 | 6.90E+03 | 0.00E+00 | 0.00E+00 | 0.00E+00 | 0.00E+00 | 0.00E+00 |
| Th-229 | 7.34E+03 | 0.00E+00 | 6.71E+02 | 1.69E+06 | 3.64E+05 | 2.05E+06 |
| Th-230 | 7.54E+04 | 0.00E+00 | 9.57E+03 | 5.08E+08 | 1.97E+08 | 7.05E+08 |
| Th-232 | 1.41E+10 | 0.00E+00 | 1.15E+00 | 7.91E+02 | 2.50E+01 | 8.17E+02 |
| Ra-226 | 1.60E+03 | 0.00E+00 | 5.91E+00 | 0.00E+00 | 0.00E+00 | 5.91E+00 |
| Pa-231 | 3.28E+04 | 0.00E+00 | 1.38E+05 | 1.88E+08 | 3.42E+07 | 2.22E+08 |
| Ac-227 | 2.18E+01 | 0.00E+00 | 4.61E+01 | 0.00E+00 | 0.00E+00 | 4.61E+01 |

**Table 8-9 Estimated radionuclide inventory (DepU) in 2130 – Scenario 3 – No reprocessing of spent fuel**

| Nuclide | Half-life [years] | Activity [Bq] |
|---|---|---|
| U-238 | 4.47E+09 | 3.43E+13 |
| U-235 | 7.04E+08 | 7.91E+11 |
| U-234 | 2.46E+05 | 7.92E+12 |
| Pa-231 | 3.28E+04 | 1.78E+09 |
| Th-230 | 7.54E+04 | 7.76E+09 |
| Ac-227 | 2.18E+01 | 1.28E+09 |
| Ra-226 | 1.60E+03 | 1.74E+08 |
| Rn-222 | 1.05E-02 | 1.74E+08 |

## 8.4. Scenario 4 – Deployment of MOX-fueled Gen III LWRs

The following figures show the development of relevant deployment and waste parameters for this scenario. The characteristics of the waste packages are summarized in Table 8-10, whereas Table 8-11 contains the estimated radionuclide inventory in 2130.

The deployment of LWR Gen III reactors starts in 2020, and reaches its maximum after about 2040. A total number of six 900 MWe reactors supply somewhat more than the anticipated 5000 MWe of electricity. Upon reaching their anticipated lifetime, the Gen III reactors are replaced by other reactors of the same type.

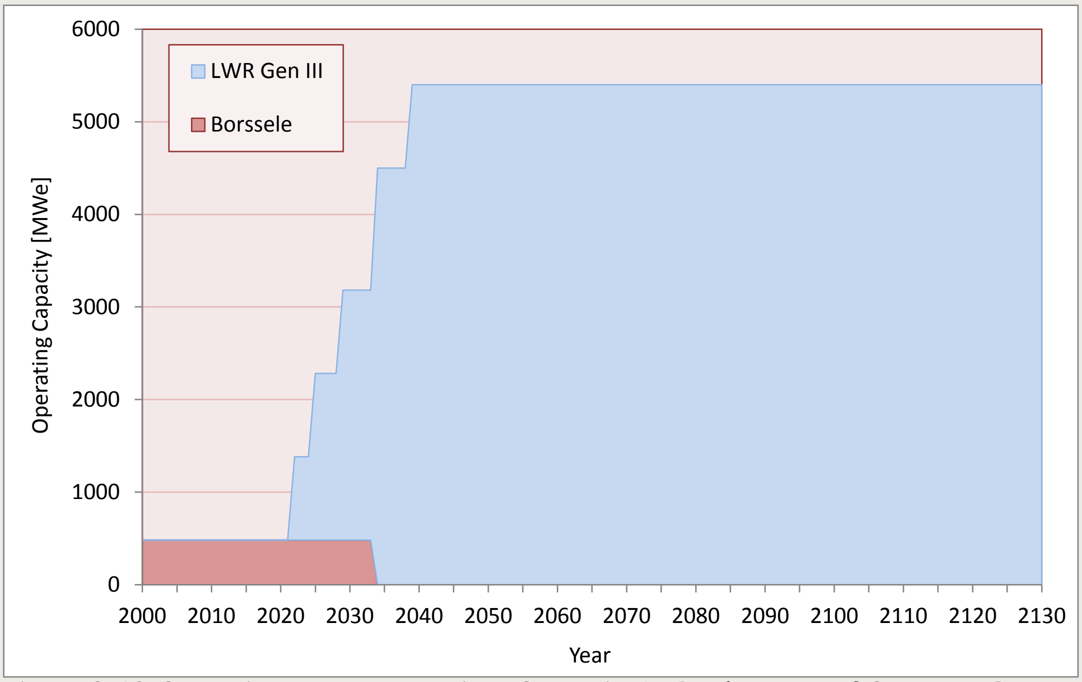


**Figure 8-10 Operating reactor capacity - Scenario 4 - Deployment of Gen III LWRs**

Figure 8-11 and Table 8-10 show the total amount of HLW CSD-V containers, resulting from the reprocessing of the different reactor fuel types. Again, the reprocessing of the formerly applied Gen-II UOX fuel results in 265 HLW CSD-V containers (see also Section 8.1).

In 2130 a total amount of about 15’000 CSD-V and 30’000 CSD-C containers would be produced under the presently adopted assumptions. These amounts will continue to increase as long as nuclear power plants will continue their operations.

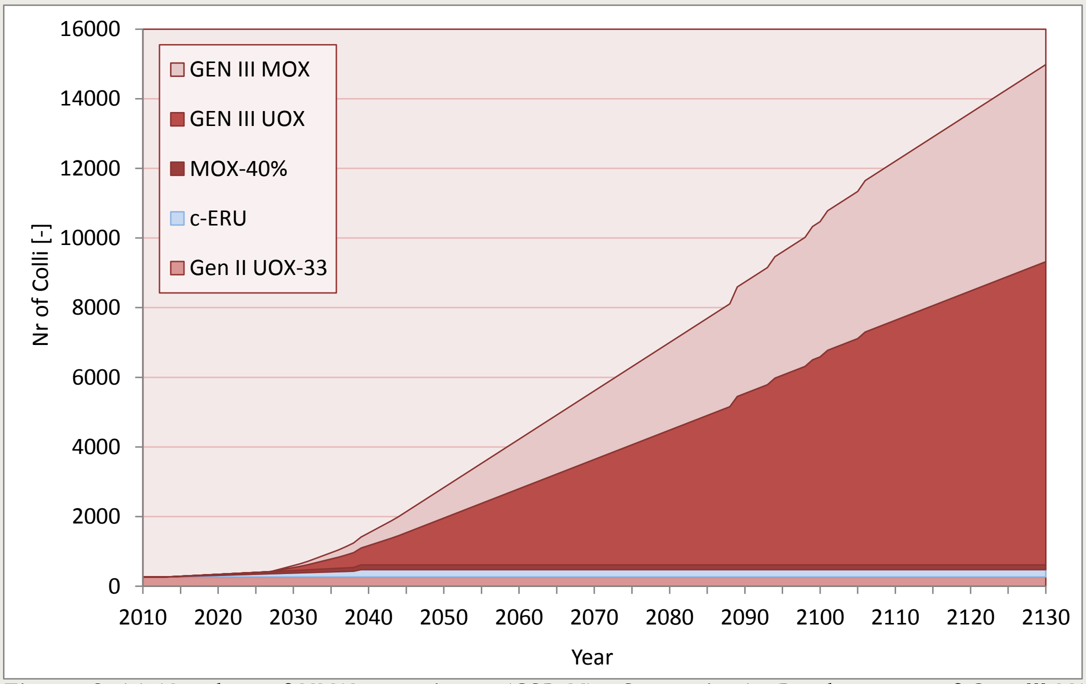


**Figure 8-11 Number of HLW containers (CSD-V) - Scenario 4 - Deployment of Gen III LWRs**

The amount of depleted uranium (DepU), generated during reactor operations from 2010, is depicted in Figure 8-12. Assuming that the DepU is conditioned in KONRAD II containers (9,40 $t_{HM}$ DepU per container), the total amount of approximately 164'200 $t_{HM}$ of DepU requires 17'465 KONRAD II containers.

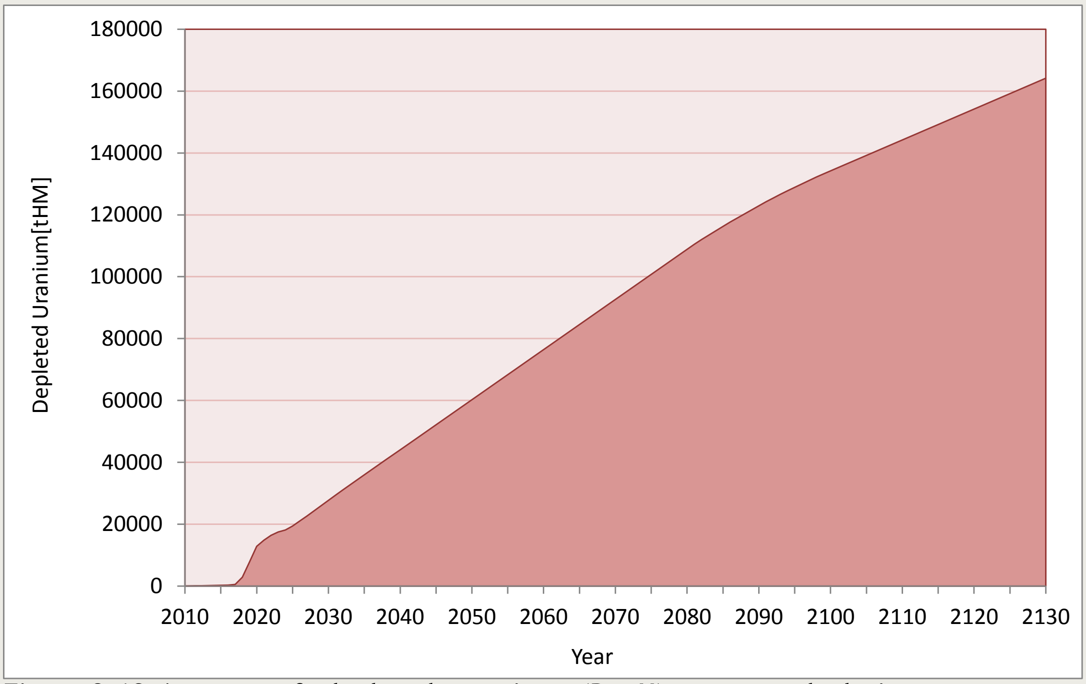


**Figure 8-12 Amount of depleted uranium (DepU) generated during reactor operations - Scenario 4 - Deployment of Gen III LWRs**

Table 8-10 Waste container characteristics per 2130 – Scenario 4 – Deployment of Gen III LWRs

| | Gen II UOX | c-ERU | MOX-40% | Gen III UOX | Gen III MOX |
|---|---|---|---|---|---|
| Number of CSD-V canisters | 285 | 210 | 136 | 8710 | 5660 |
| Number of CSD-C canisters | 570 | 420 | 273 | 17420 | 11320 |
| Number of CSD-V canisters per TWhr | | 2.88 | | 2.74 | |
| Number of CSD-C canisters per TWhr | | 5.76 | | 5.48 | |
| Number of KONRAD II containers (DepU) | 17'465 | | | | |

The radionuclide inventory estimated in the year 2130 is tabulated in Table 8-11 for the HLW, and in Table 8-12 for the depleted uranium. Because of the significant quantities of DepU, the ingrowth of relevant uranium daughter nuclides has been taken into account.

Table 8-11 Estimated radionuclide inventory in 2130 – Scenario 4 – Deployment of Gen III LWRs

| | *Activity [Bq]* | | | |
|---|---|---|---|---|
| **Nuclide** | ***Half-life [years]*** | ***CSD-V*** | ***CSD-C*** | ***Total*** |
| C-14 | 5.70E+03 | 2.79E+13 | 4.18E+14 | 4.46E+14 |
| Cl-36 | 3.01E+05 | 2.15E+13 | 0.00E+00 | 2.15E+13 |
| Ca-41 | 1.40E+05 | 8.93E+12 | 0.00E+00 | 8.93E+12 |
| Ni-59 | 7.60E+04 | 7.31E+13 | 1.08E+16 | 1.08E+16 |
| Ni-63 | 1.01E+02 | 1.37E+18 | 5.89E+17 | 1.95E+18 |
| Se-79 | 3.77E+05 | 4.05E+13 | 1.65E+12 | 4.22E+13 |
| Kr-85 | 1.08E+01 | 0.00E+00 | 0.00E+00 | 0.00E+00 |
| Sr-90 | 2.88E+01 | 5.02E+18 | 3.23E+17 | 5.34E+18 |
| Zr-93 | 1.53E+06 | 1.17E+15 | 9.00E+12 | 1.18E+15 |
| Mo-93 | 4.00E+03 | 0.00E+00 | 1.76E+14 | 1.76E+14 |
| Nb-94 | 2.00E+04 | 3.23E+13 | 1.67E+15 | 1.70E+15 |
| Tc-99 | 2.14E+05 | 1.02E+16 | 6.90E+13 | 1.03E+16 |
| Pd-107 | 6.50E+06 | 1.31E+14 | 3.51E+11 | 1.31E+14 |
| Ag-108m | 4.18E+02 | 8.38E+09 | 0.00E+00 | 8.38E+09 |
| Sn-126 | 1.00E+05 | 5.70E+14 | 2.65E+12 | 5.73E+14 |
| I-129 | 1.61E+07 | 3.13E+11 | 1.59E+12 | 1.90E+12 |
| Cs-135 | 2.30E+06 | 5.02E+14 | 2.13E+12 | 5.04E+14 |
| Cs-137 | 3.00E+01 | 1.00E+19 | 1.79E+17 | 1.02E+19 |
| Sm-151 | 9.00E+01 | 1.90E+17 | 1.26E+15 | 1.91E+17 |
| U-232 | 6.88E+01 | 2.05E+12 | 2.08E+10 | 2.07E+12 |
| U-233 | 1.59E+05 | 3.07E+10 | 9.61E+06 | 3.07E+10 |
| U-234 | 2.46E+05 | 2.75E+12 | 6.29E+11 | 3.38E+12 |
| U-235 | 7.04E+08 | 5.43E+09 | 3.74E+10 | 4.28E+10 |
| U-236 | 2.37E+07 | 1.18E+11 | 3.63E+11 | 4.81E+11 |
| U-238 | 4.47E+09 | 1.54E+11 | 5.65E+11 | 7.19E+11 |
| Pu-238 | 8.77E+01 | 6.04E+15 | 3.44E+15 | 9.47E+15 |
| Pu-239 | 2.41E+04 | 4.66E+14 | 4.68E+14 | 9.35E+14 |
| Pu-240 | 6.56E+03 | 6.13E+15 | 5.92E+14 | 6.72E+15 |
| Pu-241 | 1.43E+01 | 5.40E+15 | 6.26E+16 | 6.80E+16 |
| Pu-242 | 3.74E+05 | 6.74E+12 | 2.96E+12 | 9.69E+12 |
| Pu-244 | 8.00E+07 | 3.81E+06 | 1.47E+06 | 5.28E+06 |

| Nuclide | Half-life [years] | Activity [Bq] CSD-V | CSD-C | Total |
|---|---|---|---|---|
| Np-236 | 1.15E+05 | 0.00E+00 | 0.00E+00 | 0.00E+00 |
| Np-237 | 2.14E+06 | 1.66E+14 | 2.16E+11 | 1.66E+14 |
| Am-241 | 4.33E+02 | 4.20E+17 | 9.72E+14 | 4.21E+17 |
| Am-242m | 1.52E+02 | 2.23E+15 | 3.77E+12 | 2.23E+15 |
| Am-243 | 7.36E+03 | 1.34E+16 | 1.05E+15 | 1.45E+16 |
| Cm-243 | 2.85E+01 | 2.56E+15 | 3.20E+12 | 2.57E+15 |
| Cm-244 | 1.80E+01 | 9.00E+16 | 7.38E+14 | 9.07E+16 |
| Cm-245 | 8.50E+03 | 3.17E+14 | 3.28E+11 | 3.18E+14 |
| Cm-246 | 4.73E+03 | 6.78E+13 | 1.45E+11 | 6.79E+13 |
| Cm-247 | 1.56E+07 | 3.56E+08 | 7.90E+05 | 3.57E+08 |
| Cm-248 | 3.39E+05 | 2.39E+09 | 4.88E+06 | 2.40E+09 |
| Cm-250 | 6.90E+03 | 0.00E+00 | 0.00E+00 | 0.00E+00 |
| Th-229 | 7.34E+03 | 1.69E+08 | 3.55E+04 | 1.69E+08 |
| Th-230 | 7.54E+04 | 3.65E+10 | 5.04E+05 | 3.65E+10 |
| Th-232 | 1.41E+10 | 4.02E+04 | 6.06E+01 | 4.03E+04 |
| Ra-226 | 1.60E+03 | 0.00E+00 | 3.21E+02 | 3.21E+02 |
| Pa-231 | 3.28E+04 | 1.13E+10 | 7.28E+06 | 1.13E+10 |
| Ac-227 | 2.18E+01 | 2.69E+09 | 3.50E+04 | 2.69E+09 |

**Table 8-12 Estimated radionuclide inventory (DepU) in 2130 – Scenario 4 – Deployment of Gen III LWRs**

| Nuclide | Half-life [years] | Activity [Bq] |
|---|---|---|
| U-238 | 4.47E+09 | 2.03E+15 |
| U-235 | 7.04E+08 | 4.69E+13 |
| U-234 | 2.46E+05 | 4.69E+14 |
| Pa-231 | 3.28E+04 | 6.37E+10 |
| Th-230 | 7.54E+04 | 2.77E+11 |
| Ac-227 | 2.18E+01 | 3.94E+10 |
| Ra-226 | 1.60E+03 | 4.69E+09 |
| Rn-222 | 1.05E-02 | 4.69E+09 |

## 8.5. Scenario 5 – Large-scale deployment of HTRs

The following figures show the development of relevant deployment and waste parameters for this scenario. The characteristics of the waste packages are summarized in Table 8-13, whereas Table 8-14 contains the estimated radionuclide inventory in 2130.

The deployment of HTRs reactors starts in 2020, and reaches its maximum at about 2040. A total number of 28 HTRs (180 MWe) supply the anticipated 5000 MWe of electricity. Upon reaching their anticipated lifetime, the HTRs are replaced by other reactors of the same type.

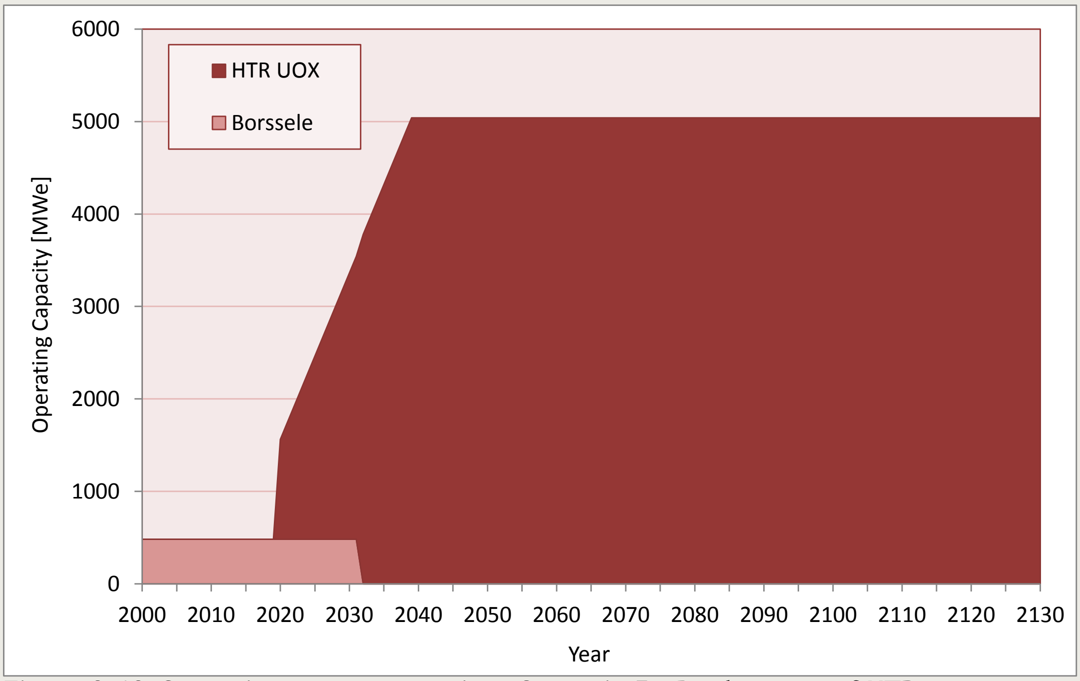


**Figure 8-13 Operating reactor capacity - Scenario 5 - Deployment of HTRs**

The number of HLW CSD-V containers is depicted in Figure 8-14. These containers originate from the operation of the Borssele NPP until 2033. The total amount of CSD-V/C containers is slightly different from the amount estimated for Scenario 2. This difference has a numerical origin and is probably caused by a slightly different decision logic in DANESS around the year of the last transfer (2037-2038) of HLW from the reprocessing plant to the surface storage "stock".

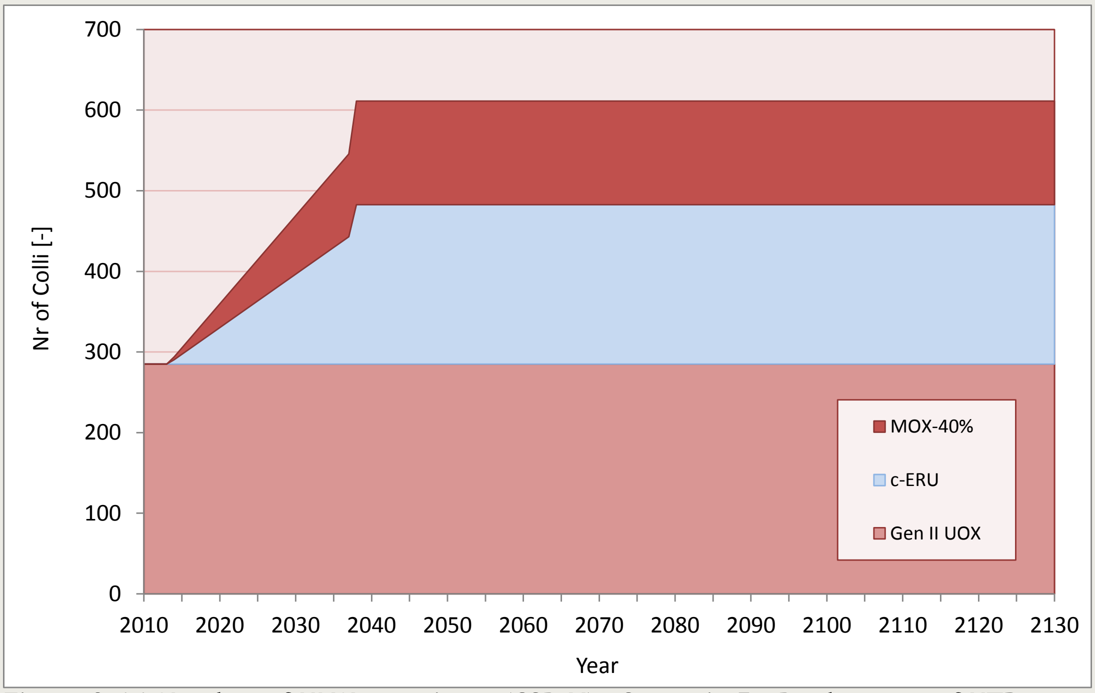


**Figure 8-14 Number of HLW containers (CSD-V) - Scenario 5 - Deployment of HTRs**

Figure 8-15 shows the number of CASTOR spent fuel containers, holding the HTR spent fuel pebbles. Due to the large volume ratio of the graphite pebbles and the UOX spent fuel coated particles the number of CASTOR containers is substantial. By the year 2130 approximately 576 million HTR spent fuel pebbles would be held in storage, having a total net volume of over 65’000 m$^3$.

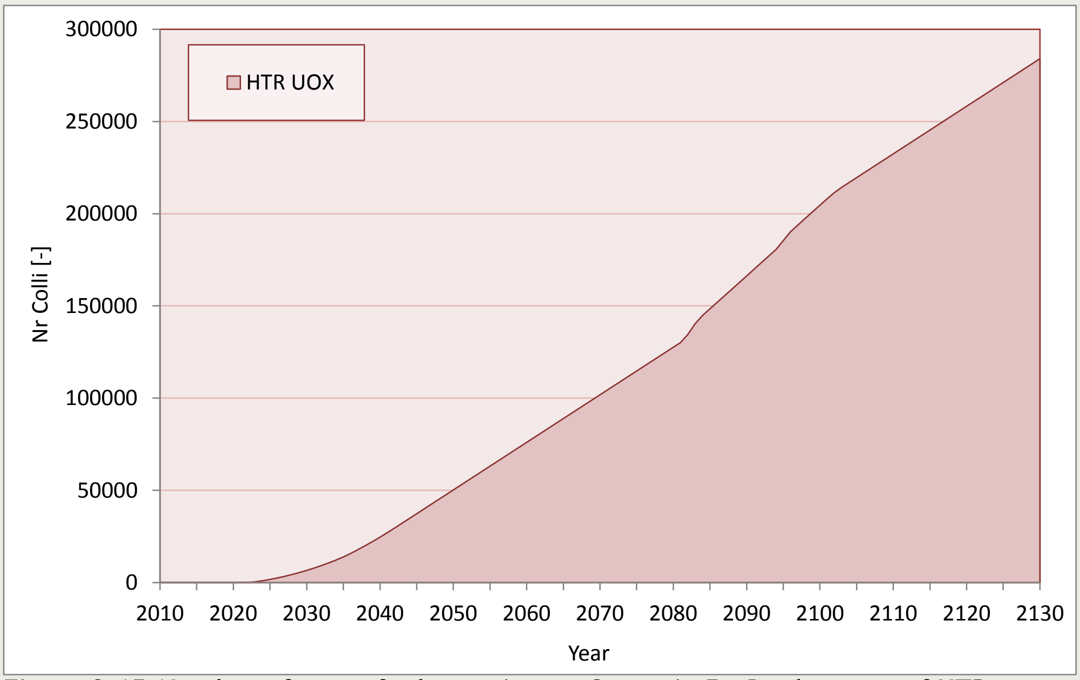


**Figure 8-15 Number of spent fuel containers - Scenario 5 - Deployment of HTRs**

The amount of depleted uranium (DepU), generated during reactor operations from 2010, is depicted in Figure 8-16. Assuming that the DepU is conditioned in KONRAD II containers (9,40 tHM DepU per container), the total amount of approximately 270’600 tHM of DepU requires 28’780 KONRAD II containers.

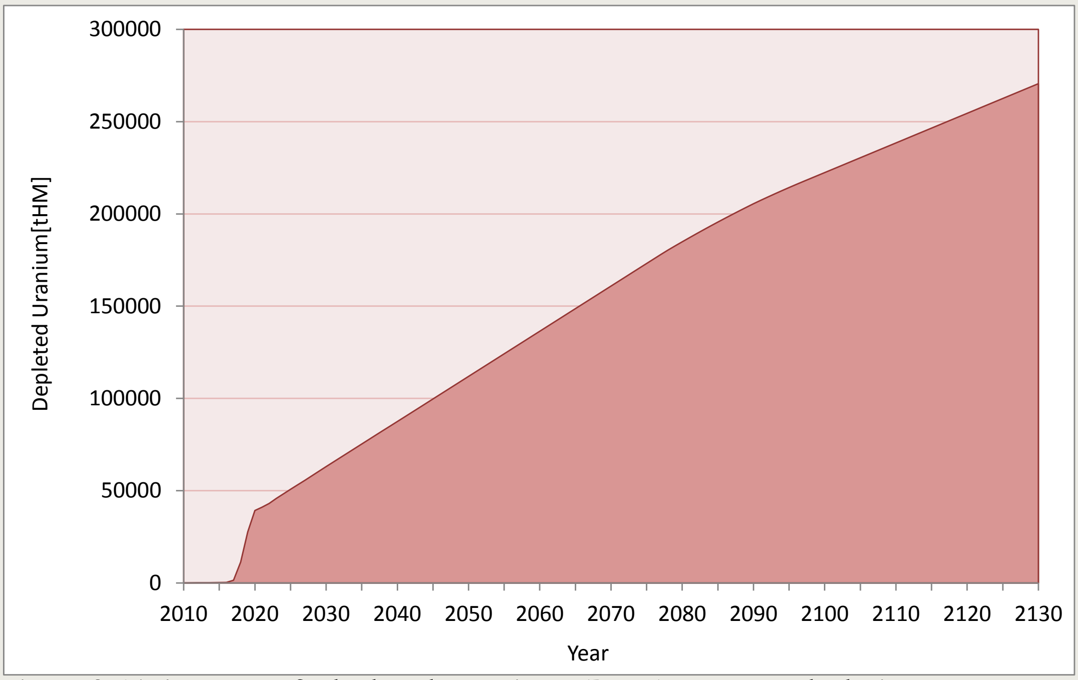


**Figure 8-16 Amount of depleted uranium (DepU) generated during reactor operations - Scenario 5 - Deployment of HTRs**

The radionuclide inventory estimated in the year 2130 is tabulated in Table 8-13 for the spent fuel and HLW, and in Table 8-15 for the depleted uranium. Because of the significant quantities of DepU, the ingrowth of relevant uranium daughter nuclides has been taken into account.

**Table 8-13 Waste characteristics per 2130 – Scenario 5 – Deployment of HTRs**

| | Gen II UOX-33 | c-ERU | MOX-40% | HTR UOX |
|---|---|---|---|---|
| Number of CSD-V canisters | 285 | 198 | 129 | |
| Number of CSD-C canisters | 570 | 396 | 258 | |
| Number of CASTOR containers (Spent Fuel) | | | | 284000 |
| Number of CSD-V canisters per TWhr | | 2.88 | | |
| Number of CSD-C canisters per TWhr | | 5.76 | | |
| Number of CASTOR containers per TWhr | | | | 55.5 |
| Number of KONRAD II containers (DepU) | 28780 | | | |

**Table 8-14 Estimated radionuclide inventory in 2130 – Scenario 5 – Deployment of HTRs**

| | *Activity [Bq]* | | | | |
|---|---|---|---|---|---|
| **Nuclide** | ***Half-life [years]*** | ***CSD-V*** | ***CSD-C*** | ***HTR SF*** | ***Total*** |
| C-14 | 5.70E+03 | 6.15E+11 | 1.69E+13 | 5.78E+12 | 2.33E+13 |
| Cl-36 | 3.01E+05 | 4.77E+11 | 0.00E+00 | 0.00E+00 | 4.77E+11 |
| Ca-41 | 1.40E+05 | 1.98E+11 | 0.00E+00 | 0.00E+00 | 1.98E+11 |
| Ni-59 | 7.60E+04 | 1.62E+12 | 4.38E+14 | 0.00E+00 | 4.40E+14 |
| Ni-63 | 1.01E+02 | 2.05E+16 | 1.54E+16 | 2.19E+10 | 3.60E+16 |
| Se-79 | 3.77E+05 | 2.20E+12 | 6.72E+10 | 2.67E+13 | 2.89E+13 |
| Kr-85 | 1.08E+01 | 0.00E+00 | 0.00E+00 | 7.16E+17 | 7.16E+17 |
| Sr-90 | 2.88E+01 | 9.61E+16 | 2.47E+15 | 1.35E+19 | 1.36E+19 |
| Zr-93 | 1.53E+06 | 5.53E+13 | 3.67E+11 | 8.15E+14 | 8.70E+14 |
| Mo-93 | 4.00E+03 | 0.00E+00 | 7.10E+12 | 0.00E+00 | 7.10E+12 |
| Nb-94 | 2.00E+04 | 7.15E+11 | 6.79E+13 | 4.37E+10 | 6.86E+13 |
| Tc-99 | 2.14E+05 | 5.75E+14 | 2.81E+12 | 6.04E+15 | 6.62E+15 |
| Pd-107 | 6.50E+06 | 4.79E+12 | 1.43E+10 | 4.78E+13 | 5.26E+13 |
| Ag-108m | 4.18E+02 | 1.70E+08 | 0.00E+00 | 6.07E+09 | 6.24E+09 |
| Sn-126 | 1.00E+05 | 2.32E+13 | 1.08E+11 | 3.58E+14 | 3.81E+14 |
| I-129 | 1.61E+07 | 7.94E+10 | 6.48E+10 | 1.35E+13 | 1.36E+13 |
| Cs-135 | 2.30E+06 | 1.95E+13 | 8.68E+10 | 1.11E+14 | 1.31E+14 |
| Cs-137 | 3.00E+01 | 1.68E+17 | 1.47E+15 | 1.91E+19 | 1.93E+19 |
| Sm-151 | 9.00E+01 | 2.72E+15 | 3.14E+13 | 7.89E+16 | 8.16E+16 |
| U-232 | 6.88E+01 | 2.55E+10 | 4.39E+08 | 1.22E+11 | 1.48E+11 |
| U-233 | 1.59E+05 | 6.80E+08 | 3.91E+05 | 2.12E+08 | 8.93E+08 |
| U-234 | 2.46E+05 | 1.02E+11 | 4.56E+10 | 7.12E+13 | 7.14E+13 |
| U-235 | 7.04E+08 | 3.02E+08 | 1.52E+09 | 3.61E+12 | 3.61E+12 |
| U-236 | 2.37E+07 | 5.32E+09 | 1.48E+10 | 1.16E+14 | 1.16E+14 |
| U-238 | 4.47E+09 | 6.62E+09 | 2.30E+10 | 4.31E+13 | 4.32E+13 |
| Pu-238 | 8.77E+01 | 1.08E+14 | 8.42E+13 | 4.56E+17 | 4.56E+17 |
| Pu-239 | 2.41E+04 | 1.59E+13 | 1.91E+13 | 4.85E+16 | 4.85E+16 |
| Pu-240 | 6.56E+03 | 2.83E+14 | 2.40E+13 | 1.45E+17 | 1.46E+17 |

| | Activity [Bq] | | | | |
|---|---|---|---|---|---|
| Nuclide | Half-life [years] | CSD-V | CSD-C | HTR SF | Total |
| Pu-241 | 1.43E+01 | 8.87E+12 | 6.70E+13 | 7.66E+18 | 7.66E+18 |
| Pu-242 | 3.74E+05 | 1.92E+11 | 1.20E+11 | 1.44E+15 | 1.44E+15 |
| Pu-244 | 8.00E+07 | 8.43E+04 | 6.00E+04 | 3.61E+08 | 3.61E+08 |
| Np-236 | 1.15E+05 | 0.00E+00 | 0.00E+00 | 1.74E+08 | 1.74E+08 |
| Np-237 | 2.14E+06 | 1.03E+13 | 8.80E+09 | 6.42E+13 | 7.45E+13 |
| Am-241 | 4.33E+02 | 3.45E+16 | 3.58E+13 | 1.24E+16 | 4.70E+16 |
| Am-242m | 1.52E+02 | 3.83E+13 | 1.15E+11 | 6.84E+14 | 7.22E+14 |
| Am-243 | 7.36E+03 | 7.75E+14 | 4.23E+13 | 8.72E+15 | 9.54E+15 |
| Cm-243 | 2.85E+01 | 1.25E+13 | 2.40E+10 | 2.06E+15 | 2.07E+15 |
| Cm-244 | 1.80E+01 | 6.35E+14 | 1.79E+12 | 5.07E+17 | 5.08E+17 |
| Cm-245 | 8.50E+03 | 1.26E+13 | 1.33E+10 | 1.44E+14 | 1.56E+14 |
| Cm-246 | 4.73E+03 | 1.49E+12 | 5.85E+09 | 3.51E+13 | 3.66E+13 |
| Cm-247 | 1.56E+07 | 7.89E+06 | 3.22E+04 | 6.86E+07 | 7.66E+07 |
| Cm-248 | 3.39E+05 | 5.31E+07 | 1.99E+05 | 2.15E+08 | 2.68E+08 |
| Cm-250 | 6.90E+03 | 0.00E+00 | 0.00E+00 | 1.81E+03 | 1.81E+03 |
| Th-229 | 7.34E+03 | 3.73E+06 | 1.44E+03 | 2.32E+06 | 6.05E+06 |
| Th-230 | 7.54E+04 | 8.09E+08 | 2.05E+04 | 4.89E+06 | 8.13E+08 |
| Th-232 | 1.41E+10 | 8.91E+02 | 2.47E+00 | 6.64E+03 | 7.54E+03 |
| Ra-226 | 1.60E+03 | 0.00E+00 | 1.27E+01 | 0.00E+00 | 1.27E+01 |
| Pa-231 | 3.28E+04 | 2.50E+08 | 2.96E+05 | 1.22E+08 | 3.72E+08 |
| Ac-227 | 2.18E+01 | 7.68E+06 | 1.46E+02 | 4.38E+05 | 8.11E+06 |

**Table 8-15 Estimated radionuclide inventory (DepU) in 2130 – Scenario 5 – Deployment of HTRs**

| Nuclide | Half-life [years] | Activity [Bq] |
|---|---|---|
| U-238 | 4.47E+09 | 3.35E+15 |
| U-235 | 7.04E+08 | 7.72E+13 |
| U-234 | 2.46E+05 | 7.73E+14 |
| Pa-231 | 3.28E+04 | 1.10E+11 |
| Th-230 | 7.54E+04 | 4.79E+11 |
| Ac-227 | 2.18E+01 | 6.97E+10 |
| Ra-226 | 1.60E+03 | 8.51E+09 |
| Rn-222 | 1.05E-02 | 8.51E+09 |

## 8.6. Scenario 6 - Deployment of fast reactors

The following figures show the development of relevant deployment and waste parameters for this scenario. The characteristics of the waste packages are summarized in Table 8-16, whereas Table 8-17 contains the estimated radionuclide inventory in 2130.

From 2020 on, LWR Gen III reactors are capable to fill the nuclear electricity demand, whereas the first Gen IV reactor starts its operation around 2040. Note the temporary drop in electricity production from about 2085 to 2095, which is likely due to a numerical issue in the decision logic of DANESS. As the Gen III reach their end of life, they are gradually replaced by Gen IV reactors. That transition would be completed around 2100.

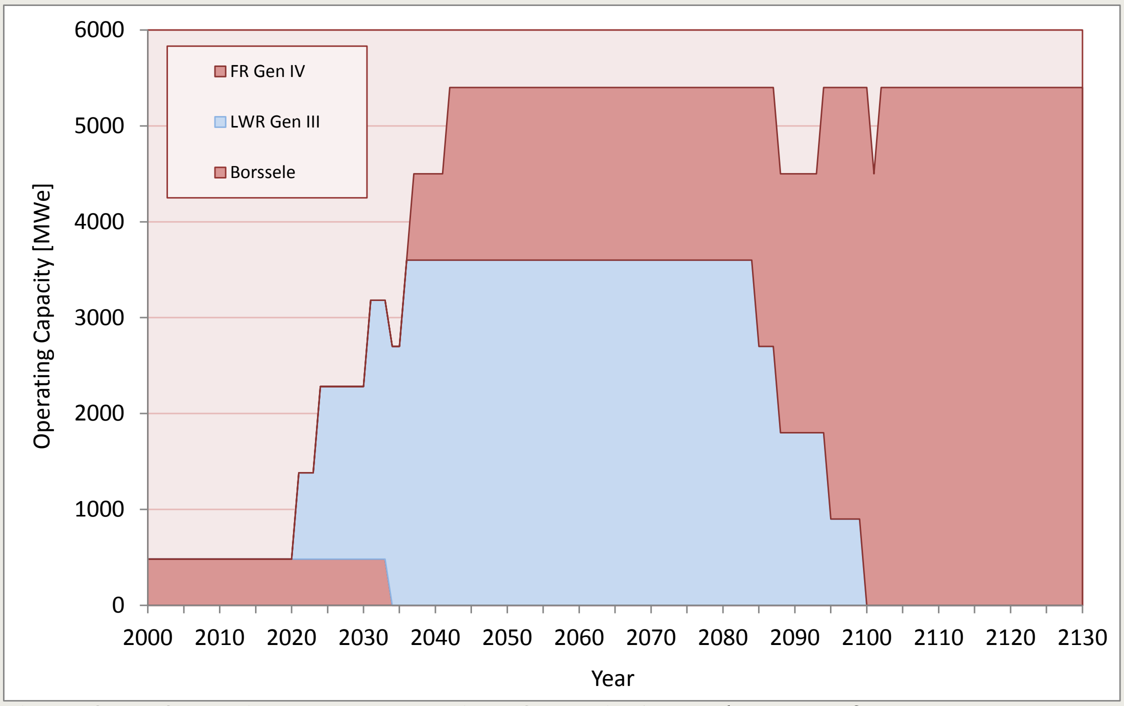


**Figure 8-17 Operating reactor capacity - Scenario 6 - Deployment of Fast Reactors**

Figure 8-18 shows that the amount of CSD-V containers originating from the reprocessing of Gen IV spent fuel is substantially less than that for the LWR-type HLW. The Gen-IV reactors generate about half the amount of HLW canisters per TWh of electricity produced compared to the LWR Gen III reactors (see also Table 8-16).

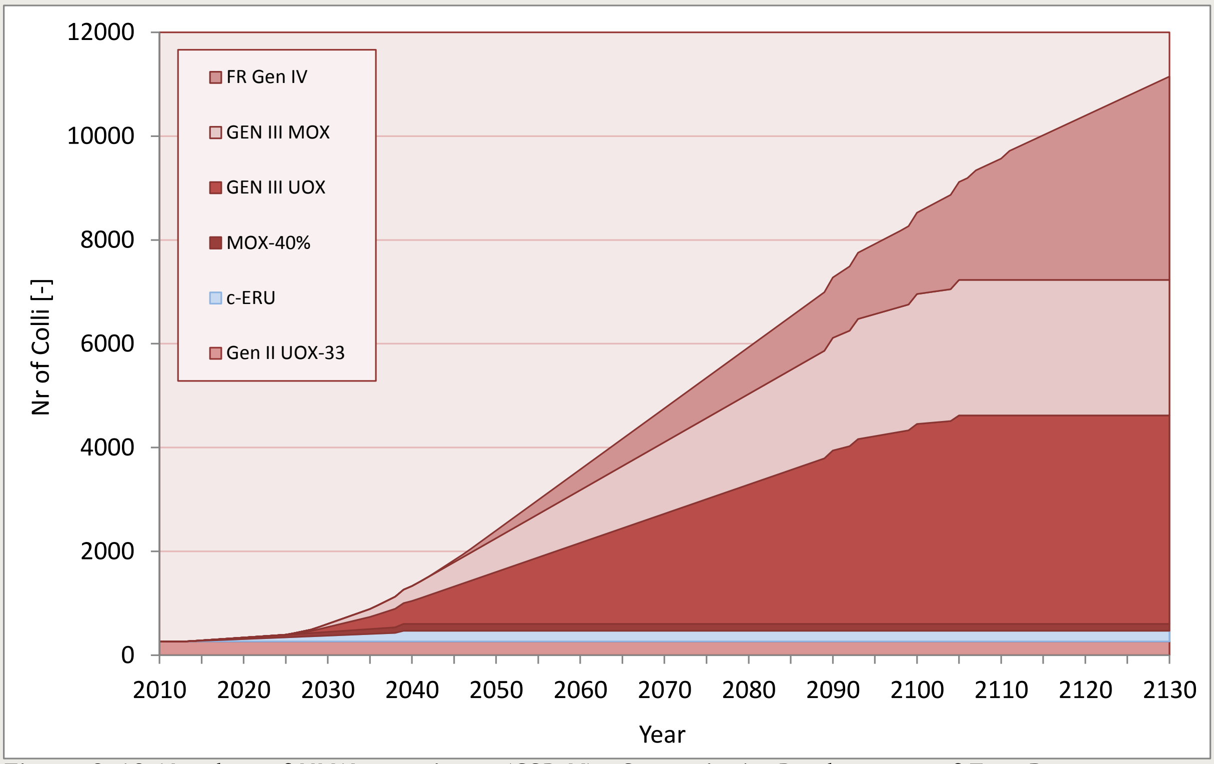


**Figure 8-18 Number of HLW containers (CSD-V) - Scenario 6 - Deployment of Fast Reactors**

The amount of depleted uranium (DepU), generated during reactor operations from 2010, is depicted in Figure 8-19. Around the turn of the century, when the LWR Gen-III reactors are replaced by Gen-IV reactors, the stock of DepU slowly decreases because DepU is used to fabricate the Gen-IV fuel. Assuming that the DepU is conditioned in KONRAD II containers (9,40 tHM DepU per container), the total amount of approximately 26’000 tHM of DepU requires 5530 KONRAD II containers.

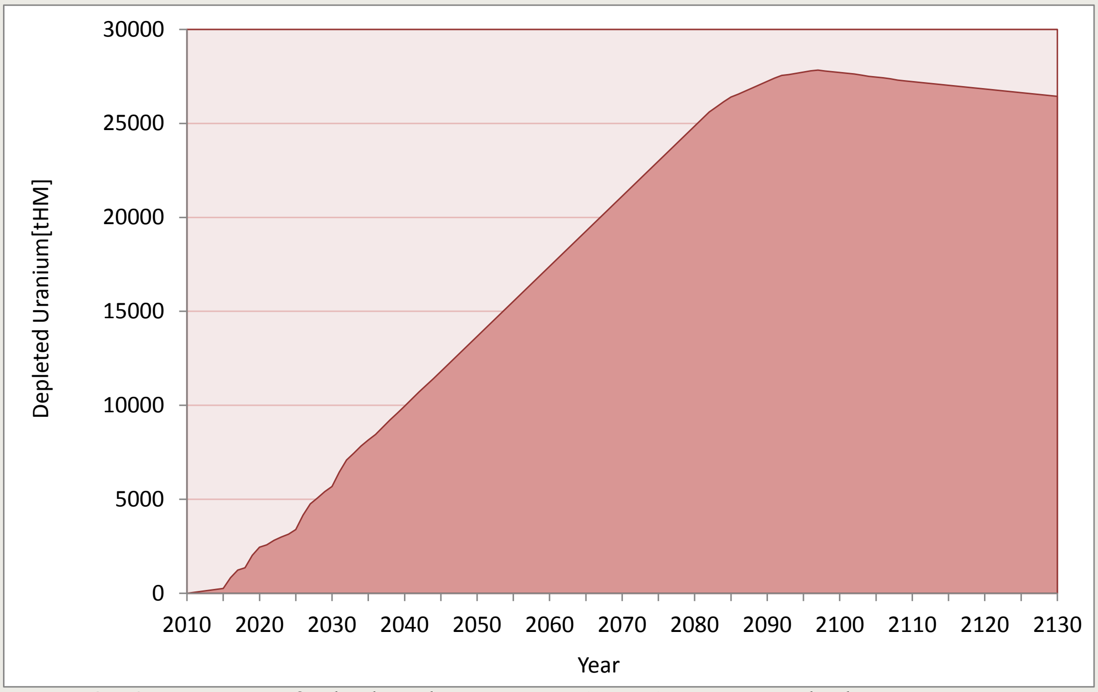


**Figure 8-19 Amount of depleted uranium (DepU) generated during reactor operations - Scenario 6 – Deployment of Fast Reactors**

**Table 8-16 Waste container characteristics per 2130 – Scenario 6 – Deployment of Fast Reactors**

| | Gen II UOX-33 | c-ERU | MOX-40% | Gen III UOX | Gen III MOX | Gen IV |
|---|---|---|---|---|---|---|
| Number of CSD-V canisters | 285 | 205 | 133 | 4015 | 2610 | 3920 |
| Number of CSD-C canisters | 570 | 410 | 263 | 8030 | 5220 | 7840 |
| Number of CSD-V canisters per TWhr | | 2.88 | | 2.92 | | 1.59 |
| Number of CSD-C canisters per TWhr | | 5.76 | | 5.48 | | 3.18 |
| Number of KONRAD II containers (DepU) | 5530 | | | | | |

The radionuclide inventory estimated in the year 2130 is tabulated in Table 8-17 for the HLW, and in Table 8-18 for the depleted uranium. Because of the significant quantities of DepU, the ingrowth of relevant uranium daughter nuclides has been taken into account.

Table 8-17 Estimated radionuclide inventory in 2130 - Scenario 6 - Deployment of Fast Reactors

| | Activity [Bq] | | | |
|---|---|---|---|---|
| **Nuclide** | ***Half-life [years]*** | ***CSD-V*** | ***CSD-C*** | ***Total*** |
| C-14 | 5.70E+03 | 6.71E+13 | 3.11E+14 | 3.78E+14 |
| Cl-36 | 3.01E+05 | 1.02E+13 | 0.00E+00 | 1.02E+13 |
| Ca-41 | 1.40E+05 | 7.17E+12 | 0.00E+00 | 7.17E+12 |
| Ni-59 | 7.60E+04 | 4.31E+13 | 8.01E+15 | 8.06E+15 |
| Ni-63 | 1.01E+02 | 5.76E+17 | 4.25E+17 | 1.00E+18 |
| Se-79 | 3.77E+05 | 3.24E+13 | 1.23E+12 | 3.37E+13 |
| Kr-85 | 1.08E+01 | 0.00E+00 | 0.00E+00 | 0.00E+00 |
| Sr-90 | 2.88E+01 | 2.75E+18 | 2.17E+17 | 2.97E+18 |
| Zr-93 | 1.53E+06 | 8.26E+14 | 6.70E+12 | 8.32E+14 |
| Mo-93 | 4.00E+03 | 0.00E+00 | 1.31E+14 | 1.31E+14 |
| Nb-94 | 2.00E+04 | 1.53E+13 | 1.24E+15 | 1.26E+15 |
| Tc-99 | 2.14E+05 | 7.51E+15 | 5.14E+13 | 7.56E+15 |
| Pd-107 | 6.50E+06 | 1.03E+14 | 2.62E+11 | 1.03E+14 |
| Ag-108m | 4.18E+02 | 1.17E+10 | 0.00E+00 | 1.17E+10 |
| Sn-126 | 1.00E+05 | 4.73E+14 | 1.97E+12 | 4.75E+14 |
| I-129 | 1.61E+07 | 2.61E+11 | 1.18E+12 | 1.44E+12 |
| Cs-135 | 2.30E+06 | 5.56E+14 | 1.59E+12 | 5.57E+14 |
| Cs-137 | 3.00E+01 | 6.64E+18 | 1.20E+17 | 6.76E+18 |
| Sm-151 | 9.00E+01 | 3.70E+17 | 9.09E+14 | 3.71E+17 |
| U-232 | 6.88E+01 | 8.83E+11 | 1.48E+10 | 8.97E+11 |
| U-233 | 1.59E+05 | 1.46E+10 | 7.15E+06 | 1.46E+10 |
| U-234 | 2.46E+05 | 2.73E+12 | 4.99E+11 | 3.23E+12 |
| U-235 | 7.04E+08 | 2.83E+09 | 2.78E+10 | 3.07E+10 |
| U-236 | 2.37E+07 | 5.98E+10 | 2.70E+11 | 3.30E+11 |
| U-238 | 4.47E+09 | 9.31E+10 | 4.21E+11 | 5.14E+11 |
| Pu-238 | 8.77E+01 | 6.36E+15 | 2.47E+15 | 8.84E+15 |
| Pu-239 | 2.41E+04 | 5.89E+14 | 3.49E+14 | 9.37E+14 |
| Pu-240 | 6.56E+03 | 3.84E+15 | 4.41E+14 | 4.28E+15 |
| Pu-241 | 1.43E+01 | 2.52E+15 | 3.88E+16 | 4.13E+16 |
| Pu-242 | 3.74E+05 | 5.42E+12 | 2.20E+12 | 7.62E+12 |
| Pu-244 | 8.00E+07 | 2.83E+06 | 1.10E+06 | 3.93E+06 |
| Np-236 | 1.15E+05 | 0.00E+00 | 0.00E+00 | 0.00E+00 |
| Np-237 | 2.14E+06 | 8.21E+13 | 1.61E+11 | 8.22E+13 |
| Am-241 | 4.33E+02 | 2.10E+17 | 7.18E+14 | 2.11E+17 |
| Am-242m | 1.52E+02 | 1.14E+15 | 2.75E+12 | 1.14E+15 |
| Am-243 | 7.36E+03 | 6.65E+15 | 7.78E+14 | 7.43E+15 |
| Cm-243 | 2.85E+01 | 7.89E+14 | 2.15E+12 | 7.91E+14 |
| Cm-244 | 1.80E+01 | 2.07E+16 | 4.71E+14 | 2.12E+16 |
| Cm-245 | 8.50E+03 | 1.59E+14 | 2.44E+11 | 1.60E+14 |
| Cm-246 | 4.73E+03 | 3.55E+13 | 1.08E+11 | 3.56E+13 |
| Cm-247 | 1.56E+07 | 2.34E+08 | 5.88E+05 | 2.35E+08 |
| Cm-248 | 3.39E+05 | 1.35E+09 | 3.63E+06 | 1.36E+09 |
| Cm-250 | 6.90E+03 | 0.00E+00 | 0.00E+00 | 0.00E+00 |
| Th-229 | 7.34E+03 | 3.41E+08 | 2.64E+04 | 3.41E+08 |
| Th-230 | 7.54E+04 | 2.73E+10 | 3.75E+05 | 2.73E+10 |
| Th-232 | 1.41E+10 | 1.96E+04 | 4.51E+01 | 1.97E+04 |
| Ra-226 | 1.60E+03 | 0.00E+00 | 2.38E+02 | 2.38E+02 |
| Pa-231 | 3.28E+04 | 5.54E+09 | 5.42E+06 | 5.54E+09 |

| Nuclide | Activity [Bq] | | | |
|---|---|---|---|---|
| | *Half-life [years]* | *CSD-V* | *CSD-C* | *Total* |
| Ac-227 | 2.18E+01 | 7.43E+08 | 2.29E+04 | 7.43E+08 |

**Table 8-18 Estimated radionuclide inventory (DepU) in 2130 - Scenario 6 - Deployment of Fast Reactors**

| Nuclide | *Half-life [years]* | *Activity [Bq]* |
|---|---|---|
| U-238 | 4.47E+09 | 3.27E+14 |
| U-235 | 7.04E+08 | 7.55E+12 |
| U-234 | 2.46E+05 | 7.55E+13 |
| Pa-231 | 3.28E+04 | 1.31E+10 |
| Th-230 | 7.54E+04 | 5.70E+10 |
| Ac-227 | 2.18E+01 | 8.49E+09 |
| Ra-226 | 1.60E+03 | 1.03E+09 |
| Rn-222 | 1.05E-02 | 1.03E+09 |

## *8.7. Scenario 7 - Deployment of thorium-based reactors.*

The following figures show the development of relevant deployment and waste parameters for this scenario. The characteristics of the waste packages are summarized in Table 8-19, whereas Table 8-20 contains the estimated radionuclide inventory in 2130.

From 2020 on, LWR Gen III reactors are capable to fill the nuclear electricity demand, whereas the first thorium-fueled reactor starts its operation around 2030. As the Gen III reactors reach their end of life, they are gradually replaced by thorium reactors. That transition would be completed around 2100.

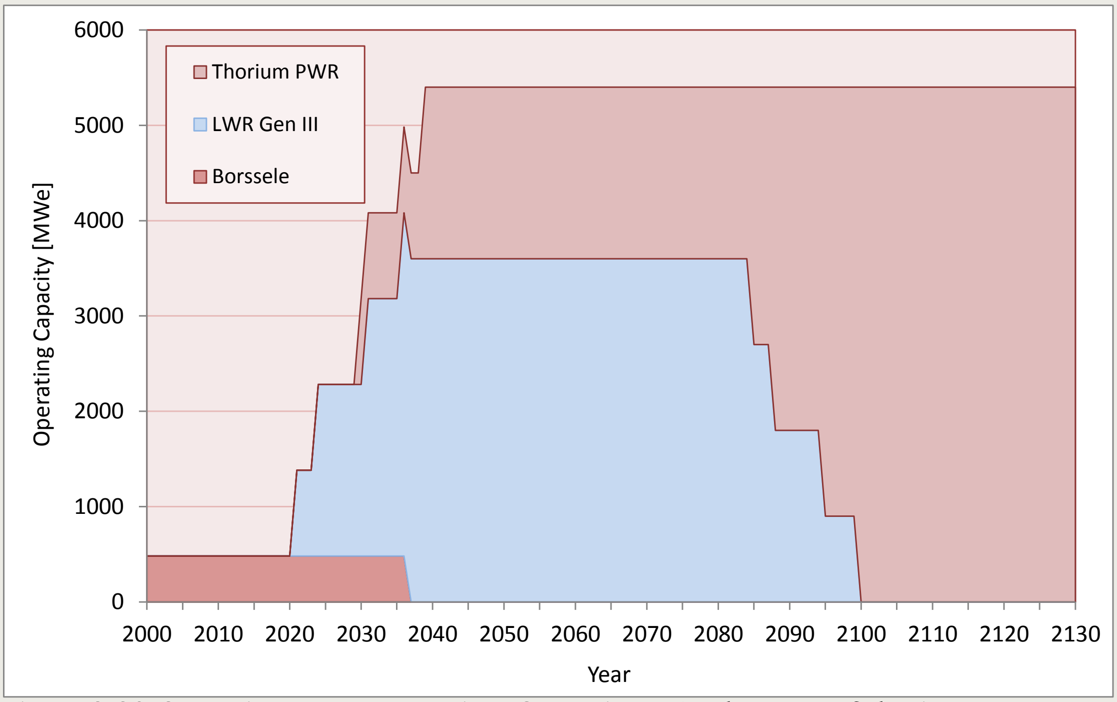


**Figure 8-20 Operating reactor capacity - Scenario 7 - Deployment of thorium reactors**

Figure 8-21 shows that the amount of CSD-V containers originating from the reprocessing of thorium spent fuel is substantially less than that for the LWR-type HLW. The thorium reactors generate about 30% the amount of HLW canisters per TWh of electricity produced, compared to the LWR Gen III reactors (see also Table 8-19).

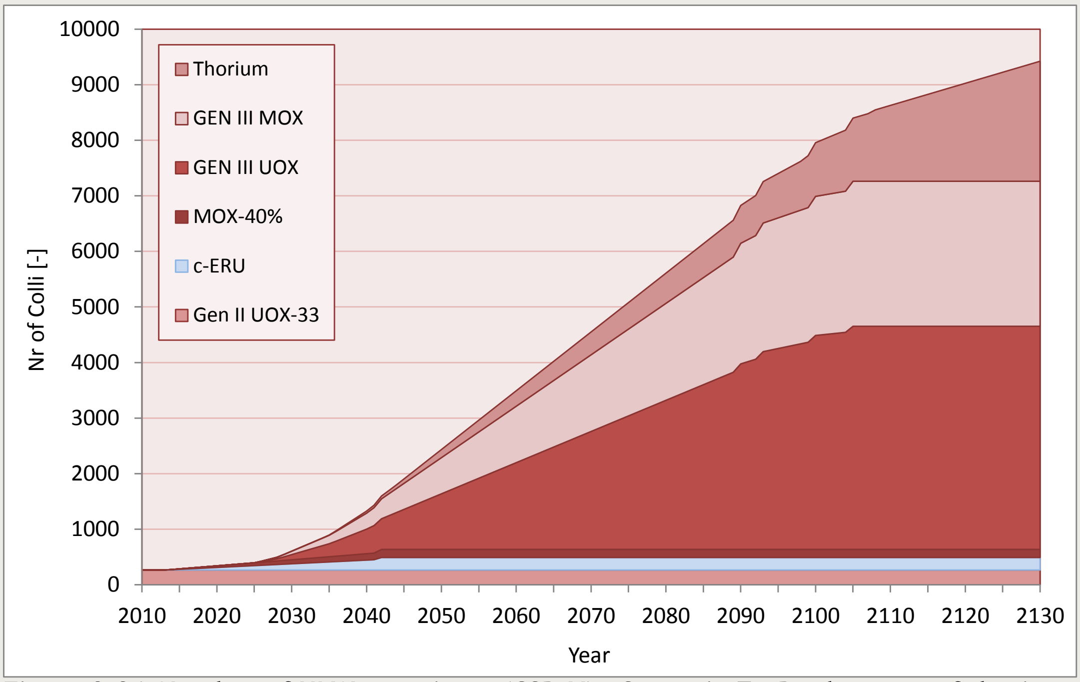


**Figure 8-21 Number of HLW containers (CSD-V) - Scenario 7 - Deployment of thorium reactors**

The amount of depleted uranium (DepU), generated during reactor operations from 2010, is depicted in Figure 8-22. From around the turn of the century, when the LWR Gen-III reactors are replaced by thorium reactors, the stock of DepU remains constant since no fresh uranium fuel is needed any more. Assuming that the DepU is conditioned in KONRAD II containers (9,40 tHM DepU per container), the total amount of approximately 25250 tHM of DepU requires 5370 KONRAD II containers.

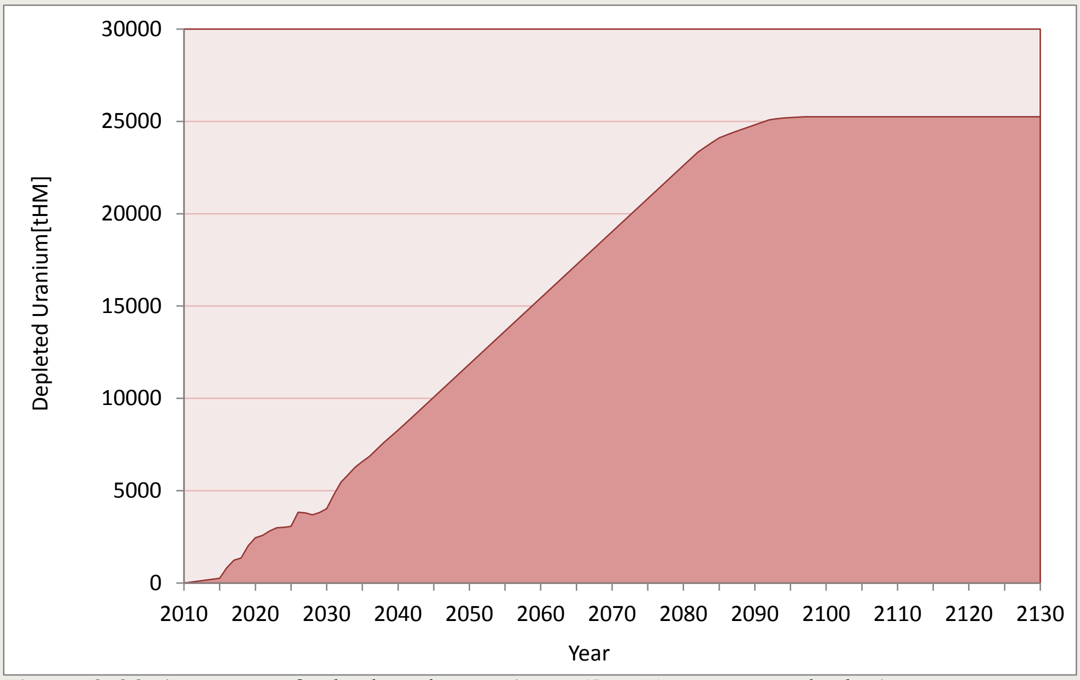


**Figure 8-22 Amount of depleted uranium (DepU) generated during reactor operations - Scenario 7 - Deployment of thorium reactors**

**Table 8-19 Waste container characteristics per 2130 - Scenario 7 - Deployment of thorium reactors**

| | Gen II UOX-33 | c-ERU | MOX-40% | Gen III UOX | Gen III MOX | Thorium Fuel |
|---|---|---|---|---|---|---|
| Number of CSD-V canisters | 285 | 225 | 146 | 4015 | 2610 | 2180 |
| Number of CSD-C canisters | 570 | 450 | 292 | 8030 | 5220 | 4360 |
| Number of CSD-V canisters per TWhr | | 2.88 | | 2.92 | | 0.85 |
| Number of CSD-C canisters per TWhr | | 5.76 | | 5.84 | | 1.70 |
| Number of KONRAD II containers (DepU) | 5370 | | | | | |

The radionuclide inventory estimated in the year 2130 is tabulated in Table 8-20 for the HLW, and in Table 8-21 for the depleted uranium. Because of the significant quantities of DepU, the ingrowth of relevant uranium daughter nuclides has been taken into account.

**Table 8-20 Estimated radionuclide inventory in 2130 - Scenario 7 - Deployment of thorium reactors**

| | | ***Activity [Bq]*** | | |
|---|---|---|---|---|
| **Nuclide** | ***Half-life [years]*** | ***CSD-V*** | ***CSD-C*** | ***Total*** |
| C-14 | 5.70E+03 | 1.33E+13 | 2.63E+14 | 2.76E+14 |
| Cl-36 | 3.01E+05 | 1.02E+13 | 0.00E+00 | 1.02E+13 |
| Ca-41 | 1.40E+05 | 4.25E+12 | 0.00E+00 | 4.25E+12 |
| Ni-59 | 7.60E+04 | 3.48E+13 | 6.79E+15 | 6.83E+15 |
| Ni-63 | 1.01E+02 | 5.78E+17 | 3.48E+17 | 9.26E+17 |
| Se-79 | 3.77E+05 | 2.04E+13 | 1.04E+12 | 2.14E+13 |
| Kr-85 | 1.08E+01 | 1.19E+16 | 0.00E+00 | 1.19E+16 |
| Sr-90 | 2.88E+01 | 1.70E+18 | 1.62E+17 | 1.86E+18 |
| Zr-93 | 1.53E+06 | 5.72E+14 | 5.68E+12 | 5.78E+14 |

| | Activity [Bq] | | | |
|---|---|---|---|---|
| **Nuclide** | *Half-life [years]* | *CSD-V* | *CSD-C* | *Total* |
| Mo-93 | 4.00E+03 | 0.00E+00 | 1.11E+14 | 1.11E+14 |
| Nb-94 | 2.00E+04 | 1.54E+13 | 1.05E+15 | 1.07E+15 |
| Tc-99 | 2.14E+05 | 5.13E+15 | 4.35E+13 | 5.17E+15 |
| Pd-107 | 6.50E+06 | 6.52E+13 | 2.22E+11 | 6.54E+13 |
| Ag-108m | 4.18E+02 | 3.88E+09 | 0.00E+00 | 3.88E+09 |
| Sn-126 | 1.00E+05 | 2.82E+14 | 1.67E+12 | 2.84E+14 |
| I-129 | 1.61E+07 | 4.35E+11 | 1.00E+12 | 1.44E+12 |
| Cs-135 | 2.30E+06 | 2.50E+14 | 1.34E+12 | 2.52E+14 |
| Cs-137 | 3.00E+01 | 3.53E+18 | 9.03E+16 | 3.62E+18 |
| Sm-151 | 9.00E+01 | 8.52E+16 | 7.41E+14 | 8.60E+16 |
| U-232 | 6.88E+01 | 5.35E+12 | 1.19E+10 | 5.36E+12 |
| U-233 | 1.59E+05 | 8.41E+11 | 6.06E+06 | 8.41E+11 |
| U-234 | 2.46E+05 | 1.72E+12 | 4.52E+11 | 2.18E+12 |
| U-235 | 7.04E+08 | 2.71E+09 | 2.36E+10 | 2.63E+10 |
| U-236 | 2.37E+07 | 5.78E+10 | 2.29E+11 | 2.87E+11 |
| U-238 | 4.47E+09 | 7.50E+10 | 3.56E+11 | 4.31E+11 |
| Pu-238 | 8.77E+01 | 3.52E+15 | 2.01E+15 | 5.53E+15 |
| Pu-239 | 2.41E+04 | 2.31E+14 | 2.95E+14 | 5.27E+14 |
| Pu-240 | 6.56E+03 | 3.09E+15 | 3.73E+14 | 3.46E+15 |
| Pu-241 | 1.43E+01 | 3.33E+15 | 2.56E+16 | 2.89E+16 |
| Pu-242 | 3.74E+05 | 3.62E+12 | 1.86E+12 | 5.49E+12 |
| Pu-244 | 8.00E+07 | 1.82E+06 | 9.29E+05 | 2.75E+06 |
| Np-236 | 1.15E+05 | 0.00E+00 | 0.00E+00 | 0.00E+00 |
| Np-237 | 2.14E+06 | 8.23E+13 | 1.36E+11 | 8.24E+13 |
| Am-241 | 4.33E+02 | 2.09E+17 | 6.04E+14 | 2.10E+17 |
| Am-242m | 1.52E+02 | 9.93E+14 | 2.28E+12 | 9.96E+14 |
| Am-243 | 7.36E+03 | 6.65E+15 | 6.59E+14 | 7.31E+15 |
| Cm-243 | 2.85E+01 | 7.68E+14 | 1.60E+12 | 7.69E+14 |
| Cm-244 | 1.80E+01 | 2.02E+16 | 3.26E+14 | 2.05E+16 |
| Cm-245 | 8.50E+03 | 1.54E+14 | 2.07E+11 | 1.54E+14 |
| Cm-246 | 4.73E+03 | 3.22E+13 | 9.12E+10 | 3.23E+13 |
| Cm-247 | 1.56E+07 | 1.69E+08 | 4.98E+05 | 1.70E+08 |
| Cm-248 | 3.39E+05 | 1.14E+09 | 3.08E+06 | 1.14E+09 |
| Cm-250 | 6.90E+03 | 0.00E+00 | 0.00E+00 | 0.00E+00 |
| Th-229 | 7.34E+03 | 8.04E+07 | 2.24E+04 | 8.04E+07 |
| Th-230 | 7.54E+04 | 1.73E+10 | 3.18E+05 | 1.73E+10 |
| Th-232 | 1.41E+10 | 2.48E+08 | 3.82E+01 | 2.48E+08 |
| Ra-226 | 1.60E+03 | 0.00E+00 | 2.02E+02 | 2.02E+02 |
| Pa-231 | 3.28E+04 | 2.49E+13 | 4.59E+06 | 2.49E+13 |
| Ac-227 | 2.18E+01 | 6.77E+08 | 1.64E+04 | 6.77E+08 |

**Table 8-21 Estimated radionuclide inventory (DepU) in 2130 - Scenario 1 - No new nuclear power plants**

| **Nuclide** | *Half-life [years]* | *Activity [Bq]* |
|---|---|---|
| U-238 | 4.47E+09 | 3.12E+14 |
| U-235 | 7.04E+08 | 7.21E+12 |
| U-234 | 2.46E+05 | 7.21E+13 |
| Pa-231 | 3.28E+04 | 1.19E+10 |
| Th-230 | 7.54E+04 | 5.17E+10 |

| Nuclide | *Half-life [years]* | *Activity [Bq]* |
|---|---|---|
| Ac-227 | 2.18E+01 | 7.62E+09 |
| Ra-226 | 1.60E+03 | 9.14E+08 |
| Rn-222 | 1.05E-02 | 9.14E+08 |

It has to be noted that the DANESS has been set up as a uranium fuel cycle analysis tool. In order to apply DANESS to a thorium fuel cycle the code would need significant modifications, e.g. including the thorium mining, conversion, enrichment steps in the fuel cycle, provisions to properly model thorium reprocessing steps, and adding other thorium-specific features (resources, price, etc.). For those reasons, the results of the presently assessed thorium fuel cycle must be regarded as indicative.

## 8.8. Summary and evaluation of the results

A summarizing overview of the radionuclide inventories of the respective anticipated types of radioactive waste in the year 2130, generated by the seven considered scenarios is given in Table 8-22. For each scenario the activities of the spent fuels and high-level wastes (both CSD-V and CSD-C) have been agregated. An overview of the radionuclide inventories due to the storage of depleted uranium, including relevant daughters due to the ingrowth from U-234, U-235, and U-238, is provided in Table 8-23.

Characteristics of the waste forms (containers, canisters) are provided in Table 8-24. The following observations apply:

- The number of HLW containers per TWhr, both CSD-V and CSD-C, is similar for the scenarios that utilize UOX or a mixture of UOX and MOX fuel.
- Comparing the inventories estimated for Scenarios 1 (no new reactors), and Scenario 2 (Application of MOX fuel) shows a larger total activity for Scenario 1. The main contributors to the total activities in both scenarios are Sr-90 and Cs-137. For Scenario 1 these inventories are about 2 times higher than for Scenario 3. Hereby it must be taken into account that the inventories of the HLW in Scenario 1 have been obtained from COVRA, whereas the compositions of the UOX and MOX spent fuel in Scenario 2 are based on information provided by the RED-IMPACT project (see also Section 7.2).
- Comparing the inventories estimated for Scenarios 2 (Application of MOX fuel) and 3 (No reprocessing) shows that in the last scenario considerable more plutonium and uranium (several hundred times more), and about 10-20 times more curium must be disposed. During the reprocessing step (Scenario 2) these nuclides are removed from the nuclear waste and stored at locations outside the Netherlands.
- For the thorium cycle, the number of HLW containers per TWhr, both CSD-V and CSD-C, is somewhat less that for the scenarios that utilize UOX or MOX fuel only. Reprocessing of the thorium fuel only generates about one third of the amount of HLW containers per TWhr compared to the reprocessing of the uranium fuel.
- The HTR fuel cycle generates by far the the largest amount of waste containers, both in total and per generated TWhr. One reason is that the HTR (spent) fuel pebbles take up a relatively large volume per fissile mass compared to the other (UOX, MOX) fuels. The second reason is that the HTR fresh fuel is assumed to consist of UOX fuel that is 9% enriched in U-235, implying that about twice the amount of natural uranium is required per tonne to manufacture fresh HTR fuel compared to fresh Gen II/III UOX fuel (approx. 4.0-4.5% enriched). This practice generates more DepU when deploying HTRs than LWR Gen II/II reactors.

- The fuel cycles utilizing Fast Reactors and thorium reactors generate considerable less DepU per TWhr than the other fuel cycles. DepU is generated as a result of the necessary deployment of UOX-fueled reactors in the next decades, i.e. before the deployment of thorium reactors only becomes feasible.
- In the scenario “Fast Reactors”, LWR Gen III reactors are necessary to fill up the nuclear electricity demand before fast reactors can be deployed, viz. from about 2040 on. In the time period up to 2040 a stock pile of DepU will accumulate. Upon the deployment of fast reactors, DepU can serve as fissile material in those reactors, and the DepU stocks can be used for that purpose. As a consequence the DepU stocks may decrease, although at a relatively low rate, and only later in the century.

Table 8-22 Activities of radionuclides (spent fuel, HLW) generated in the considered scenarios in the year 2130

| | | *Activity [Bq]* | | | | | | |
|---|---|---|---|---|---|---|---|---|
| Nuclide | *Half-life [years]* | *Scenario 1 No new NPPs* | *Scenario 2 MOX Fuel* | *Scenario 3 No Reprocessing* | *Scenario 4 Gen III LWR* | *Scenario 5 HTRs* | *Scenario 6 Fast Reactors* | *Scenario 7 Thorium cycle* |
| **C-14** | 5.70E+03 | 1.72E+13 | 1.77E+13 | 1.33E+13 | 4.46E+14 | 2.33E+13 | 3.78E+14 | 2.76E+14 |
| **Cl-36** | 3.01E+05 | 0.00E+00 | 4.03E+11 | 5.54E+11 | 2.15E+13 | 4.77E+11 | 1.02E+13 | 1.02E+13 |
| **Ca-41** | 1.40E+05 | 0.00E+00 | 1.67E+11 | 1.75E+11 | 8.93E+12 | 1.98E+11 | 7.17E+12 | 4.25E+12 |
| **Ni-59** | 7.60E+04 | 4.47E+14 | 4.48E+14 | 2.06E+14 | 1.08E+16 | 4.40E+14 | 8.06E+15 | 6.83E+15 |
| **Ni-63** | 1.01E+02 | 1.57E+16 | 3.35E+16 | 6.78E+15 | 1.95E+18 | 3.60E+16 | 1.00E+18 | 9.26E+17 |
| **Se-79** | 3.77E+05 | 2.98E+12 | 2.42E+12 | 2.13E+12 | 4.22E+13 | 2.89E+13 | 3.37E+13 | 2.14E+13 |
| **Kr-85** | 1.08E+01 | 0.00E+00 | 0.00E+00 | 1.11E+14 | 0.00E+00 | 7.16E+17 | 0.00E+00 | 1.19E+16 |
| **Sr-90** | 2.88E+01 | 2.09E+17 | 1.15E+17 | 1.34E+17 | 5.34E+18 | 1.36E+19 | 2.97E+18 | 1.86E+18 |
| **Zr-93** | 1.53E+06 | 6.61E+13 | 5.83E+13 | 5.25E+13 | 1.18E+15 | 8.70E+14 | 8.32E+14 | 5.78E+14 |
| **Mo-93** | 4.00E+03 | 7.24E+12 | 7.23E+12 | 3.30E+12 | 1.76E+14 | 7.10E+12 | 1.31E+14 | 1.11E+14 |
| **Nb-94** | 2.00E+04 | 6.92E+13 | 6.98E+13 | 3.16E+13 | 1.70E+15 | 6.86E+13 | 1.26E+15 | 1.07E+15 |
| **Tc-99** | 2.14E+05 | 7.84E+14 | 6.22E+14 | 5.51E+14 | 1.03E+16 | 6.62E+15 | 7.56E+15 | 5.17E+15 |
| **Pd-107** | 6.50E+06 | 4.24E+12 | 4.78E+12 | 4.45E+12 | 1.31E+14 | 5.26E+13 | 1.03E+14 | 6.54E+13 |
| **Ag-108m** | 4.18E+02 | 0.00E+00 | 1.44E+08 | 1.90E+08 | 8.38E+09 | 6.24E+09 | 1.17E+10 | 3.88E+09 |
| **Sn-126** | 1.00E+05 | 2.38E+13 | 2.38E+13 | 2.18E+13 | 5.73E+14 | 3.81E+14 | 4.75E+14 | 2.84E+14 |
| **I-129** | 1.61E+07 | 2.28E+11 | 1.61E+11 | 5.70E+11 | 1.90E+12 | 1.36E+13 | 1.44E+12 | 1.44E+12 |
| **Cs-135** | 2.30E+06 | 1.88E+13 | 1.98E+13 | 1.82E+13 | 5.04E+14 | 1.31E+14 | 5.57E+14 | 2.52E+14 |
| **Cs-137** | 3.00E+01 | 3.30E+17 | 1.94E+17 | 2.43E+17 | 1.02E+19 | 1.93E+19 | 6.76E+18 | 3.62E+18 |
| **Sm-151** | 9.00E+01 | 3.19E+13 | 2.39E+15 | 3.35E+15 | 1.91E+17 | 8.16E+16 | 3.71E+17 | 8.60E+16 |
| **U-232** | 6.88E+01 | 4.47E+08 | 2.27E+10 | 1.06E+11 | 2.07E+12 | 1.48E+11 | 8.97E+11 | 5.36E+12 |
| **U-233** | 1.59E+05 | 3.99E+05 | 5.75E+08 | 1.81E+08 | 3.07E+10 | 8.93E+08 | 1.46E+10 | 8.41E+11 |
| **U-234** | 2.46E+05 | 9.74E+10 | 1.40E+11 | 5.40E+13 | 3.38E+12 | 7.14E+13 | 3.23E+12 | 2.18E+12 |
| **U-235** | 7.04E+08 | 1.96E+09 | 1.88E+09 | 1.04E+11 | 4.28E+10 | 3.61E+12 | 3.07E+10 | 2.63E+10 |
| **U-236** | 2.37E+07 | 2.11E+10 | 2.06E+10 | 2.18E+12 | 4.81E+11 | 1.16E+14 | 3.30E+11 | 2.87E+11 |
| **U-238** | 4.47E+09 | 3.06E+10 | 3.03E+10 | 2.96E+12 | 7.19E+11 | 4.32E+13 | 5.14E+11 | 4.31E+11 |
| **Pu-238** | 8.77E+01 | 1.41E+14 | 1.88E+14 | 9.52E+16 | 9.47E+15 | 4.56E+17 | 8.84E+15 | 5.53E+15 |

| | | *Activity [Bq]* | | | | | | |
|---|---|---|---|---|---|---|---|---|
| **Nuclide** | ***Half-life [years]*** | ***Scenario 1 No new NPPs*** | ***Scenario 2 MOX Fuel*** | ***Scenario 3 No Reprocessing*** | ***Scenario 4 Gen III LWR*** | ***Scenario 5 HTRs*** | ***Scenario 6 Fast Reactors*** | ***Scenario 7 Thorium cycle*** |
| **Pu-239** | 2.41E+04 | 3.19E+13 | 3.50E+13 | 8.31E+15 | 9.35E+14 | 4.85E+16 | 9.37E+14 | 5.27E+14 |
| **Pu-240** | 6.56E+03 | 3.43E+14 | 3.19E+14 | 2.12E+16 | 6.72E+15 | 1.46E+17 | 4.28E+15 | 3.46E+15 |
| **Pu-241** | 1.43E+01 | 8.57E+13 | 8.05E+13 | 3.06E+16 | 6.80E+16 | 7.66E+18 | 4.13E+16 | 2.89E+16 |
| **Pu-242** | 3.74E+05 | 2.19E+11 | 3.02E+11 | 1.29E+14 | 9.69E+12 | 1.44E+15 | 7.62E+12 | 5.49E+12 |
| **Pu-244** | 8.00E+07 | 6.12E+04 | 1.32E+05 | 7.35E+07 | 5.28E+06 | 3.61E+08 | 3.93E+06 | 2.75E+06 |
| **Np-236** | 1.15E+05 | 0.00E+00 | 0.00E+00 | 1.62E+08 | 0.00E+00 | 1.74E+08 | 0.00E+00 | 0.00E+00 |
| **Np-237** | 2.14E+06 | 1.48E+13 | 1.12E+13 | 1.03E+13 | 1.66E+14 | 7.45E+13 | 8.22E+13 | 8.24E+13 |
| **Am-241** | 4.33E+02 | 5.90E+16 | 3.92E+16 | 7.44E+16 | 4.21E+17 | 4.70E+16 | 2.11E+17 | 2.10E+17 |
| **Am-242m** | 1.52E+02 | 1.17E+11 | 3.30E+13 | 8.87E+14 | 2.23E+15 | 7.22E+14 | 1.14E+15 | 9.96E+14 |
| **Am-243** | 7.36E+03 | 1.12E+15 | 8.81E+14 | 2.44E+15 | 1.45E+16 | 9.54E+15 | 7.43E+15 | 7.31E+15 |
| **Cm-243** | 2.85E+01 | 2.43E+10 | 1.14E+13 | 2.33E+14 | 2.57E+15 | 2.07E+15 | 7.91E+14 | 7.69E+14 |
| **Cm-244** | 1.80E+01 | 1.69E+15 | 7.67E+14 | 8.10E+15 | 9.07E+16 | 5.08E+17 | 2.12E+16 | 2.05E+16 |
| **Cm-245** | 8.50E+03 | 1.26E+13 | 1.28E+13 | 1.42E+14 | 3.18E+14 | 1.56E+14 | 1.60E+14 | 1.54E+14 |
| **Cm-246** | 4.73E+03 | 5.96E+09 | 1.27E+12 | 1.75E+13 | 6.79E+13 | 3.66E+13 | 3.56E+13 | 3.23E+13 |
| **Cm-247** | 1.56E+07 | 3.28E+04 | 6.71E+06 | 1.36E+08 | 3.57E+08 | 7.66E+07 | 2.35E+08 | 1.70E+08 |
| **Cm-248** | 3.39E+05 | 2.03E+05 | 4.51E+07 | 1.34E+09 | 2.40E+09 | 2.68E+08 | 1.36E+09 | 1.14E+09 |
| **Cm-250** | 6.90E+03 | 0.00E+00 | 0.00E+00 | 0.00E+00 | 0.00E+00 | 1.81E+03 | 0.00E+00 | 0.00E+00 |
| **Th-229** | 7.34E+03 | 1.47E+03 | 3.16E+06 | 2.05E+06 | 1.69E+08 | 6.05E+06 | 3.41E+08 | 8.04E+07 |
| **Th-230** | 7.54E+04 | 2.09E+04 | 6.83E+08 | 7.05E+08 | 3.65E+10 | 8.13E+08 | 2.73E+10 | 1.73E+10 |
| **Th-232** | 1.41E+10 | 2.52E+00 | 7.56E+02 | 8.17E+02 | 4.03E+04 | 7.54E+03 | 1.97E+04 | 2.48E+08 |
| **Ra-226** | 1.60E+03 | 1.30E+01 | 1.30E+01 | 5.91E+00 | 3.21E+02 | 1.27E+01 | 2.38E+02 | 2.02E+02 |
| **Pa-231** | 3.28E+04 | 3.02E+05 | 2.12E+08 | 2.22E+08 | 1.13E+10 | 3.72E+08 | 5.54E+09 | 2.49E+13 |
| **Ac-227** | 2.18E+01 | 1.47E+02 | 7.12E+06 | 4.61E+01 | 2.69E+09 | 8.11E+06 | 7.43E+08 | 6.77E+08 |
| | | **6.18E+17** | **3.88E+17** | **6.29E+17** | **1.83E+19** | **4.27E+19** | **1.14E+19** | **6.80E+18** |

Table 8-23 Inventories of radionuclides (depleted uranium) generated in the considered scenarios in the year 2130

| | | *Activity [Bq]* | | | | | | |
|---|---|---|---|---|---|---|---|---|
| Nuclide | *Half-life [years]* | *Scenario 1 No new NPPs* | *Scenario 2 MOX Fuel* | *Scenario 3 No Reprocessing* | *Scenario 4 Gen III LWR* | *Scenario 5 HTRs* | *Scenario 6 Fast Reactors* | *Scenario 7 Thorium cycle* |
| U-238 | 4.47E+09 | 5.56E+13 | 3.43E+13 | 3.43E+13 | 2.03E+15 | 3.35E+15 | 3.27E+14 | 3.12E+14 |
| U-235 | 7.04E+08 | 1.28E+12 | 7.91E+11 | 7.91E+11 | 4.69E+13 | 7.72E+13 | 7.55E+12 | 7.21E+12 |
| U-234 | 2.46E+05 | 1.28E+13 | 7.92E+12 | 7.92E+12 | 4.69E+14 | 7.73E+14 | 7.55E+13 | 7.21E+13 |
| Pa-231 | 3.28E+04 | 2.91E+09 | 1.78E+09 | 1.78E+09 | 6.37E+10 | 1.10E+11 | 1.31E+10 | 1.19E+10 |
| Th-230 | 7.54E+04 | 1.27E+10 | 7.76E+09 | 7.76E+09 | 2.77E+11 | 4.79E+11 | 5.70E+10 | 5.17E+10 |
| Ac-227 | 2.18E+01 | 2.10E+09 | 1.28E+09 | 1.28E+09 | 3.94E+10 | 6.97E+10 | 8.49E+09 | 7.62E+09 |
| Ra-226 | 1.60E+03 | 2.91E+08 | 1.74E+08 | 1.74E+08 | 4.69E+09 | 8.51E+09 | 1.03E+09 | 9.14E+08 |
| Rn-222 | 1.05E-02 | 2.91E+08 | 1.74E+08 | 1.74E+08 | 4.69E+09 | 8.51E+09 | 1.03E+09 | 9.14E+08 |
| **Total** | | **6.97E+13** | **4.30E+13** | **4.30E+13** | **2.55E+15** | **4.20E+15** | **4.10E+14** | **3.92E+14** |

Table 8-24 Waste characteristics per 2130 for the considered scenarios

| Characteristic | *Scenario 1 No new NPPs* | *Scenario 2 MOX Fuel* | *Scenario 3 No Reprocessing* | *Scenario 4 Gen III LWR* | *Scenario 5 HTRs* | *Scenario 6 Fast Reactors* | *Scenario 7 Thorium cycle* |
|---|---|---|---|---|---|---|---|
| # CSD-V canisters | 624 | 623 | 285 | 15’000 | 612 | 11’170 | 9465 |
| # CSD-C canisters | 1247 | 1246 | 570 | 30’000 | 1224 | 23’240 | 18’930 |
| # CSD-V canisters per TWh(e) | 3.08 | 2.76 | 3.08 | 2.75 | 2.88 | 2.51 | 2.28 |
| # CSD-C canisters per TWh(e) | 6.16 | 5.53 | 6.16 | 5.50 | 5.76 | 5.02 | 4.56 |
| # Spent fuel canisters | - | - | 318 | - | 284’000 | - | - |
| # Spent fuel canisters per TWh(e) | - | - | 2.70 | - | 55.5 | - | - |
| # KONRAD II containers (DepU) | 477 | 319 | 295 | 17’465 | 28’785 | 5530 | 5370 |
| # KONRAD II containers per TWh(e) (DepU) | 6.35 | 4.19 | 4.28 | 3.72 | 7.03 | 1.71 | 1.64 |

An overview of the summed radionuclide inventories and radiotoxicity values generated by the different scenarios by the year 2130 is given in Figure 8-23 for the fission products and in Figure 8-24 for the actinides (only for radionuclides with half lives > 10 years and total estimated radiotoxicities > $10^3$ Sv). The blue bars represent the “no new nuclear” scenarios, whereas the orange bars represent the growth scenarios. For the radionuclide inventories the following observations apply:

- For scenarios assuming direct disposal of spent fuel, (Scenario 3 *No reprocessing*; Scenario 5 *HTRs*) obviously considerable more plutonium and uranium, and about 10-20 times more curium must be finally disposed than for the “reprocessing” scenarios. During the reprocessing step these compounds are removed from the nuclear waste and stored at locations outside the Netherlands.
- The fission products that contribute most to the total radionuclide inventory and radiotoxicity in all scenarios at the foreseen time of emplacement in a disposal facility (the year 2130) are Ni-63, Sr-90, Tc-99, Cs-137, and Sm-151 (and Kr-85 for Scenario 3 *HTRs*). In a post-closure safety assessment these nuclides would contribute most to the radiological consequences of *short-term* scenarios.
- Considering a post-closure safety assessment the long-lived isotopes Ni-59, Se-79, Zr-93, Nb-94, Tc-99, Sn-129, I-129, and Cs-135 would contribute most to the long-term radiological effects.
- The actinides that contribute most to the total radionuclide inventory and radiotoxicity in all scenarios at the foreseen time of emplacement in a disposal facility (the year 2130) are isotopes of Pu, Am, and Cm.
- Considering a post-closure safety assessment the long-lived actinides Pu-239, Pu-240 (mid-term), Am-241, and Cm-245 (mid-term) would contribute most to the ultimate radiological effects in the biosphere.

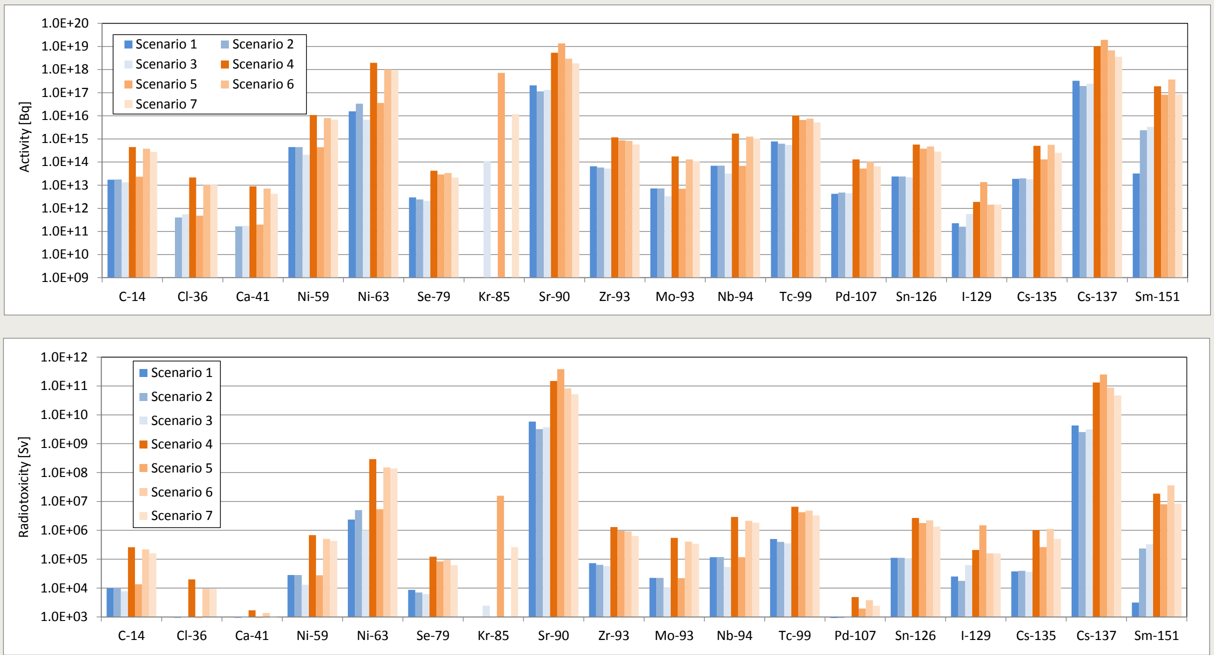


**Figure 8-23** **Total estimated fission product inventory (top) and radiotoxicity (bottom) for the year 2130 - blue: no new nuclear scenarios; orange: nuclear growth scenarios**

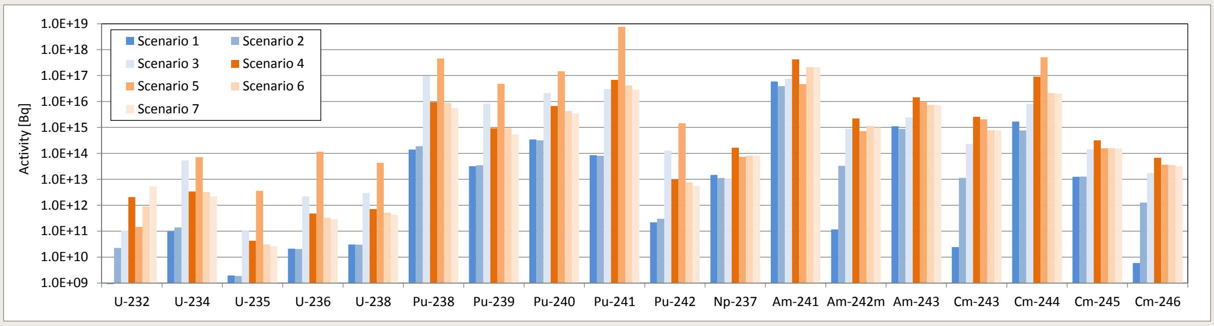


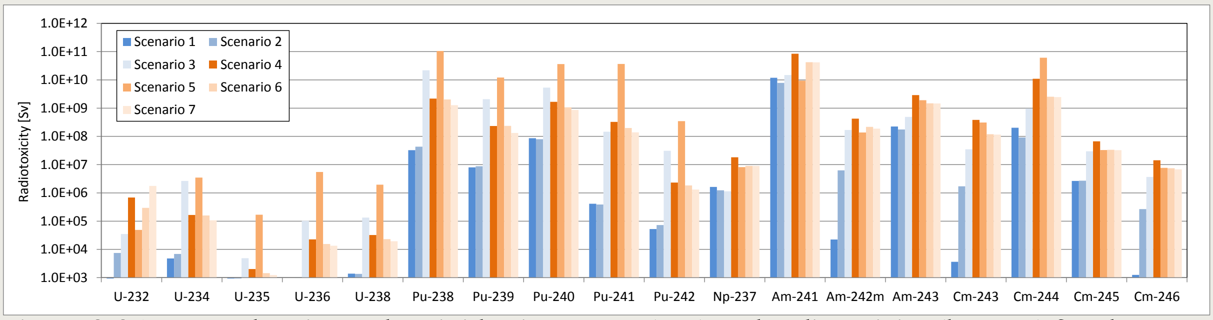


**Figure 8-24** **Total estimated actinides inventory (top) and radiotoxicity (bottom) for the year 2130 - blue: no new nuclear scenarios; orange: nuclear growth scenarios**

# 9. Concluding remarks

The present report addresses Milestone M1.1.2.1, “Report on alternative waste scenario’s”, as part of the OPERA project OPCHAR, OPERA Waste Characteristics, Work Package 1.1, “Waste Characteristics”, Task 1.1.2, “Alternative waste scenarios”.

The present report describes the results of OPCHAR Task 1.1.2 with regard to the following topics:

- The introduction of a set of alternative future fuel cycle scenarios in the Netherlands, that are in compliance with scenarios formulated in the ‘Energierapport 2008’ (MinEZ, 2008; p.88), and that have been analysed with DANESS;
- The introduction of a travel time based indicator that allows comparing different nuclear energy usage scenarios;
- A summary description of the DANESS code that has been applied to simulate the fuel cycle scenarios;
- A description of the assumptions for the calculations;
- A description of technology parameters of the back-end of the fuel cycle, since that has been the focus of the simulations;
- An overview of the main results obtained with DANESS, with the focus on the types and amounts of radioactive waste, viz. spent fuel, vitrified HLW, and depleted uranium.

It has to be noted that the DANESS code has been set up as a uranium fuel cycle analysis tool. In order to apply DANESS to a thorium fuel cycle the code requires important modifications, e.g. including the thorium mining, conversion, enrichment steps in the fuel cycle, provisions to properly model thorium reprocessing steps, and adding other thorium-specific features (resources, price, etc.). In the present DANESS code, no provisions have yet been implemented to properly model all these steps for the thorium fuel cycle. For those reasons, the results of the presently assessed thorium fuel cycle must be regarded as indicative.

## Index of Figures


Figure 2-1 Process scheme of Scenario 1 – No new nuclear power plants .................. 10
Figure 2-2 Process scheme of Scenario 2 – Application of MOX fuel ......................... 10
Figure 2-3 Process scheme of Scenario 3 – No reprocessing of spent fuel .................. 11
Figure 2-4 Process scheme of Scenario 4 – Deployment of MOX-fueled Gen III LWRs ..... 11
Figure 2-5 Process scheme of Scenario 5 – Large-scale deployment of HTRs............... 11
Figure 2-6 Process scheme of Scenario 6 – Deployment of fast reactors.................... 12
Figure 2-7 Process scheme of Scenario 7 - Deployment of thorium-based reactors....... 13
Figure 3-1 Reference value divided by relative flow rate and radiotoxicity inventory as function of adjusted radionuclide half-life, example adapted from (Schröder, 2011) ........ 20
Figure 3-2 Reference value divided by relative flow rate and radiotoxicity inventory as function of adjusted radionuclide half-life, example adapted from (Schröder, 2011) ........ 23
Figure 3-3 Reference value divided by relative flow rate and radiotoxicity inventory of selected radionuclides as function time ........ 24
Figure 4-1 Architecture of the DANESS model ........ 26
Figure 4-2 Fuel cycle model of the DANESS program ........ 26
Figure 5-1 Forecast of the installed nuclear electricity generating capacity in the Netherlands for the adopted growth scenario ........ 28
Figure 5-2 Overview of the Sodium-cooled Fast Reactor ........ 30
Figure 5-3 Spherical fuel element ........ 31
Figure 5-4 View of the HTR-PM........ 32
Figure 6-1 Spent fuel assembly for spent UOX fuel ........ 35
Figure 6-2 Spent fuel assembly for spent MOX fuel ........ 36
Figure 6-3 Spent fuel storage in CASTOR casks ........ 36
Figure 6-4 Universal canister for vitrified high level waste ........ 37
Figure 8-1 Operating reactor capacity - Scenario 1 – No new nuclear power plants ...... 41
Figure 8-2 Number of HLW colli (CSD-V) - Scenario 1 – No new nuclear power plants .... 42
Figure 8-3 Amount of depleted uranium (DepU) generated during reactor operations – Scenario 1 – No new nuclear power plants ........ 42
Figure 8-4 Operating reactor capacity – Scenario 2 – Application of MOX fuel ............ 45
Figure 8-5 Number of HLW containers (CSD-V) – Scenario 2 – Application of MOX fuel ... 45
Figure 8-6 Amount of depleted uranium (DepU) generated during reactor operations – Scenario 2 – Application of MOX fuel ........ 46
Figure 8-7 Operating reactor capacity – Scenario 3 – No reprocessing of spent fuel ...... 48
Figure 8-8 Number of containers (spent fuel; CSD-V) – Scenario 3 – No reprocessing of spent fuel........ 49
Figure 8-9 Amount of depleted uranium (DepU) generated during reactor operations – Scenario 3 – No reprocessing of spent fuel ........ 50
Figure 8-10 Operating reactor capacity – Scenario 4 – Deployment of Gen III LWRs ........ 52
Figure 8-11 Number of HLW containers (CSD-V) – Scenario 4 – Deployment of Gen III LWRs 53
Figure 8-12 Amount of depleted uranium (DepU) generated during reactor operations – Scenario 4 – Deployment of Gen III LWRs ........ 53
Figure 8-13 Operating reactor capacity - Scenario 5 – Deployment of HTRs ................ 56
Figure 8-14 Number of HLW containers (CSD-V) – Scenario 5 – Deployment of HTRs ....... 56
Figure 8-15 Number of spent fuel containers – Scenario 5 – Deployment of HTRs .......... 57
Figure 8-16 Amount of depleted uranium (DepU) generated during reactor operations – Scenario 5 – Deployment of HTRs ........ 57
Figure 8-17 Operating reactor capacity – Scenario 6 – Deployment of Fast Reactors....... 60

Figure 8-18 Number of HLW containers (CSD-V) – Scenario 6 – Deployment of Fast Reactors 60
Figure 8-19 Amount of depleted uranium (DepU) generated during reactor operations - Scenario 6 – Deployment of Fast Reactors ........ 61
Figure 8-20 Operating reactor capacity – Scenario 7 – Deployment of thorium reactors... 63
Figure 8-21 Number of HLW containers (CSD-V) – Scenario 7 – Deployment of thorium reactors ........ 64
Figure 8-22 Amount of depleted uranium (DepU) generated during reactor operations - Scenario 7 – Deployment of thorium reactors ........ 65
**Figure 8-23 Total estimated fission product inventory (top) and radiotoxicity (bottom) for the year 2130 - blue: no new nuclear scenarios; orange: nuclear growth scenarios** ........ 72
**Figure 8-24 Total estimated actinides inventory (top) and radiotoxicity (bottom) for the year 2130 - blue: no new nuclear scenarios; orange: nuclear growth scenarios** ........ 73

## Index of Tables

Table 3-1 Safety and performance indicators recommended for OPERA ........ 16
Table 3-2 Example of original and adjusted radionuclide half-lives and effective radionuclide inventory, adapted from (Schröder et al., 2009) ........ 21
Table 5-1 Main features of the Borssele reactor ........ 29
Table 5-2 Main features of the Gen III LWR ........ 29
Table 5-3 Main characteristics of the SFR ........ 30
Table 5-4 Main charactistics of the HTR-PM ........ 32
Table 5-5 Main features of the thorium PWR ........ 33
Table 7-1 NPP-type characteristics used in scenario analysis ........ 38
Table 7-2 Fuel-type characteristics used in scenario analysis ........ 40
Table 8-1 Waste characteristics per 2130 – Scenario 1 – No new nuclear power plants.. 43
Table 8-2 Estimated radionuclide inventory in 2130 - Scenario 1 – No new nuclear power plants ........ 43
Table 8-3 Estimated radionuclide inventory (DepU) in 2130 - Scenario 1 – No new nuclear power plants ........ 44
Table 8-4 Waste characteristics per 2130 – Scenario 2 – Application of MOX fuel ........ 46
Table 8-5 Estimated radionuclide inventory in 2130 – Scenario 2 – Application of MOX fuel ........ 46
Table 8-6 Estimated radionuclide inventory (DepU) in 2130 – Scenario 2 – Application of MOX fuel ........ 47
Table 8-7 Waste characteristics per 2130 – Scenario 3 – No reprocessing of spent fuel.. 49
Table 8-8 Estimated radionuclide inventory in 2130 – Scenario 3 – No reprocessing of spent fuel ........ 50
Table 8-9 Estimated radionuclide inventory (DepU) in 2130 – Scenario 3 – No reprocessing of spent fuel ........ 51
Table 8-10 Waste container characteristics per 2130 – Scenario 4 – Deployment of Gen III LWRs ........ 54
Table 8-11 Estimated radionuclide inventory in 2130 – Scenario 4 – Deployment of Gen III LWRs ........ 54
Table 8-12 Estimated radionuclide inventory (DepU) in 2130 – Scenario 4 – Deployment of Gen III LWRs ........ 55
Table 8-13 Waste characteristics per 2130 – Scenario 5 – Deployment of HTRs ........ 58
Table 8-14 Estimated radionuclide inventory in 2130 – Scenario 5 – Deployment of HTRs 58
Table 8-15 Estimated radionuclide inventory (DepU) in 2130 – Scenario 5 – Deployment of HTRs ........ 59

Table 8-16 Waste container characteristics per 2130 – Scenario 6 – Deployment of Fast Reactors ... 61
Table 8-17 Estimated radionuclide inventory in 2130 – Scenario 6 – Deployment of Fast Reactors ... 62
Table 8-18 Estimated radionuclide inventory (DepU) in 2130 – Scenario 6 – Deployment of Fast Reactors ... 63
Table 8-19 Waste container characteristics per 2130 – Scenario 7 – Deployment of thorium reactors ... 65
Table 8-20 Estimated radionuclide inventory in 2130 – Scenario 7 – Deployment of thorium reactors ... 65
Table 8-21 Estimated radionuclide inventory (DepU) in 2130 – Scenario 1 – No new nuclear power plants ... 66
Table 8-22 Activities of radionuclides (spent fuel, HLW) generated in the considered scenarios in the year 2130 ... 69
Table 8-23 Inventories of radionuclides (depleted uranium) generated in the considered scenarios in the year 2130 ... 71
Table 8-24 Waste characteristics per 2130 for the considered scenarios ... 71

# 10. References


ANDRA, 2005, Dossier 2005 – Argile – Synthesis; Evaluation of the feasibility of a geological repository in an argillaceous formation - Meuse/Haute-Marne site, ANDRA, Paris, December 2005.

AREVA, 2005, EPR, Paris-La Défense Cedex – France, March, 2005.

Areva, 2007, Finnish EPR Olkiluoto 3, The world's first third-generation reactor now under construction, AREVA, 2007.

Argonne National Laboratory (ANL). Analysis of Nuclear Energy System Strategies, DANESS v1 Description. Argonne National Laboratory, Nuclear Engineering Division NE, Argonne, Illinois, USA, 2005.

Astilleros, JM, 2002, Pina, CM, Fernández-Díaz, L, Putnis, A, Molecular-scale surface processes during the growth of calcite in the presence of manganese, Geochim. Cosmochim. Acta 66 (2002) p.3177–3189.

Becker, D-A, 2013, Grupa, JB, Wolf, J, Methods for uncertainty analysis, OPERA report OPERA-PU-GRS7321, 13 December 2013, 1-35.

Berner, U, 1998, Geochemical Modelling of Repository Systems: Limitations of the Thermodynamic Approach, Radiochim. Acta 82 (1998) p.423-428.

Boucher L, 2004. "Detailed Description of Selected Fuel Cycle Scenarios" Deliverable 1.4 of EU FP6 Red-Impact project, FI6W-CT-2004-002408 (2004).

Bruno, J, 2003, Duro, L, Grivé, M, The applicability and limitations of thermodynamic geochemical models to simulate trace element behaviour in natural waters. Lessons learned from natural analogue studies. Chemical Geology 190 (2003) p.371-393.

Bultman, JH Technology Assessment HTR, Part 5: Thorium fueled High Temperature gas cooled Reactors. ECN~C--96-045, Petten, June 1996.

Carter, JT,2012, Luptak AJ, Gastelum J, Stockman C, Miller A, Fuel Cycle Potential Waste Inventory for Disposition, Chapter 9. Thorium Based Fuel Cycle Potential Waste, FCR&D-USED-2010-000031 Rev 5, July 2012.

CBS, 2013, Centraal Bureau voor de Statistiek – "Elektriciteitsbalans; aanbod en verbruik", http://statline.cbs.nl/StatWeb/publication/?DM=SLNL&PA=00377&D1=a&D2=a&HDR=G1&STB=T&VW=T last accessed on 5 March 2014.

CORA, 2001, Commissie Opberging Radioactief Afval (CORA). Terugneembare berging, een begaanbaar pad? Onderzoek naar de mogelijkheden van terugneembare berging van radioactief afval in Nederland. Ministry of Economic Affairs, The Hague, February 2001.

COVRA, 2013, Kwartaalrapport Nr. 103, Week 14 tot en met 26, Rapport nr. 13203, 30 September 2013.

De Cannière, P, 2010, Mae, A, Williams, S, Bruggeman, C, Beauwens, T, Maes, N, Cowper, M, Behaviour of Selenium in Boom Clay, SCK•CEN report SCK•CEN-ER-120, May 2010, 1-328.

EPZ, 2008, Brandstofdiversificatie Kerncentrale Borssele, EPZ, 24 april 2008.

EPZ, 2010, Milieueffectrapportage Brandstofdiversificatie, July 2010.

Ganor, J, 1998, Lasaga, AC, Simple mechanistic models for inhibition of a dissolution reaction, Geochim. Cosmochim. Acta 62 (1998) p.1295–1306.

GIF, 2011, Annual Report 2010, Generation IV International Forum, August, 2011.

González Romero, EM, 2005 RED-IMPACT Deliverable 3.1, Definition of technical data and detailed hypotheses, RED-IMPACT: Impact of Partitioning, Transmutation and Waste Reduction Technologies on the Final Nuclear Waste Disposal, EC Contract FI6W-CT-2004-002408, November 2005.

Grauer, R, 1997, Solubility Limitations. An “Old Timer’s” View, In: Grenthe, I, Puigdomenech, I (ed.): Modelling in aquatic chemistry. OECD Publications, ISBN 92-64-15569-4 (1997) p.131-152.

Grupa, JB, 2013, Wildenborg, T, Relevant scenarios for a repository in Boom Clay, OPERA report OPERA-PU-NRG7111, December 2013, 1-41.

Hart, J, 2008, Effects of future deployment of nuclear power in the Netherlands, Paper presented at the “12th International High-Level Radioactive Waste Management Conference (IHLRWM), September 7-11, 2008, Las Vegas.

Hart, J, DANESS Analysis of RED-IMPACT Scenarios A1 and B1 - Assessment of Environmental Impact of Radionuclide Releases, NRG-22358/09.98684/P, Petten, 15 November 2009.

Hart, J, 2010, Impact of the Introduction of (V)HTRs on the Nuclear Fuel Cycle Update of PUMA Report D322/D331, NRG-22572/102559/P, Petten, 21 September 2010.

Hart, J, 2014, Determination of the inventory, Part A: Radionuclides, OPERA-PU-NRG1112A, February 2014.

Heberling, F, 2008, Denecke, MA, Bosbach, D, Neptunium(V) Coprecipitation with Calcite, Environ. Sci. Technol. 42 (2008) p.471–476.

Hummel, W, 2003, Curti, E, Nickel Aqueous Speciation and Solubility at Ambient Conditions: A Thermodynamic Elegy, Monatshefte für Chemie 134 (2003) p.941-973.

IAEA, 1998, Technologies for gas cooled reactor decommissioning, fuel storage and waste disposal Proceedings of a Technical Committee meeting held in Julich, Germany, 8-10 September 1997 IAEA-TECDOC-1043, Vienna, September 1998.

IAEA, 2004, Operational and decommissioning experience with fast reactors, Proceedings of a technical meeting held in Cadarache, France, 11-15 March 2002. IAEA-TECDOC-1405, Vienna, August 2004.

IAEA, 2005, Thorium fuel cycle – potential benefits and challenges, IAEA-Tecdoc-1450, Vienna, May 2005.

IAEA, 2008, INPRO, International Atomic Energy Agency, International Project on Innovative Nuclear Reactors and Fuel Cycles. www.iaea.org/inpro.

IAEA, 2010, High Temperature Gas Cooled Reactor Fuels and Materials, IAEA-TECDOC-1645, Vienna, 2010.

IAEA, 2012, Nuclear Power Reactors in the World, Reference Data Series No. 2, 2012 Edition, IAEA-RDS-2/31, Vienna, June 2012. http://www.iaea.org/PRIS/CountryStatistics/ReactorDetails.aspx?current=423 (last accessed 22 April 2014).

Isee Systems, 2009. iThink software, www.iseesystems.com.

Kellett, MA, 2009, Bersillon, O, Mills, RW, The JEFF-3.1/-3.1.1 radioactive decay data and fission yields sub-libraries, JEFF Report 20, ISBN 978-92-64-99087-6, OECD/NEA report 6287, Paris, 2009, 1-147.

Liljenzin, JO, 2001, The Nuclear Fuel Cycle, Chapter 21.

Listo, 2014, DEEA - Dynamic Energy Economics Analysis, LISTO bvba, Belgium; http://forio.com/simulation/deea/index.html, last accessed on 6 March 2014.

Lützenkirchen, J, 2009, Huber, F, Interaction of uranyl with quartz - influence of dissolved silica, In: Buckau, G, L Duro, B Kienzler, V Montoya, A Delos (eds.), 4th Annual Workshop Proceedings of the Integrated Project “Fundamental Processes of Radionuclide Migration” (6th EC FP IP FUNMIG), Forschungzentrum Karlsruhe GmbH, Karlsruhe, 2009, p.297-303.

Meeussen JCL, 2014, Rosca-Bocancea E, Determination of the inventory: part B matrix composition, OPERA-IR-NRG1112B, 24 February 2014.

MinEZ, 2008, Ministry of Economic Affairs. Energierapport 2008. Publication number 08 ET 14, The Hague, Juni 2008.

Kuijper, JC, 2010, Somers J, Van Den Durpel L, Chauvet V, Cerullo N, Cetnar J, Abram T, Bakker K, Bomboni E, Bernnat W, Domanska JG, Girardi E, de Haas JBM, Hesketh K, Hiernaut JP, Hossain K, Jonnet J, Kim Y, Kloosterman JL, Kopec M, Murgatroyd J, Lecarpentier D, Lomonaco G, McEachern D, Meier A, Mignanelli M, Nabielek H, Oppe J, Petrov BY, Pohl C, Rütten HJ, Schihab S, Toury G, Trakas C, Venneri F, Verfondern K, Wiss T, Zakova J, European Commission 6th Framework Programme Project Plutonium and Minor Actinides Management in Thermal High Temperature Reactors. Publishable Final Activity Report, Contract Number: FP6-036457, June 2010.

Mathieu L, 2006, Heuer D, Brissot R, Garzenne C, Le Brun C, Lecarpentier D, Liatard E, Loiseaux J-M, Meplan O, Merle-Lucotte E., Nuttin A, Walle E, Wilson J, The thorium molten salt reactor: Moving on from the MSBR. Progress in Nuclear Energy, 48(7) 664-679, 2006.

NEI, 2009, Nuclear Engineering International, World Nuclear Industry Handbook 2009.

NEI, 2012, Nuclear Engineering International, World Nuclear Industry Handbook 2012.

ONDRAF/NIRAS, 2001, SAFIR 2 - Safety Assessment and Feasibility Interim Report 2, NIROND 2001–06 E, Mol, December 2001.

OPLA, 1989, Commissie Opberging te Land (OPLA). Onderzoek naar geologische opberging van radioactief afval in Nederland, Eindrapport Fase 1. ISBN 90-9002867-6, Ministry of Economic affairs, The Hague, May 1989.

Schröder, TJ, 2013, Rosca-Bocancea, E, Safety and performance indicator calculation methodology, OPERA report OPERA-PU-NRG7312, December 2013, 1-29.

Renault C, 2009, Hron M, Konings RJM, Holcomb DE, The Molten Salt Reactor (MSR) in Generation-IV: Overview and perspectives. Proceedings of the GIF symposium in Paris, France (2009) 191-199, 2009.

Robertson RC, 1971. Conceptual design study of a single-fluid Molten Salt Breeder Reactor. Oak Ridge National Laboratory report ORNL-4541, USA, June 1971.

Roelofs, F, 2011, Hart J, van Heek A, European new build and fuel cycles in the 21st century, Nuclear Engineering and Design, 241 (2307-2317), 2011.

Rosca-Bocancea, E, 2013, Schröder, TJ, Development of Safety and Performance Indicators, OPERA report OPERA-CF-NRG010, October 2013, 1-32.

Rosenthal MW, 1972, Nabenreich PN, Briggs RB, The development status of Molten Salt Breeder Reactors, Oak Ridge National Laboratory report ORNL-4812, USA, August 1972.

Schröder, TJ, 2009, Rosca-Bocancea E, and Hart J, PAMINA Task WP3.4, Other methodological advancements: Safety Indicators and Performance Indicators Calculation results of a repository design in argillaceous rock, PAMINA Milestone Report M3.4.15, NRG report NRG-21952/09.95482, Petten, June 2009.

Schröder, TJ, 2009, Rosca-Bocancea E, Hart J, PAMINA, Calculation results of a repository design in argillaceous rock, PAMINA Milestone Report M3.4.21, 2009, 1-84.

Schröder, TJ,2009a, Rosca-Bocancea, E, Hart, J, Costescu-Badea, A, Bolado Lavin, R, PAMINA, Analysis of a repository design in argillaceous rock, PAMINA Milestone Report M2.1D.12, 2009, 1-225.

Schröder, TJ, 2011, TRUCK_NB. Verkennend vooronderzoek naar veiligheidsrelevante aspecten voor een Nederlandse eindberging in Boomse Klei, NRG report NRG-22151.30/10.104836, January 2011, 1-98.

SCK•CEN, 2002, BENIPA Project. 3. Plastic clay reference case: Data for radionuclide transport calculations, Revision 1, SCK•CEN, Augustus 2002, 1-7.

Seebregts, AJ, Snoep HJM, van Deurzen J, Lako P, Poley AD, Kernenergie & Brandstofmix, Effecten van nieuwe kerncentrales na 2020 in de kernenergiescenario's uit het Energierapport 2008, ECN-E--10-033, Petten, March 2010.

Seebregts, AJ, 2011, Summary of 'Nuclear Energy and Fuel Mix: Effects of new nuclear power plants after 2020 as defined in the Dutch Energy Report 2008, ECN-E--11-018, Petten, March 2011.

Temmam, M,2000,  Paquette, J, Vali, H, Mn and Zn incorporation into calcite as a function of chloride aqueous concentration, Geochim. Cosmochim. Acta 64 (2000) p.2417–2430.

Todosow, M, 2010, Raitses G, Thorium based fuel cycle options for PWRs, Paper 10305, Proceedings of ICAPP '10, San Diego, USA, 13-17 June 2010.

Van den Durpel, L, 2005, Wade DC, Yacout A, From Gen-II to Gen-IV: A Systems View on Nuclear Energy Development Scenarios, ICAPP05, Paper 5467, Seoul, Korea, 2005.

Van Den Durpel L, 2008, Yacout A, Wade DC, Taiwo T, DANESS v4.0: an integrated nuclear energy system assessment code. PHYSOR 2008, Interlaken, Switzerland.

Van Den Durpel L, 2009, van Heek A, Impact on the Nuclear Fuel Cycle, PUMA-0908-D322/D331. October 2009.

Van Dril, AWN, 2005, and Elzenga HE, "Referentieramingen energie en emissies 2005-2020", ECN-C—05-018, Petten, May, 2005.

Van Heek AI, 2012, Hart J, Wakker A, Roelofs F, A high nuclear new build scenario for the EU-27: impacts on electricity production cost, fuel cycle, resources, and geological repository footprint, NRG-23152, Petten, 26 October 2012.

Vercouter, T, 2009, Amekraz, B, Moulin, C, Silicate complexation of trivalent lanthanides and actinides, In: Buckau, G, L Duro, Kienzler, V Montoya, A. Delos (eds.), 4th Annual Workshop Proceedings of the Integrated Project "Fundamental Processes of Radionuclide Migration" (6th EC FP IP FUNMIG), Forschungzentrum Karlsruhe GmbH, Karlsruhe, 2009, p.367-374.

Verhoef E, 2011a, Neeft E, Grupa J, Poley A, Outline of a disposal concept in clay, OPERA-PG-COV008, 2011-07-05, 1-17.

Verhoef, E, 2011b, Schröder, TJ, OPERA Research Plan, OPERA report OPERA-PG-COV004, 21 June 2011, 1-49.

Von Lensa W, 2001, W., Nabbi R, and Rossbach M. RED-IMPACT – Impact of Partitioning, Transmutation and Waste Reduction Technologies on the Final Nuclear Waste Disposal – Synthesis Report, FP6 Contract No. FI6W-CT-2004-002408, ISBN 978-3-89336-538-8, Forschungszentrum Jülich, Germany, September 2007.

VROM, 2001, Ministerie van Volkshuisvesting, Ruimtelijke Ordening en Milieubeheer (VROM), Besluit stralingsbescherming, 2001, 1-131.

Zhang, Z, 2007, Chinese HTR Program: HTR-10 results & Work Progress on HTR-PM, Preseted at ICAPP 2007, Nice.

Zhang Z, 2009, Zongxin Wu, Dazhong Wang, Yuanhui Xu, Yuliang Sun, Fu Li, Yujie Dong, Current status and technical description of Chinese 2 x 250 MWth HTR-PM demonstration plant, Nuclear En~neeting and Design 239 (2009) 1212-1219.

## Disclaimer

This report has been prepared at the request and for the sole use of the Client and for the intended purposes as stated in the agreement between the Client and Contractors under which this work was completed.

Contractors have exercised due and customary care in preparing this report, but have not, save as specifically stated, independently verified all information provided by the Client and others. No warranty, expressed or implied is made in relation to the preparation of the report or the contents of this report. Therefore, Contractors are not liable for any damages and/or losses resulting from errors, omissions or misrepresentations of the report.

Any recommendations, opinions and/or findings stated in this report are based on circumstances and facts as received from the Client before the performance of the work by Contractors and/or as they existed at the time Contractors performed the work. Any changes in such circumstances and facts upon which this report is based may adversely affect any recommendations, opinions or findings contained in this report. Contractors have not sought to update the information contained in this report from the time Contractors performed the work.

The Client can only rely on or rights can be derived from the final version of the report; a draft of the report does not bind or obligate Contractors in any way. A third party cannot derive rights from this report and Contractors shall in no event be liable for any use of (the information stated in) this report by third parties.

OPERA

Meer informatie:

Postadres
Postbus 202
4380 AE
Vlissingen

T 0113-616 666
F 0113-616 650
E info@covra.nl

www.covra.nl